OBSERVATION OF QUANTIZED CIRCULATION IN SUPERFLUID HELIUM

A THESIS

SUBMITTED TO THE FACULTY OF THE GRADUATE SCHOOL

OF THE UNIVERSITY OF MINNESOTA

By

STEPHEN CARR WHITMORE

IN PARTIAL FULFILLMENT OF THE REQUIREMENTS

FOR THE DEGREE OF

DOCTOR OF PHILOSOPHY

DECEMBER, 1966

DISCLAIMER

OBSERVATION OF QUANTIZED CIRCULATION IN SUPERFLUID HELIUM

A THESIS

SUBMITTED TO THE FACULTY OF THE GRADUATE SCHOOL

OF THE UNIVERSITY OF MINNESOTA

By

STEPHEN CARR WHITMORE

IN PARTIAL FULFILLMENT OF THE REQUIREMENTS

FOR THE DEGREE OF

DOCTOR OF PHILOSOPHY

DECEMBER, 1966

ABSTRACT

OBSERVATION OF QUANTIZED CIRCULATION IN SUPERFLUID HELIUM

Circulation of the superfluid component of liquid-helium II around a fine wire has been measured by means of the influence that the circulation exerts on the transverse vibrations of the wire. The work is a repetition and extension of an experiment performed earlier by Vinen.[1] It gives new evidence in support of the Onsager-Feynman hypothesis that circulation of superfluid helium is quantized in units of h/m, where h is Planck's constant and m is the mass of the helium atom.

A fine wire is stretched down the center of a cylindrical vessel containing liquid helium, and the circulation is prepared by rotating the vessel around the axis of the wire while cooling from above T_λ. Then the rotation of the vessel is stopped, and the wire is set into vibration by passing a current pulse through it in the presence of a transverse magnetic field. The free, slowly damped vibrations which follow can then be observed by means of the oscillatory e.m.f. induced along the wire. If circulation exists around the wire its influence on a cylindrically symmetric wire is to cause the plane of vibration of the wire to precess at a rate proportional to the circulation, in the same direction as the circulation. As the plane of

vibration precesses the induced e.m.f. sweeps out a decaying beat pattern with beat frequency proportional to the circulation. More accurately, the beat frequency is proportional to a weighted average of the circulation around the wire taken along the wire's length, a quantity we call the apparent circulation. Measurements of the beat frequency can be repeated indefinitely by repeatedly setting the wire into vibration with a current pulse.

Vinen's experiment has been extended in three ways. (1) The sensitivity of the electrical system which detects the vibrations of the wire has been increased, so that it has been possible to make virtually continuous records of circulation as a function of time for periods of several hours, and to make measurements over a temperature range from $1.2^{\circ}K$ to $1.9^{\circ}K$. (2) The measurements have been extended to wires of larger diameter than 25 μ, the size which Vinen used. (3) The direction of the apparent circulation around the wire has been measured as well as its magnitude. However, unlike Vinen's work circulation measurements have not been made while the vessel containing the helium was rotating.

There are two principal results of this experiment. (1) Motion of the superfluid can persist around the wire for long periods of time even though the vessel containing the liquid helium is stationary. Moreover, this motion is not steady. Smooth changes in apparent circulation take place throughout a

run, changes which can include reversals in direction. (2) The apparent circulation tends to show markedly greater stability at the anticipated quantum levels than at other values. Long periods of stability have been observed at the level of zero, one, two, and three quantum units. Another significant result of the experiment is that as the wire diameter has been increased, the maximum value of stable circulation observed has also increased.

However, the details of the fluid dynamics in this experiment remain far from clear. The observations of circulation values intermediate to the quantum levels and of spontaneous changes in circulation are not understood. The observation of transitions between stable values of +3 and -3 quantum units, with no evidence of stability at the intervening quantum levels during the transition, is especially surprising.

---

1. W. F. Vinen, Proc. Roy. Soc. (London) A260, 218 (1961).

CONTENTS

CONTENTS (continued)

LIST OF FIGURES

LIST OF TABLES

I. INTRODUCTION

A. The Two-Fluid Model

^{4}He liquifies under atmospheric pressure at 4.18°K and is thought to remain liquid down to 0°K so long as the pressure is kept below 25 atmospheres.[1-5] At a temperature called T_λ, which under saturated vapor pressure is 2.17°K, the liquid undergoes an anomalous phase transition. At temperatures well above T_λ the liquid behaves very much like a classical viscous fluid. At T_λ it appears to have a logarithmic singularity in its specific heat, and below T_λ the liquid behaves as though it were a mixture of two fluids, which are called the normal fluid and superfluid components. Above T_λ the liquid is called helium I and below T_λ it is called helium II. The normal fluid component of helium II has a measurable viscosity not very different from the viscosity of helium I, whereas at low velocities the superfluid component flows without resistance through very small channels, so small as to be essentially impervious to the normal fluid.

According to the two-fluid model the normal and superfluid components of helium II are assumed to have densities ρ_n and ρ_s respectively, connected by the relation

$$\rho_n + \rho_s = \rho \tag{1}$$

where ρ is the actual density of the total fluid. ρ_n was measured by Andronikashvili[6] in 1946, in a remarkable experiment

supporting the two-fluid model. ρ_s/ρ is plotted as a function of temperature in Figure 1. The ratio is zero at T_λ, 99% at 1^oK, and is thought to be identically unity at 0^oK.

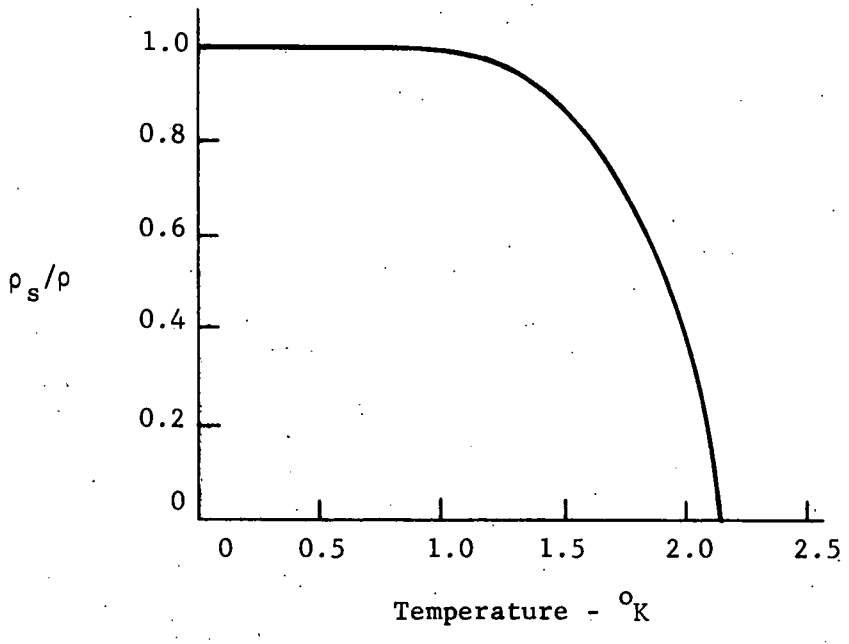

Figure 1. ρ_s/ρ as a Function of Temperature

Landau[7] successfully interpreted the two-fluid model of liquid helium in terms of elementary excitations. At 0^oK the liquid is in its ground state, has no entropy, and is presumed to be entirely superfluid. As the temperature is raised, collective excitations are created superimposed on the superfluid background. At temperatures not too close to T_λ the excitations

can be thought of as quasi-particles of an ideal Bose gas. It is these excitations which comprise the normal fluid and give the liquid its thermodynamic properties. Using certain plausible assumptions about the nature of the excitations Landau obtained a form for their dispersion curve, and showed that the curve accounts for the ability of the superfluid to flow without resistance and for the observed values of ρ_n and the specific heat of the liquid. He also predicted the existence of second sound and with Khalatnikov[8] calculated the viscosity of the normal fluid.

Landau also proposed a set of hydrodynamic equations to describe the flow of the two fluids at low velocities. The two components are assumed to have independent velocity fields, $\vec{v}_s$ and $\vec{v}_n$, and independent mass current densities, $\rho_s\vec{v}_s$ and $\rho_n\vec{v}_n$. Then mass conservation requires that

$$\frac{\partial(\rho_s+\rho_n)}{\partial t} + \mathrm{div}(\rho_s\vec{v}_s + \rho_n\vec{v}_n) = 0 \ . \qquad (2)$$

It is assumed that the normal fluid carries all the entropy of the liquid; then entropy conservation in the absence of dissipative processes requires that

$$\frac{\partial(\rho s)}{\partial t} + \mathrm{div}(\rho s\vec{v}_n) = 0 \qquad (3)$$

where s is the entropy per unit mass of the whole liquid. The equation of motion for the fluid as a whole, corresponding to the Navier-Stokes equation of classical fluid dynamics, is

$$\rho_s \frac{D_s \vec{v}_s}{D_s t} + \rho_n \frac{D_n \vec{v}_n}{D_n t} = - \text{grad } P + (\eta_n + \eta'_n) \text{ grad div } \vec{v}_n$$

$$- \eta_n \text{ curl curl } \vec{v}_n \qquad (4)$$

Here $\frac{D_s}{D_s t}$ and $\frac{D_n}{D_n t}$ are time derivatives in coordinate systems moving with the superfluid and normal fluid respectively, P is the pressure, and η_n and η'_n are viscosity coefficients of the normal fluid. The set of hydrodynamic equations is completed by the addition of a fourth equation proposed by Landau, for the motion of the superfluid component. Using these equations Landau was able to calculate the speed of second sound. In addition an attempt to formulate a quantum theory of fluid dynamics led him to postulate that the superfluid flows with potential flow, so that

$$\text{curl } \vec{v}_s = 0 \; . \qquad (5)$$

The two-fluid model has provided understanding of a great many experiments performed with liquid helium and was relied upon throughout the work reported here. The terminology of the model will be used throughout the discussion of this work which follows. In order to avoid possible misunderstanding it is helpful to bear in mind a comment from Landau's original paper.[9]

> It must be stressed that when we look upon helium as a mixture of two liquids it is no more than a method of expression, convenient for describing phenomena which take place in helium II. Like every description of quantum phenomena in classical terms it is not quite adequate. Actually one must say that in a quantum liquid two movements can exist simultaneously, each of which is connected with its own "effective

mass" (so that the sum of both these masses equals the total real mass of the liquid). One of these movements is normal, i.e., possesses the same properties as the movements of usual liquids; the other is superfluid. Both of these motions take place without a transfer of momentum from one to the other. We particularly emphasize that there is no division of the real particles of the liquid into "superfluid" and "normal" ones here. In a certain sense one can speak of "superfluid" and "normal" masses of liquid as of masses connected with two simultaneously possible movements, but this by no means signifies the possibility of a real division of the liquid into two parts.

B. Superfluid Flow

A second line of investigation which complements the two-fluid model emphasizes that the remarkable properties of liquid helium are a manifestation of wave mechanics on a macroscopic scale. Fritz London[10] first called attention to the similarity between the lambda transition in helium and condensation of an ideal Bose-Einstein gas into its ground state. It may be supposed that even in the real liquid a macroscopic fraction of the helium atoms occupies the same quantum state;[11] a recent calculation[12] estimates that the fraction is 11% at $T = 0^{\circ}K$. In uniform flow with velocity $\vec{v}_s$ the macroscopic occupation would be of the momentum state $\vec{p} = m\vec{v}_s$, where m is the mass of a helium atom.

By analogy with the wave mechanics of a single particle Onsager[13] and Feynman[14] independently made some surprising predictions about superfluid flow. Suppose that the quantum state with flow $\vec{v}_s$ can be characterized by a wave function with phase ϕ such that

$$m\vec{v}_s = \hbar \text{ grad } \phi \qquad (6)$$

where $\hbar$ is Planck's constant divided by 2π, just as one has in the wave mechanics of a single particle. As a consequence we would have curl $\vec{v}_s = 0$ identically, and the superfluid would perform potential flow. This means that the circulation of the superfluid, which is the line integral $\oint \vec{v}_s \cdot \vec{d\ell}$ around a closed contour, would be zero around any contour which does not enclose an internal boundary. In addition, in order for the wave function to be single-valued its phase would have to change by an integral multiple of 2π around any closed path. Consequently we would have

$$\oint \vec{v}_s \cdot \vec{d\ell} = \frac{nh}{m}, \quad n = 0, \pm 1, \pm 2, \ldots \quad . \tag{7}$$

The circulation around a contour which encloses either a solid cylinder or a line singularity in the velocity field would be quantized in units of h/m.

We shall be concerned primarily with circulation around a solid cylinder; however, let us consider briefly the possibility of a line singularity. If such a singularity should exist, and if for simplicity we assume that the singularity is a straight line in an unbounded fluid, so that the velocity field is cylindrically symmetric about the singularity, then according to the Onsager-Feynman picture we would have

$$v_s(r)\ 2\pi r = \frac{nh}{m} \tag{8}$$

$$v_s(r) = \frac{n\hbar}{mr} \ , \tag{9}$$

where r is the perpendicular distance from the field point to the singularity. $\vec{v}_s$ would be curl-free everywhere except along the line r = 0. This is the velocity field which characterizes a free vortex line in classical fluid dynamics. According to the Onsager-Feynman picture the circulation of a vortex line in superfluid helium would be quantized. Such a vortex line could not terminate in the fluid. In a real vessel it would either attach itself at both ends to walls of the vessel, or it might close on itself in a vortex ring. It could exchange energy with quasi-particles of the normal fluid by changing its length, or in the case of a ring its radius, but it is unlikely that its circulation would be affected. Once formed it would in all likelihood persist indefinitely unless destroyed at the walls or by annihilation with a vortex of opposite circulation, or perhaps until it had shrunk to the size and energy of an elementary excitation.

Real quantized vortex rings answering this description have been observed in liquid helium at 0.3°K by Rayfield and Reif,[15] and Gamota and Sanders,[16] using energetic ions to create rings and then detect them. The radius of the rings was typically a few microns. The radius of the core, which is roughly the region from which superfluid is excluded, was about 1.3Å. All of the observations were of rings with one quantum unit of circulation. Richards and Anderson[17] have provided additional convincing evidence for the existence of quantized

free vortices, although it was not clear at what level of circulation or of what configuration. In addition there exists a large body of more indirect evidence supporting the existence of quantized free vortices.[18-20]

C. The Vinen Experiment

Another attempt to verify directly the proposal that the circulation of superfluid helium is quantized was made by W. F. Vinen[21] in an ingenious experiment completed in 1960. Vinen stretched a fine wire down the center of a cylindrical vessel containing liquid helium, and measured circulation around the wire by means of the influence that circulation exerts on the transverse vibrations of the wire. In one method of proceeding, with which we shall be concerned here, Vinen created circulation by rotating the vessel around the axis of the wire while cooling from above T_λ, then made measurements on the circulation which persisted after the rotation of the vessel had been stopped.

The principle of the measurement can be understood by considering the case of a cylindrically symmetric wire with no stiffness. In the absence of circulation such a wire can be regarded as having as its lowest modes of transverse vibration two degenerate circularly polarized modes. With circulation κ around the wire the degeneracy of these modes is removed by the "lift" force, resulting in a splitting $\Delta\omega_\kappa = \frac{\rho_s \kappa}{\mu}$ between the

angular frequencies of the two modes. Here μ is very nearly equal to the mass per unit length of the wire plus that of the fluid displaced. If the two modes are excited simultaneously with equal amplitude, the result is vibration of the wire in a plane which precesses with angular frequency $\frac{\Delta\omega_\kappa}{2}$ in the same sense as the fluid is circulating.

The wire can be set into vibration by passing a current pulse through it in the presence of a steady transverse magnetic field. The free, slowly-damped vibrations which follow can then be observed by means of the oscillatory e.m.f. induced along the wire. The amplitude of the induced e.m.f. depends on the orientation of the plane of vibration in the magnetic field. As the plane of vibration precesses, the induced e.m.f. sweeps out a slowly decaying beat pattern, with beat period $\frac{2\pi}{\Delta\omega_\kappa} = \frac{2\pi\mu}{\rho_s\kappa}$. Thus, for a cylindrically symmetric wire with no stiffness, the circulation around the wire can be determined simply by measuring the beat period once μ and ρ_s are known. If the circulation around the wire is a function $\kappa(z)$ of position along the wire, then the circulation measured this way is the integral

$$\bar{\kappa} = \frac{2}{L}\int_{-L/2}^{L/2} \kappa(z)\cos^2\frac{\pi z}{L}\,dz \qquad (10)$$

where L is the length of the wire. The measured quantity $\bar{\kappa}$ will be called the apparent circulation.

In practice, however, the lowest vibrational normal modes of a wire in the absence of circulation are rarely degenerate, presumably because of some inherent asymmetry in the wire or its mounting. Vinen found that these modes always appear to be plane-polarized, with mutually perpendicular planes of polarization. In such a case the effect of circulation is to produce elliptically polarized modes whose total angular frequency difference, $\Delta\omega$, is given by $(\Delta\omega)^2 \cong (\Delta\omega_o)^2 + (\Delta\omega_\kappa)^2$, where $\Delta\omega_o$ is the angular frequency difference in the absence of circulation. Since the measured beat period is now $\frac{2\pi}{\Delta\omega}$, it is necessary in practice to know $\Delta\omega_o$ as well as μ and ρ_s in order to determine $\overline{\kappa}$. It is helpful that at the beginning of an experimental run $\Delta\omega_o$ can be adjusted to a convenient value by twisting the wire.

Vinen's technique is sensitive enough to measure a single quantum unit of circulation with an accuracy of a few percent. Nevertheless his results were not very conclusive. He did find that circulation persisted in the superfluid for several hours after the vessel stopped rotating, but the measured values were in general not quantized, and varied both from one experimental run to another and during the course of a single run. However, he also found that apparent circulation of one quantum unit was especially stable against repeated vibrations of the wire with very large amplitude. He was led by these observations to suggest that when a fraction of a quantum unit is measured it

indicates that one end of a free vortex line is attached to the wire at some point along its length. $\kappa(z)$ would change at such a point by an amount equal to the circulation of the free vortex line, yielding a value for $\bar{\kappa}$ intermediate to the quantum levels. If the wire should move violently, the end of the line might be expected to move along the wire, resulting in a change in the apparent circulation. Circulation which was uniform along the length of the wire would be stable under this kind of motion. In a more detailed analysis Griffiths[22] was able to show that the configuration proposed by Vinen, of a vortex line attached at one end to the wire and at the other to a wall of the vessel, would be metastable under certain circumstances.

In this manner Vinen's experiment can be interpreted as giving evidence for the quantization of circulation. His results would have been more convincing if they had included observations of stable circulation at higher quantum levels, with $n = 2,3,4$, etc. Because the hypothesis of the quantization of circulation is central to the theory of liquid ^{4}He, and because Vinen's technique provided the most direct way known of testing this hypothesis, it was felt that an attempt should be made to repeat his experiment, and if possible extend it to obtain more conclusive results. With this incentive the work presented in this thesis was undertaken. The work has been partially successful, in that it has provided more accurate and detailed information about the circulation around the wire than Vinen was able

to get. It has given additional evidence in support of the hypothesis of quantization of circulation. In particular, stable circulation was observed at the level of one, two, and three quantum units. It has also been possible to measure the direction of circulation around the wire, whether the liquid flows clockwise or counter-clockwise, as well as its magnitude. However, the results of this work have many features which are still not understood.

II. MOTION OF THE WIRE

A. Forces Exerted by the Liquid on the Vibrating Wire

In order to analyze the influence of liquid helium on a vibrating wire we shall rely on Landau's two-fluid equations for a description of the motion of the liquid. In order to simplify the equations we shall make the plausible assumption that ρ_s, ρ_n, and the entropy per unit mass, s, are constant in time and uniform throughout the liquid. These assumptions are satisfied if the liquid has constant, uniform temperature and density. Then Eq. (3) requires that

$$\text{div } \vec{v}_n = 0, \tag{11}$$

and it follows from Eq. (2) that

$$\text{div } \vec{v}_s = 0. \tag{12}$$

In short we assume that the two fluids are separately incompressible. Of course in practice this assumption is not obeyed exactly. For example, the vibrating wire creates fluctuations in both the temperature and density of the liquid. However, in practice these fluctuations were very weak, and we take (11) and (12) to be valid approximations to the real fluid. In that case the problem of finding the forces exerted by the liquid on the vibrating wire separates into two independent problems, each of which can be solved within the framework of classical fluid dynamics.

In order to show that this separation is possible we first put Eq. (4) into a different form. For simplicity we use Cartesian coordinates. In these coordinates we have curl curl = grad div $- \nabla^2$, and because of Eq. (11), (4) reduces to

$$\rho_s \frac{D_s \vec{v}_s}{D_s t} + \rho_n \frac{D_n \vec{v}_n}{D_n t} = - \text{grad } P + \eta_n \nabla^2 \vec{v}_n \ . \tag{13}$$

The derivative $D_s \vec{v}_s / D_s t$ can be expanded in the form

$$\frac{D_s \vec{v}_s}{D_s t} = \frac{\partial \vec{v}_s}{\partial t} + \text{grad } \frac{v_s^2}{2} - \vec{v}_s \times \text{curl } \vec{v}_s , \tag{14}$$

and since we postulate that curl $\vec{v}_s = 0$, the derivative reduces to

$$\frac{D_s \vec{v}_s}{D_s t} = \frac{\partial \vec{v}_s}{\partial t} + \text{grad } \frac{v_s^2}{2} \ . \tag{15}$$

Furthermore, since $\vec{v}_s$ has zero curl it can be derived from a velocity potential ϕ_s, so that

$$\vec{v}_s = \text{grad } \phi_s \ . \tag{16}$$

Then the derivative (15) is

$$\frac{D_s \vec{v}_s}{D_s t} = \text{grad} \left(\frac{\partial \phi_s}{\partial t} + \frac{v_s^2}{2} \right) \ . \tag{17}$$

With this simplification (13) becomes

$$\rho_n \frac{D_n \vec{v}_n}{D_n t} = - \text{grad} \left(P + \rho_s \frac{\partial \phi_s}{\partial t} + \rho_s \frac{v_s^2}{2} \right) + \eta_n \nabla^2 \vec{v}_n \ . \tag{18}$$

Now we expand the derivative $D_n \vec{v}_n / D_n t$ in the same form as (14) and take the curl of Eq. (18). The result can be expressed in Cartesian coordinates as

$$\frac{D_n}{D_n t}(\text{curl}\ \vec{v}_n) = (\text{curl}\ \vec{v}_n \cdot \text{grad})\vec{v}_n + \nu_n \nabla^2\ \text{curl}\ \vec{v}_n . \quad (19)$$

Here ν_n is the kinematic viscosity of the normal fluid, given by

$$\nu_n = \eta_n/\rho_n . \quad (20)$$

Equation (19) is the vorticity equation for the normal fluid. Together with (11) it completely specifies the normal fluid velocity field for a given complete set of boundary conditions. Furthermore, Eqs. (11) and (19) are identical to the classical continuity and vorticity equations for flow of an incompressible viscous liquid. Therefore we may determine $\vec{v}_n$ uniquely by solving a problem in classical fluid dynamics.

The superfluid velocity field is determined for a given complete set of boundary conditions by Eqs. (5) and (12), which are the usual requirements for irrotational flow of an incompressible liquid. Taken together they require that the velocity potential ϕ_s satisfy Laplace's equation

$$\nabla^2\phi_s = 0 . \quad (21)$$

Then $\vec{v}_s$ is given by (16), so that $\vec{v}_s$ is also determined by solving a problem in classical fluid dynamics.

With $\vec{v}_n$ known Eq. (18) determines the quantity $P+\rho_s\frac{\partial\phi_s}{\partial t} + \rho_s\frac{v_s^2}{2}$ throughout the liquid, to within an additive function of time only. In fact (18) is identical to the Navier-Stokes equation provided that this quantity takes the place of the classical

pressure. We can think of $P+\rho_s \frac{\partial \phi_s}{\partial t} + \rho_s \frac{v_s^2}{2}$ as a fictitious pressure due to flow of the normal fluid component, which we call P_n.

With $\vec{v}_s$ known we may define a fictitious pressure P_s to within an additive function of time only by the relation

$$P_s = - \rho_s \frac{\partial \phi_s}{\partial t} - \rho_s \frac{v_s^2}{2} , \qquad (22)$$

which is the classical formula for the pressure due to irrotational flow of an incompressible fluid. For convenience we shall refer to P_s as the pressure due to flow of the superfluid component.

With both P_n and P_s determined the real pressure P is given by

$$P = P_n + P_s + P_o(t), \qquad (23)$$

where $P_o(t)$ is a function of time only. The total normal force exerted by the liquid on the vibrating wire can then be found by integrating each term in (23) separately over the surface of the wire and adding the results. Since $P_o(t)$ is uniform in space its integral is zero. In addition, there is a tangential force per unit area on the wire due to the viscosity of the normal fluid which is assumed to have the classical form. Therefore the total force exerted by the liquid on the vibrating wire can be calculated as if it were the sum of forces exerted by the superfluid and normal fluid components acting independently, where these forces are calculated just as they are in the corresponding classical problems.

B. Forces Due to Motion of the Normal Fluid

We consider first the forces on the wire due to motion of the normal fluid. We want to find solutions to Eqs. (11) and (19) which satisfy certain boundary conditions. We assume that the motion of the normal fluid is caused just by motion of the vibrating wire. The cylindrical vessel containing the liquid helium is at rest, and any motion of the normal fluid due to rotation of the vessel has vanished. Then the correct boundary conditions are that the fluid is at rest at the wall of the vessel, and that its velocity is equal to the velocity of the vibrating wire at the surface of the wire. Of course the velocity of the wire varies with distance along the length of the wire.

The exact solution to this problem is not known, but certain plausible approximations can be made which make it tractable. The first of these is that Eqs. (11) and (19) can be solved for each segment of the wire independently, treating each segment as an oscillating cylinder in two dimensions, where the velocity of the cylinder is equal to the velocity of the segment. This means that we assume that the force which the fluid exerts on each small segment of the wire depends on the motion of just that segment. In two dimensions the first term on the right hand side of Eq. (19) vanishes identically. The equation reduces to

$$\frac{D_n}{D_n t} (\text{curl } \vec{v}_n) = \nu_n \nabla^2 \text{ curl } \vec{v}_n \tag{24}$$

which can be written

$$\frac{\partial}{\partial t} (\text{curl } \vec{v}_n) = - (\vec{v}_n \cdot \text{grad}) \text{ curl } \vec{v}_n + \nu_n \nabla^2 \text{ curl } \vec{v}_n . \tag{25}$$

The left hand side of this equation is the rate of change of vorticity in a differential volume element fixed in space. The first term on the right hand side is the negative of the rate at which vorticity enters or leaves the volume element by convection. The second term on the right hand side is the rate of change of vorticity in the element due to diffusion.

We want to determine conditions under which the rate of change of vorticity due to diffusion is large compared to the rate of change due to convection. Since vorticity originates with motion of the wire the total rate of change of vorticity, which is the left hand member of (25), must be of order ω curl $\vec{v}_n$ or larger, where ω is the angular frequency of vibration of the wire. Vorticity diffuses outwards from the surface of the wire with a characteristic decay length δ called the penetration depth, so that the diffusion term in (25) is of order $\frac{\nu_n}{\delta^2}$ curl $\vec{v}_n$. The convection term is of order $\frac{u_o}{\delta}$ curl $\vec{v}_n$ or smaller, where u_o is the velocity amplitude of the wire. Diffusion will predominate over convection provided that $\frac{u_o}{\delta} \ll \omega$. If this condition is satisfied it must be true that $\frac{\nu_n}{\delta^2} \cong \omega$, so that $\delta \cong (\frac{\nu_n}{\omega})^{\frac{1}{2}}$. Since $u_o = \omega r_o$, where r_o is the displacement amplitude of the wire, the inequality is satisfied if

$r_o \ll \delta$. We see therefore that the convection term in Eq. (25) can be neglected provided that the displacement amplitude of the wire is small compared with the penetration depth.

In the present experiment r_o/δ was typically about 30% at 1.2^oK, and 10% at 1.6^oK. Although one could wish for stronger justification, nevertheless we make the assumption that r_o/δ is small enough so that the convection term in (25) can be discarded. The approximation is necessary in order to reduce (25) to a linear equation. It is interesting to note that measured values of the damping of the wire due to the normal fluid agreed with calculated values in all cases to within a few percent. It will become apparent that the normal fluid had very little effect on the measured values of circulation.

With the convection term discarded (25) becomes

$$\frac{\partial}{\partial t} (\text{curl } \vec{v}_n) = \nu_n \nabla^2 \text{ curl } \vec{v}_n \qquad (26)$$

which is the usual diffusion equation. For example, the same equation describes heat conduction; here it describes the diffusion of vorticity through the normal fluid. Vorticity is created at the surface of the wire by the shear force which exists by virtue of the fluid viscosity. Motion of the wire sets up velocity gradients in the fluid in directions perpendicular to the velocity. Vorticity diffuses outwards from the surface of the wire, passing through a decay length δ in a time ω^{-1}.

We have seen that the decay length must be of order $\delta \cong (\frac{\nu_n}{\omega})^{\frac{1}{2}}$. An exact solution to (26) given below shows that the correct decay length is $\delta = (\frac{2\nu_n}{\omega})^{\frac{1}{2}}$.

Equations (11) and (26) in two dimensions have been solved by Segel[23] for flow between two circular cylinders when the outer cylinder is fixed and the inner cylinder vibrates about a slightly eccentric axis. The same equations were solved by Stokes[24,25] in 1851 for vibration of a circular cylinder in an unbounded fluid, assuming that the fluid is at rest at infinity. The solution in this case is much more accessible than for the bounded fluid and has been used in the analysis of this experiment. This is a valid approximation under the conditions of this experiment because corrections to Stokes' solution due to the outer boundary are of order α^2 or less, where α is the ratio of the radius of the inner cylinder to the radius of the outer cylinder. For this experiment α^2 ranged from 10^{-4} to 10^{-3}.

Stokes' solution for the force per unit length on a circular cylinder of radius a vibrating with small amplitude in an unbounded fluid can be expressed as

$$\frac{\vec{F}_n}{L} = - \mu_n K \frac{d\vec{u}}{dt} - \mu_n \omega K' \vec{u} \qquad (27)$$

where

$$K = 1 - \frac{4}{\beta} \operatorname{Im} \frac{\sqrt{i}\, H_1^{(1)}(\sqrt{i}\,\beta)}{H_o^{(1)}(\sqrt{i}\,\beta)} \qquad (28)$$

$$K' = \frac{4}{\beta} \operatorname{Re} \frac{\sqrt{i}\, H_1^{(1)}(\sqrt{i}\,\beta)}{H_o^{(1)}(\sqrt{i}\,\beta)} \quad . \tag{29}$$

Here $\vec{u}$ is the velocity of the cylinder, given by $\vec{u} = \operatorname{Re} \vec{u}_o e^{-i\omega t}$; μ_n is the mass of normal fluid displaced by a unit length of the cylinder, given by $\mu_n = \pi a^2 \rho_n$; and β is given by $\beta = a(\frac{\omega}{\nu_n})^{\frac{1}{2}} = \sqrt{2}\,\frac{a}{\delta}$. H_1 and H_o are Hankel functions, or Bessel functions of the third kind.[26] $\sqrt{i}\, H_1^{(1)}(\sqrt{i}\,\beta)$ and $H_o^{(1)}(\sqrt{i}\,\beta)$ are tabulated as functions of β in Jahnke and Emde, Tables of Functions.[27]

The functions K and K' are plotted against β in Figure 2 for a useful range of β. Numerical values of K and K' were taken from a table furnished by Stokes. It is apparent that K and K' are both positive, and that $K > 1$. As $\beta \to 0$, $K \to \infty$ and $K' \to \infty$. As $\beta \to \infty$, $K \to 1$ and $K' \to 0$. For $\beta \gtrsim 1$, K and K' can be approximated to 5% or better by the first two terms in their respective series expansions.

$$K \cong 1 + 2\frac{\sqrt{2}}{\beta} = 1 + 2\frac{\delta}{a} \tag{30}$$

$$K' \cong 2\frac{\sqrt{2}}{\beta} + \frac{2}{\beta^2} = 2\frac{\delta}{a} + \left(\frac{\delta}{a}\right)^2 \tag{31}$$

Equation (27) shows that the force per unit length on the cylinder is the sum of two forces, one of them proportional to the acceleration, the other to the velocity. The first force, proportional to the acceleration but opposite in direction, is the reaction to the force which the cylinder must exert in order to accelerate the fluid. Its effect is just to add to the inertia with which the cylinder responds to other forces

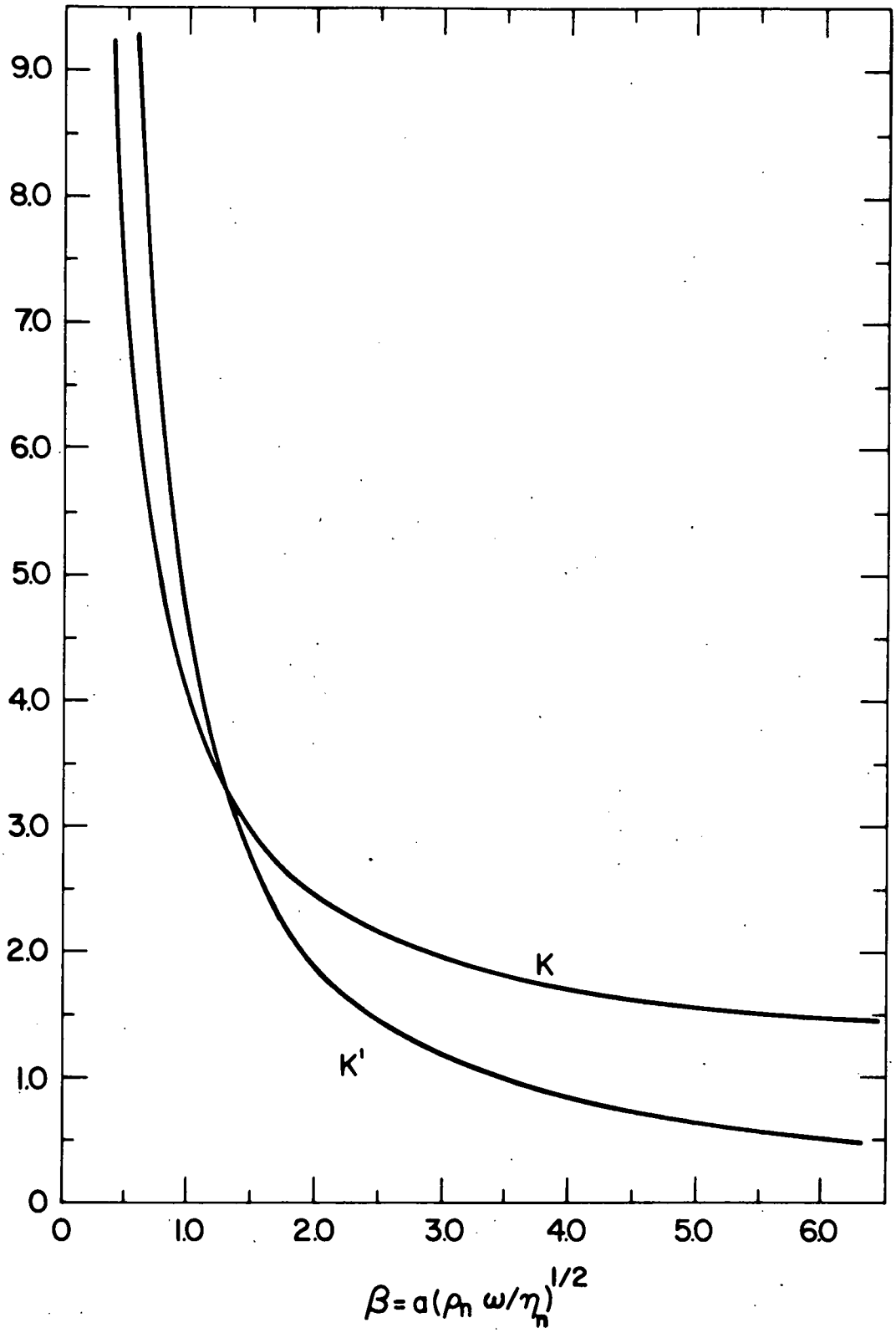

Figure 2. K and K' as Functions of β.

which may be acting on it. The inertial force can be incorporated into the equation of motion for the cylinder just by adding $\mu_n K$ to the cylinder's mass per unit length. $\mu_n K$ is then called the hydrodynamic or virtual mass per unit length of the wire. For a non-viscous fluid $\beta = \infty$ and $K = 1$. For a viscous fluid the inertial force is enhanced because the wire accelerates fluid by viscous drag as well as by pressure forces. In fact it is easy to see by substituting (30) into (27) that in the first approximation the hydrodynamic mass per unit length is enhanced by an amount $\rho_n 2\pi a\delta$, which if δ is small is just the mass per unit length of fluid contained in a cylindrical shell of radius a and thickness δ.

The second term on the right hand side of (27), which is proportional to the velocity but opposite in direction, is a dissipative force. It is the damping force per unit length on the cylinder. In a non-viscous liquid $K' = 0$ and there is no damping. It is easy to show by substituting the first term of the series expansion for K' into (27) that in the first approximation the damping force per unit length is $- 2\pi a\rho_n \delta\omega \vec{u} = - 2\pi a(2\rho_n \eta\omega)^{\frac{1}{2}} \vec{u}$.

When instead of allowing the fluid to extend to infinity it is assumed bounded by a fixed outer cylinder, the force per unit length on the inner cylinder is still given to first order in β by (27), when $\beta \geq 1$, but K and K' are different. If the new

functions are $\tilde{K}$ and $\tilde{K}'$, the first terms in their series expansions are[28]

$$\tilde{K} \cong (1 - \alpha^2)^{-1} (1 + \alpha^2 + 2\sqrt{\frac{2}{\beta}}) \tag{32}$$

$$\tilde{K}' \cong (1 - \alpha^2)^{-1} 2\sqrt{\frac{2}{\beta}} . \tag{33}$$

It is apparent that since α^2 ranged from 10^{-4} to 10^{-3} the outer cylinder had no discernible effect on the force on the wire due to normal fluid.

At a temperature of 1.2°K, where most of the measurements were made in this experiment, the kinematic viscosity ν_n of the normal fluid component of liquid helium is 4.2×10^{-3} cm^2/sec. The angular frequency of vibration of the wire was typically $10^3\pi$ radians/sec, so that at 1.2°K the penetration depth was typically 20 μ. The wires used varied in radius from 13 μ to 50 μ, so the expansion parameter β ranged from 1 to 4. It is interesting to note that if the Reynolds number for flow around a vibrating cylinder is $R = u_o a/\nu_n = \omega r_o a/\nu_n$, then $R = \beta^2 r_o/a$. In this experiment r_o/a ranged from 40% for the thinnest wires to 8% for the thickest, so that at 1.2°K the Reynolds number varied from 0.4 to 1.3. Measurements were also made at 1.6°K using the thicker wires. At that temperature the kinematic viscosity ν_n is 5.6×10^{-2} cm^2/sec, so that penetration depth was typically 60 μ, β was about 1, and R was about 0.1. Of course these considerations apply only to the normal fluid.

If r_o is the maximum displacement of the vibrating wire then its maximum velocity and acceleration are ωr_o and $\omega^2 r_o$ respectively. Representative values of these three quantities were 5 μ, 1.5 cm/sec, and 5×10^3 cm/sec^2. Useful parameters are tabulated for several experimental runs in Tables 1a-d.

The analysis given above for the forces exerted by the normal fluid assumes that the wire has a circular cross-section. In practice the wires used were slightly asymmetric. Solutions for the force on a cylinder of elliptical cross-section vibrating in an unbounded viscous fluid have been obtained by Kanwal,[29] when the vibration is along either the major or minor axis of the ellipse. The solutions have the same form as (27), being the sum of an inertial force, proportional to acceleration, and a drag force, proportional to velocity. However the coefficients of each term now contain infinite series of Bessel functions. In the simplest case, when the fluid viscosity is zero, the drag force is also zero and the inertial force is $-\pi b^2 \rho_n \frac{d\vec{u}}{dt}$, where b is half the length of the minor axis if the motion is along the major axis.[30] In practice, errors in the damping and virtual mass of the wire due to asymmetry were not significant to the experiment. Fortunately the lift force exerted by the superfluid, which is the critical effect for measuring circulation, is independent of the shape and size of the cross-section of the wire.

C. Forces Due to Motion of the Superfluid

We consider next the forces on the vibrating wire due to motion of the superfluid. We want to find solutions to Eq. (21) satisfying the condition that at the boundary the normal gradient of ϕ_s equals the normal velocity of the boundary. Then $\vec{v}_s$ will be determined by (16), and the forces can be found by integrating (22) over the surface of the wire.

There are two features to Eq. (21) which make this problem much simpler than the problem of the normal fluid. They are that in contrast to (19) Eq. (21) is linear and makes no reference to time. The first feature means that solutions to (21) can be formed by superposition. The second means that the velocity field $\vec{v}_s$ responds instantaneously to an arbitrary motion of the boundaries: $\vec{v}_s$ assumes just that configuration which it would have if the boundaries were moving at a steady rate with their contemporary instantaneous velocity.

Of course in real liquids a disturbance in the fluid velocity can not propagate faster than the speed of sound in the liquid. This means that Eq. (21) will apply to the present experiment only if the maximum velocity amplitude of the vibrating wire is small compared with the speed of sound in liquid helium. In practice this ratio was of order 10^{-4}.

We suppose for the superfluid that in addition to the flow produced by motion of the wire there is an independent

circulation around it. This is the flow expected of the superfluid component after liquid helium has been cooled in rotation from above T_λ, provided that circulation of the superfluid persists after the rotation of the apparatus has been stopped. Again we treat each segment of the wire independently, as an oscillating cylinder in two dimensions. We assume that the forces exerted by the fluid on each segment of the wire depend on the motion of just that segment.

Equation (21) in two dimensions has been solved by Lamb for flow produced by a circular cylinder with circulation around it moving arbitrarily in an unbounded fluid.[31] The result for the force per unit length on the cylinder is

$$\frac{\vec{F}_s}{L} = -\mu_s \frac{d\vec{u}}{dt} + \rho_s \vec{\kappa} \times \vec{u} \,. \tag{34}$$

Here $\vec{u}$ is the velocity of the wire, which is arbitrary; μ_s is the mass of superfluid displaced by a unit length of the cylinder, given by $\mu_s = \pi a^2 \rho_s$; and $\vec{\kappa}$ is the circulation of the superfluid around the cylinder. The circulation strength is given by the line integral of the fluid velocity on any contour enclosing the cylinder.

$$\kappa = \oint_{cyl} \vec{v}_s \cdot d\vec{\ell} \tag{35}$$

The positive direction of the vector $\vec{\kappa}$ is given by the same right hand rule which relates the magnetic induction around a wire to the electric current.

The first term in Eq. (34), proportional to the acceleration, is the same as the inertial force encountered in the discussion of the normal fluid in the zero-viscosity limit. The hydrodynamic mass of the cylinder in superfluid is just the mass of the fluid actually displaced by the cylinder, provided that the cylinder has a circular cross-section. The second term in (34), proportional to the velocity, is the Magnus force, frequently called the lift force. Its direction is transverse to the motion of the wire. It is the force which makes a baseball curve and keeps airplanes aloft. In the case of the vibrating wire the lift force is a consequence of the pressure difference on opposite sides of the wire which results from the superposition of symmetric flow around the wire and uniform flow past it. The force is independent of the size of the wire, and as Lamb shows in a more general calculation,[32] it is independent of the shape of the wire's cross-section.

When instead of allowing the superfluid to extend to infinity it is assumed bounded by a fixed outer cylinder, the force per unit length on each segment of the wire when the wire coincides with the axis of the outer cylinder is

$$\frac{\vec{F}_s}{L} \simeq (1 - \alpha^2) \left[- (1 + \alpha^2) \mu_s \frac{d\vec{u}}{dt} + \rho_s \vec{\kappa} \times \vec{u} \right] \qquad (36)$$

where again α is the ratio of the radius of the wire to the radius of the outer cylinder. Since α^2 was of order 10^{-4} to 10^{-3} the outer cylinder had no discernible effect on the wire.

D. Motion of the Wire

We have found solutions to the classical problems corresponding to motion of the normal fluid and superfluid respectively. Then within the approximations used the force per unit length exerted on the vibrating wire by the fluid as a whole is given by the sum of Eqs. (27) and (34).

$$\frac{\vec{F}}{L} \cong - (\mu_s + K \mu_n) \frac{d\vec{u}}{dt} - \mu_n \omega K' \vec{u} + \rho_s \vec{\kappa} \times \vec{u} \qquad (37)$$

The first term on the right hand side of (37) is the inertial reaction to acceleration of the wire. The hydrodynamic or virtual mass of the wire is $\mu_s + K \mu_n$. The second term is a dissipative force, proportional to the velocity of the wire; and the third term is the Magnus force, perpendicular to the velocity of the wire.

In addition to the forces exerted on the wire by the fluid there are forces due to stiffness and tension in the wire itself.[33] We proceed to examine the motion of the wire under the influence of these forces. There are two equations of motion, corresponding to the two degrees of freedom for the wire. In the absence of circulation the equations should reduce to two independent equations in one dimension, consistent with the observation made during the experiment that in the absence of circulation the normal modes of the wire are nearly always plane-polarized, with mutually perpendicular planes of polarization. We choose the z axis to be parallel to the wire, and the x-z and y-z planes

to be the planes of polarization, which are determined by the physical characteristics of the wire. The equations of motion are

$$\mu_x \frac{\partial^2 x}{\partial t^2} = T \frac{\partial^2 x}{\partial z^2} - S_x \frac{\partial^4 x}{\partial z^4} - 2\mu_x \lambda_x \frac{\partial x}{\partial t} - \rho_s \varkappa \frac{\partial y}{\partial t} \qquad (38a)$$

$$\mu_y \frac{\partial^2 y}{\partial t^2} = T \frac{\partial^2 y}{\partial z^2} - S_y \frac{\partial^4 y}{\partial z^4} - 2\mu_y \lambda_y \frac{\partial y}{\partial t} + \rho_s \varkappa \frac{\partial x}{\partial t} . \qquad (38b)$$

Here μ is the mass per unit length of the wire plus $(\mu_s + K\mu_n)$. T is the tension in the wire. S is the stiffness constant given by

$$S = YAR^2, \qquad (39)$$

where Y is Young's modulus, A is the cross-sectional area of the wire, and R is the radius of gyration of a cross-section about an axis through its centroid and in the plane of the cross-section, perpendicular to the plane of polarization. For a circular cross-section R = a/2, where a is the radius of the wire. The damping is caused by the normal fluid, so that the damping constant λ is a function of frequency. For a wire of circular cross-section λ is given by

$$\lambda = \mu_n \frac{\omega K'}{2\mu} . \qquad (40)$$

In general the coefficients μ, S, and λ are different for the two different sets of normal modes. For example, we might suppose that the wire has an elliptical cross-section, and that the planes of polarization are given by the major and minor axes

of the ellipse. Obviously the wire will have different radii of gyration about its major and minor axes and different virtual masses for motion along these axes. Of course for a cylindrically symmetric wire when there is no circulation Eqs. (38a) and (38b) are identical, and the two sets of normal modes are degenerate.

We shall assume that μ, T, S, and λ for both sets of plane-polarized modes are uniform along the length of the wire, but that the circulation around the wire may vary with z. $\varkappa(z)$ will change at points where a free vortex line terminates on the wire, by an amount equal to the circulation of the free vortex. We ignore the slight additional force exerted on the wire by an attached free vortex line which exists because of tension in the line. This force is smaller than the lift force on the wire by a factor of about 10^{-4}. An attached free vortex line also distorts the velocity field $\vec{v}_s$ from the two-dimensional flow we have assumed. We also ignore this effect.

E. Motion of the Wire with Zero Circulation

When $\varkappa = 0$ for all z, Eqs. (38a) and (38b) have solutions of the form

$$x_o(z,t) = \text{Re } f_o(z)\, e^{i\eta_o^x t} \qquad (41a)$$

$$y_o(z,t) = \text{Re } g_o(z)\, e^{i\eta_o^y t} \,. \qquad (41b)$$

The boundary conditions on the wire are that the displacement and slope of the wire must be zero at each end. Since the

boundary conditions are symmetric we choose the origin of the z axis at the midpoint of the wire. The normal modes (41) will then be either even or odd functions of z. In either case if the boundary conditions are satisfied at one end of the wire they will be satisfied at the other end. Then the boundary conditions can be written

$$f_o(z)\Big|_{L/2} = 0 \ , \ f_o'(z)\Big|_{L/2} = 0; \tag{42a}$$

$$g_o(z)\Big|_{L/2} = 0 \ , \ g_o'(z)\Big|_{L/2} = 0 \ . \tag{42b}$$

L is the length of the wire.

We shall examine one set of plane-polarized normal modes in detail, set (41a).[34] The complex frequency η_o^x has the form

$$\eta_o^x = \sqrt{\omega_o^{x\,2} - \lambda_x^2} + i\,\lambda_x . \tag{43}$$

The even modes have

$$f_o(z) = A \cos \frac{m_1 \pi z}{L} + B \cosh \frac{m_2 \pi z}{L} \tag{44}$$

and the odd modes have

$$f_o(z) = C \sin \frac{m_1 \pi z}{L} + D \sinh \frac{m_2 \pi z}{L} . \tag{45}$$

Because of the linearity of Eq. (38a) the sinusoidal and hyperbolic sinusoidal solutions must separately satisfy (38a). It follows that

$$\left(\frac{m_1 \pi}{L}\right)^2 = \sqrt{\left(\frac{T}{2S_x}\right)^2 + \frac{\omega_o^{x\,2}\,\mu_x}{S_x}} - \frac{T}{2S_x} \tag{46}$$

$$\left(\frac{m_2\pi}{L}\right)^2 = \sqrt{\left(\frac{T}{2S_x}\right)^2 + \frac{\omega_o^{x^2}\mu_x}{S_x}} + \frac{T}{2S_x} \tag{47}$$

$$\omega_o^x = \frac{m_1\pi}{L}\sqrt{\frac{T}{\mu_x}\left(1 + \frac{m_1\pi}{L}\frac{S_x}{T}\right)} \quad . \tag{48}$$

The boundary conditions (42a) require that for the even modes

$$m_1 \tan\frac{m_1\pi}{2} + m_2 \tanh\frac{m_2\pi}{2} = 0 \tag{49}$$

and for the odd modes that

$$\frac{1}{m_1}\tan\frac{m_1\pi}{2} - \frac{1}{m_2}\tanh\frac{m_2\pi}{2} = 0. \tag{50}$$

Then by substitution from (47) it follows for the even modes that

$$\tan\frac{m_1\pi}{2} = -\sqrt{1 + \left(\frac{L}{m_1\pi}\right)^2\frac{T}{S_x}}\,\tanh\left(\frac{m_1\pi}{2}\sqrt{1 + \left(\frac{L}{m_1\pi}\right)^2\frac{T}{S_x}}\right) \tag{51}$$

and for the odd modes that

$$\sqrt{1 + \left(\frac{L}{m_1\pi}\right)^2\frac{T}{S_x}}\,\tan\frac{m_1\pi}{2} = \tanh\left(\frac{m_1\pi}{2}\sqrt{1 + \left(\frac{L}{m_1\pi}\right)^2\frac{T}{S_x}}\right). \tag{52}$$

Equations (51) and (52) can be solved for the allowed values of m_1. Then the allowed values of m_2 and ω_o^x are determined by (47) and (48).

In general (51) and (52) must be solved numerically. However, if S_x/L^2T is small, so that the tension provides a much more important restoring force than the stiffness, m_1 can be found approximately by expanding both sides of (51) and (52) and retaining only the leading terms. For both (51) and (52) the

first three terms give

$$m_1 \cong n\left[1 + \frac{2}{L}\sqrt{\frac{S_x}{T}} + \left(1 + \frac{n^2\pi^2}{8}\right)\left(\frac{2}{L}\right)^2 \frac{S_x}{T}\right] \qquad (53)$$

where n = 1,3,5,...for the even modes, and n = 2,4,6,... for the odd modes. This approximation is valid only for low modes, when $n^2 < L^2T/\pi^2S_x$. We shall see in Chapter IV that in fact only the low modes were important in this experiment. To the same approximation the allowed values of ω_o^x are

$$\omega_o^x \cong \frac{n\pi}{L}\sqrt{\frac{T}{\mu_x}}\left[1 + \frac{2}{L}\sqrt{\frac{S_x}{T}} + \left(1 + \frac{n^2\pi^2}{8}\right)\left(\frac{2}{L}\right)^2 \frac{S_x}{T}\right] \qquad (54)$$

The expansion parameter for these series is $\frac{2}{L}\sqrt{\frac{S_x}{T}}$. It is apparent that when this parameter is zero m_1 is an integer and (54) reduces to the familiar expression for the allowed angular frequencies on a flexible string of length L, fixed at each end, when there is no damping. Then the normalized even modes are $\sqrt{\frac{2}{L}}\cos\frac{n\pi z}{L}$, n = 1,3,5,... , and the normalized odd modes are $\sqrt{\frac{2}{L}}\sin\frac{n\pi z}{L}$, n = 2,4,6,... .

It is interesting that in the next approximation, when terms of order 1 and $\frac{2}{L}\sqrt{\frac{S_x}{T}}$ are retained and higher order terms are discarded, the wire behaves in its low modes just like a flexible string of length $L - 2\sqrt{\frac{S_x}{T}}$. We set $L^* = L - 2\sqrt{\frac{S_x}{T}}$. In this approximation the allowed values of ω_o^x are

$$\omega_o^x \cong \frac{n\pi}{L^*}\sqrt{\frac{T}{\mu_x}} \quad . \qquad (55)$$

The normalized even modes are

$$f_o(z) \cong \sqrt{\frac{2}{L^*}} \cos \frac{n\pi z}{L^*} \quad , \quad n = 1,3,5,... \tag{56}$$

and the normalized odd modes are

$$f_o(z) \cong \sqrt{\frac{2}{L^*}} \sin \frac{n\pi z}{L^*} \quad , \quad n = 2,4,6,... \quad . \tag{57}$$

The stiffness in the wire and the boundary condition that the slope of the wire be zero at each end effectively shorten the wire, so that in its low modes it vibrates flexibly over a length L*. In practice the stiffer wires used in this experiment were effectively shortened by about 10%. Corrections of higher order in $\frac{2}{L}\sqrt{\frac{S_x}{T}}$ were then about 1%.

The actual angular frequency of the normal modes is given by Re $\eta_o^x = \sqrt{\omega_o^{x\,2} - \lambda_x^2}$; it is a function of the decay constant λ_x. Furthermore λ_x depends on the frequency. If the effect of damping is small enough it is possible to determine Re η_o^x by a perturbation approximation. We evaluate λ_x at Re $\eta_o^x \cong \omega_o^x$, then use this value of λ_x to determine a corrected value for Re η_o^x. In fact however the damping was so small in this experiment that even this first correction was of order 10^{-6}, whereas the fractional shift in frequency caused by circulation was typically of order 10^{-3}. Therefore in practice the effect of damping on the frequency could be ignored altogether. The important effect of the damping was to make the normal modes decay exponentially with time constant $1/\lambda_x$.

We have seen that corresponding to each positive integer n there is a pair of normal modes x_n, y_n given by

$$x_{no}(z,t) = \text{Re } f_{no}(z)\, e^{i\eta^x_{no} t} \tag{58a}$$

$$y_{no}(z,t) = \text{Re } g_{no}(z)\, e^{i\eta^y_{no} t} \tag{58b}$$

where for example $f_{no}(z)$ is given by (44) and (45) when m_1 and m_2 have their $n^{\underline{th}}$ allowed values. These functions are just the $n^{\underline{th}}$ pair of the whole set of functions represented in Eqs. (41). The complex frequency η^x_{no} is equal to $\sqrt{\omega^{x\,2}_{no} - \lambda^2_{nx}} + i\,\lambda_{nx}$, where ω^x_{no} is given by (48) when m_1 has its $n^{\underline{th}}$ allowed value, and λ_{nx} is a function of ω^x_{no}. The functions $f_{no}(z)$ when normalized constitute a complete orthonormal set of functions. Any function which satisfies the boundary conditions (42a) and has continuous first and second and piecewise continuous third and fourth derivatives may be expanded in terms of these functions in an absolutely and uniformly convergent series.[35] It is apparent that in the case of a cylindrically symmetric wire $f_{no}(z) = g_{no}(z)$ for all n.

It should be pointed out that although we have assumed that the boundary conditions (42) are the same for motion in both the x-z and y-z planes, in practice they may be slightly different. For example, it is conceivable that the supports which hold the wire at each end are slightly flexible for motion in one plane but rigid for motion in the other. We shall not

consider such an asymmetry formally. Its principal effect would be to contribute to a frequency difference $\omega_o^x - \omega_o^y$.

F. Motion of the Wire with Non-Zero Circulation

When circulation exists around the wire the equations of motion (38a) and (38b) are coupled by the Magnus force. In order to look for normal modes of the new system we assume that Eqs. (38a) and (38b) with circulation present have solutions of the form

$$x_m(z,t) = \text{Re } f_m(z)\, e^{i\eta_m t} \tag{59a}$$

$$y_m(z,t) = \text{Re } g_m(z)\, e^{i\eta_m t} \tag{59b}$$

where $f_m(z)$ and $g_m(z)$ can be expanded in terms of the normal modes of the system without circulation.

$$f_m(z) = \sum_{n=1}^{\infty} \alpha_{mn}\, f_{no}(z) \tag{60a}$$

$$g_m(z) = \sum_{n=1}^{\infty} \beta_{mn}\, g_{no}(z) \,. \tag{60b}$$

The coefficients α_{mn}, β_{mn} are complex. When x_m and y_m are substituted into Eqs. (38a) and (38b) respectively the following algebraic equations result.

$$\sum_{n=1}^{\infty} \left\{ \alpha_{mn}\mu_x \left[2i\lambda_{mx}(\eta_m - \eta_{no}^x) - (\eta_m^2 - \eta_{no}^{x\,2}) \right] f_{no} + \beta_{mn} i\eta_m \rho_s \varkappa(z) g_{no} \right\} = 0 \tag{61a}$$

$$\sum_{n=1}^{\infty}\left\{\beta_{mn}\mu_y\left[2i\lambda_{my}(\eta_m-\eta_{no}^y) - (\eta_m^2-\eta_{mo}^{y^2})\right]g_{no} - \alpha_{mn}i\eta_m\rho_s\varkappa(z)f_{no}\right\} = 0. \tag{61b}$$

We then multiply (61a) and (61b) by $f_{mo}(z)$ and $g_{mo}(z)$ respectively and integrate both equations over z, using the fact that

$$\int_{-L/2}^{L/2} f_{mo}(z)\, f_{no}(z)\, dz = \delta_{mn} \tag{62a}$$

$$\int_{-L/2}^{L/2} g_{mo}(z)\, g_{no}(z)\, dz = \delta_{mn}\,. \tag{62b}$$

The result is

$$\alpha_{mm}\mu_x\left[2i\lambda_{mx}(\eta_m-\eta_{mo}^x) - (\eta_m^2-\eta_{mo}^{x^2})\right] + \sum_{n=1}^{\infty}\beta_{mn}i\eta_m\rho_s\int\varkappa(z)f_{mo}g_{no}dz = 0 \tag{63a}$$

$$\beta_{mm}\mu_y\left[2i\lambda_{my}(\eta_m-\eta_{mo}^y) - (\eta_m^2-\eta_{mo}^{y^2})\right] - \sum_{n=1}^{\infty}\alpha_{mn}i\eta_m\rho_s\int\varkappa(z)g_{mo}f_{no}dz = 0. \tag{63b}$$

If the wire is symmetric and $\varkappa(z)$ is uniform over the length of the wire then all the integrals in the summations in Eqs. (63) vanish except those for which n=m. Then Eqs. (63) determine α_{mm}/β_{mm}, and it is possible to form the $m^{\underline{th}}$ normal mode of the new system just by a superposition of the $m^{\underline{th}}$ pair of plane-polarized modes of the old system. The new normal modes are circularly polarized and have slightly different sets of frequencies than the old modes. We shall assume in the more general case, when the wire is not symmetric and circulation is not uniform along the wire, that the contribution of other pairs

than f_{no}, g_{no} to the $m^{\underline{th}}$ normal mode of the new system is still negligible. That is we assume in the expansions (60) that

$$|\alpha_{mn}|_{n\neq m} \ll |\alpha_{mm}| \tag{64a}$$

$$|\beta_{mn}|_{n\neq m} \ll |\beta_{mm}| \tag{64b}$$

Then Eqs. (63) reduce to

$$\alpha_{mm}\mu_x\left[2i\lambda_{mx}(\eta_m-\eta_{mo}^x) - (\eta_m^2-\eta_{mo}^{x^2})\right] + \beta_{mm}i\eta_m\rho_s\bar{\kappa}_m = 0 \tag{65a}$$

$$\beta_{mm}\mu_y\left[2i\lambda_{my}(\eta_m-\eta_{mo}^y) - (\eta_m^2-\eta_{mo}^{y^2})\right] - \alpha_{mm}i\eta_m\rho_s\bar{\kappa}_m = 0 \tag{65b}$$

where

$$\bar{\kappa}_m = \int_{-L/2}^{L/2} \kappa(z)\, f_{mo}(z)\, g_{mo}(z)\, dz. \tag{66}$$

In order for solutions α_{mm}, β_{mm} of Eqs. (65) to exist it is necessary that the determinant of the coefficients of α_{mm}, β_{mm} be zero. This condition determines the allowed complex frequencies η_m of the normal modes of the system. There are two solutions for each positive integer m. We shall again assume that the influence of damping on the real angular frequencies of the system is negligible, so that for example in computing these frequencies the terms in Eqs. (65a) and (65b) which are proportional to λ_{mx} and λ_{my} respectively may be discarded. We also keep only the lowest order terms in $\bar{\kappa}_m$. With these approximations the angular frequencies of the $m^{\underline{th}}$ pair of normal modes are

$$\omega_m^{\pm} \cong \omega_{mo} \pm \frac{1}{2}\sqrt{(\Delta\omega_{mo})^2 + (\Delta\omega_{m\mathcal{M}})^2} \tag{67}$$

where

$$\omega_{mo} \cong \sqrt{\frac{\omega_{mo}^{x\,2} + \omega_{mo}^{y\,2}}{2}} \tag{68}$$

$$\Delta\omega_{mo} \cong \omega_{mo}^{x} - \omega_{mo}^{y} \tag{69}$$

$$\Delta\omega_{m\mathcal{M}} \cong \frac{\rho_s \bar{\kappa}_m}{\sqrt{\mu_x \mu_y}} \quad . \tag{70}$$

The frequency splitting between the $m^{\underline{th}}$ pair of normal modes is

$$\Delta\omega_m \cong \sqrt{(\Delta\omega_{mo})^2 + (\Delta\omega_{m\mathcal{M}})^2} \quad . \tag{71}$$

$\Delta\omega_{mo}$ will be called the intrinsic frequency splitting of the $m^{\underline{th}}$ pair of modes.

In the case of a symmetric wire we let $\omega_{mo}^{x} = \omega_{mo}^{y} = \omega_{mo}$, and $\mu_x = \mu_y = \mu$. Then

$$\omega_m^{\pm} \cong \omega_{mo} \pm \frac{\rho_s \bar{\kappa}_m}{2\mu} \tag{72}$$

$$\Delta\omega_m \cong \frac{\rho_s \bar{\kappa}_m}{\mu} \quad . \tag{73}$$

If in addition $\kappa(z)$ is uniform over the length of the wire (66) reduces to $\bar{\kappa}_m = \kappa$ for all m; the apparent circulation is equal to the actual circulation of the superfluid. If the wire is asymmetric and $\kappa(z)$ is uniform then

$$\bar{\kappa}_m = \kappa \int_{-L/2}^{L/2} f_{mo}(z)\, g_{mo}(z)\, dz \tag{74}$$

The apparent circulation differs from the actual circulation to the degree that the integral in (60) differs from unity. However the discrepancy for low modes is of order $(\Delta\omega_{mo}/\omega^{x}_{mo})^2 \cong 10^{-3}$, too small to be observed experimentally. Also the difference between $\sqrt{\mu_x\mu_y}$ and μ, where μ is equal either to μ_x or μ_y, was at most about 0.6%, in practice, again too small a discrepancy to measure.

In order to find the normal modes of the system we substitute the allowed frequencies (67) into either one of Eqs. (65). Consider the symmetric wire first. In this case we find that $\beta_{mm} \cong \mp i\,\alpha_{mm}$ when $\omega_m \cong \omega_{mo} \pm \Delta\omega_{m\ell}/2$. Let $\alpha^{\pm}_{mm} = A^{\pm}_m e^{i\phi^{\pm}_m}$, where $A^{\pm}_m$ and $\phi^{\pm}_m$ are real. The solutions (59a) and (59b) can then be written

$$x^{\pm}_m \cong \mathrm{Re}\ \alpha^{\pm}_{mm}\, f_{mo}(z)\, e^{i\eta^{\pm}_m t}$$

$$\cong A^{\pm}_m\, f_{mo}(z)\, e^{-\lambda_m t} \cos\left[\left(\omega_{mo} \pm \frac{\Delta\omega_{m\ell}}{2}\right)t + \phi^{\pm}_m\right] \qquad (75a)$$

$$y^{\pm}_m \cong \mathrm{Re}\ \mp i\,\alpha^{\pm}_{mm}\, f_{mo}(z)\, e^{i\eta^{\pm}_m t}$$

$$\cong \pm A^{\pm}_m\, f_{mo}(z)\, e^{-\lambda_m t} \sin\left[\left(\omega_{mo} \pm \frac{\Delta\omega_{m\ell}}{2}\right)t + \phi^{\pm}_m\right]. \qquad (75b)$$

Here $\omega_{mo} = \omega^{x}_{mo} = \omega^{y}_{mo}$. It is convenient to represent the normal modes of the system with the new complex quantities $\Psi^{\pm}_m = x^{\pm}_m + i\,y^{\pm}_m$. By substitution from (75) these functions are

$$\Psi^{+}_m \cong A^{+}_m\, f_{mo}(z)\, e^{-\lambda_m t}\, e^{i\left[\left(\omega_{mo} + \frac{\Delta\omega_{m\ell}}{2}\right)t + \phi^{+}_m\right]} \qquad (76a)$$

$$\Psi_m^- \cong A_m^- f_{mo}(z)\, e^{-\lambda_m t}\, e^{-i\left[\left(\omega_{mo} - \frac{\Delta\omega_{m\kappa}}{2}\right)t + \phi_m^-\right]} \quad . \qquad (76b)$$

These functions characterize the circularly polarized normal modes of the symmetric wire with circulation. There are two of them corresponding to each positive integer m, each pair differing in angular frequency by $\Delta\omega_{m\kappa}$. The frequency splitting has the same sign as the apparent circulation $\bar{\kappa}_m$. Suppose for example that the circulation is uniform along the length of the wire and counter-clockwise around the wire. Then $\bar{\kappa}_m = \kappa$ is positive, and Ψ_m^+, which itself rotates counter-clockwise, has the higher frequency. In general, for a given pair of normal modes the one with the higher frequency rotates in the same sense as the circulation.

Suppose now that the two normal modes represented by (76) are excited with equal amplitude and phase. This would be true, for example, of a symmetric wire which was excited by the method used in this experiment to measure circulation. Then the sum of these modes is represented by the sum

$$\Psi_m^+ + \Psi_m^- = 2A_m\, f_{mo}(z)\, e^{-\lambda_m t} \cos(\omega_{mo} t + \phi_m)\, e^{i\Delta\omega_{m\kappa} t/2} \quad . (77)$$

Suppose further that the circulation is uniform over the length of the wire. Then for low modes we have $\Delta\omega_{m\kappa} = \Delta\omega_\kappa$ independent of m, and the sum of all the functions $\Psi^{\pm}$, which within the approximations we have used represents the net displacement of the wire as a function of z and t, is

$$\sum_{m=1}^{\infty} (\Psi_m^+ + \Psi_m^-) = \left[\sum_{m=1}^{\infty} 2A_m f_{mo}(z)\, e^{-\lambda_m t} \cos(\omega_{mo} t + \phi_m) \right] e^{i\Delta\omega_\mu t/2} . \tag{78}$$

The wire oscillates in a plane which precesses in the same sense as the circulation with angular frequency $\Delta\omega_\mu/2$.

Now we look for the normal modes of an asymmetric wire. By substituting the frequencies (67) into either one of Eqs. (65) and discarding small terms we find that $\beta_{mm} \cong - iR_m\alpha_{mm}$ when $\omega_m \cong \omega_{mo} + \frac{\Delta\omega_m}{2}$, and $\beta_{mm} \cong i\alpha_{mm}/R_m$ when $\omega_m \cong \omega_{mo} - \frac{\Delta\omega_m}{2}$. Here R_m is given by

$$R_m = \frac{\Delta\omega_m + \Delta\omega_{mo}}{\Delta\omega_{m\mu}} . \tag{79}$$

Let $\alpha_{mm}^{\pm} = A_m^{\pm} e^{i\phi_m^{\pm}}$, where $A_m^{\pm}$ and $\phi_m^{\pm}$ are real. Again we form the quantities $\Psi_m^{\pm} = x_m \pm iy_m$. We assume that $f_{mo}(z) \cong g_{mo}(z)$. In fact these functions differ for low modes by amounts of order $\frac{\Delta\omega_{mo}}{\omega_{mo}} \cong 10^{-3}$. Although it is essential to retain frequency corrections of this order of magnitude, since they are what determine $\bar{\nu}_m$, it is not important to make corrections of this size in the amplitude functions.

$$\begin{aligned}\Psi_m^+ &= A_m^+ f_{mo}(z) e^{-\lambda_m^+ t}\left[\cos(\omega_m^+ t+\phi_m^+) + i\, R_m \sin(\omega_m^+ t+\phi_m^+)\right] \\ &= A_m^+ f_{mo}(z) e^{-\lambda_m^+ t}\left[\cos^2(\omega_m^+ t+\phi_m^+)+R_m^2\sin^2(\omega_m^+ t+\phi_m^+)\right]^{\frac{1}{2}} e^{i\theta_m^+}\end{aligned} \tag{80a}$$

$$\begin{aligned}\Psi_m^- &= A_m^- f_{mo}(z) e^{-\lambda_m^- t}\left[\cos(\omega_m^- t+\phi_m^-) - \frac{i}{R_m}\sin(\omega_m^- t+\phi_m^-)\right] \\ &= A_m^- f_{mo}(z) e^{-\lambda_m^- t}\left[\cos^2(\omega_m^- t+\phi_m^-)+\frac{\sin^2}{R_m^2}(\omega_m^- t+\phi_m^-)\right]^{\frac{1}{2}} e^{-i\theta_m^-} .\end{aligned} \tag{80b}$$

Here

$$\tan \theta_m^+ = R_m \tan(\omega_m^+ t+\phi_m^+) \qquad (81a)$$

$$\tan \theta_m^- = \frac{1}{R_m} \tan(\omega_m^- t+\phi_m^-) \qquad (81b)$$

These functions $\Psi_m^{\pm}$ represent elliptically polarized normal modes. There are two modes corresponding to each integer m, each pair differing in angular frequency by $\Delta\omega_m$. In a given mode each point on the wire traces out an ellipse. For each pair of modes there are two ellipses for each point on the wire, oriented at right angles to each other, traced out in opposite senses. R_m is the ratio of the major to the minor axis of each ellipse of the pair, so that the two are geometrically similar. The ellipse which is traced with the higher frequency is traced in the same sense as the circulation. For example, if the apparent circulation is counter-clockwise around the wire, then $\Delta\omega_{m\ell}$ is positive. Then R_m is positive, and from (80a) and (81a) Ψ_m^+ rotates counter-clockwise.

The amplitudes $A_m^{\pm}$ and phase angles $\phi_m^{\pm}$ are determined by initial conditions. In the present experiment circulation measurements were made with the wire oriented so that its plane-polarized modes were nearly at 45^o to the direction of the magnetic field. The current pulse was chosen so that when the current was turned off the wire was nearly at rest with a displacement given by $\frac{r(z,0)}{\sqrt{2}}(\hat{x}+\hat{y})$. $r(z,0)$ can be expanded in the functions $f_{mo}(z)$.

$$r(z,0) = \sum_{m=1}^{\infty} r_m f_{mo}(z) \tag{82}$$

Then the initial conditions require that

$$A_m^+ = \frac{r_m}{\sqrt{2(1+R_m^2)}} \tag{83a}$$

$$A_m^- = \frac{R_m r_m}{\sqrt{2(1+R_m^2)}} \tag{83b}$$

$$\tan \phi_m^+ = R_m = \frac{A_m^-}{A_m^+} \tag{84a}$$

$$\tan \phi_m^- = -\frac{1}{R_m} = -\frac{A_m^+}{A_m^-} . \tag{84b}$$

We see that with the wire oriented as it was during circulation measurements the two normal modes of a given pair are equally excited. The diagram in Figure 3 represents one such pair for a given point on the wire. The relative amplitudes with which different pairs are excited are given by the coefficients r_m, which depend on the detailed shape of the current pulse and magnetic field. They are calculated in chapter IV, section B.

In order to understand what signal will be observed from the vibrating wire, let $(\Psi_m^+ + \Psi_m^-)_p$ be the projection of $\Psi_m^+ + \Psi_m^-$ onto the axis perpendicular to the magnetic field. Then if the magnetic field is uniform over the length of the wire the e.m.f. induced

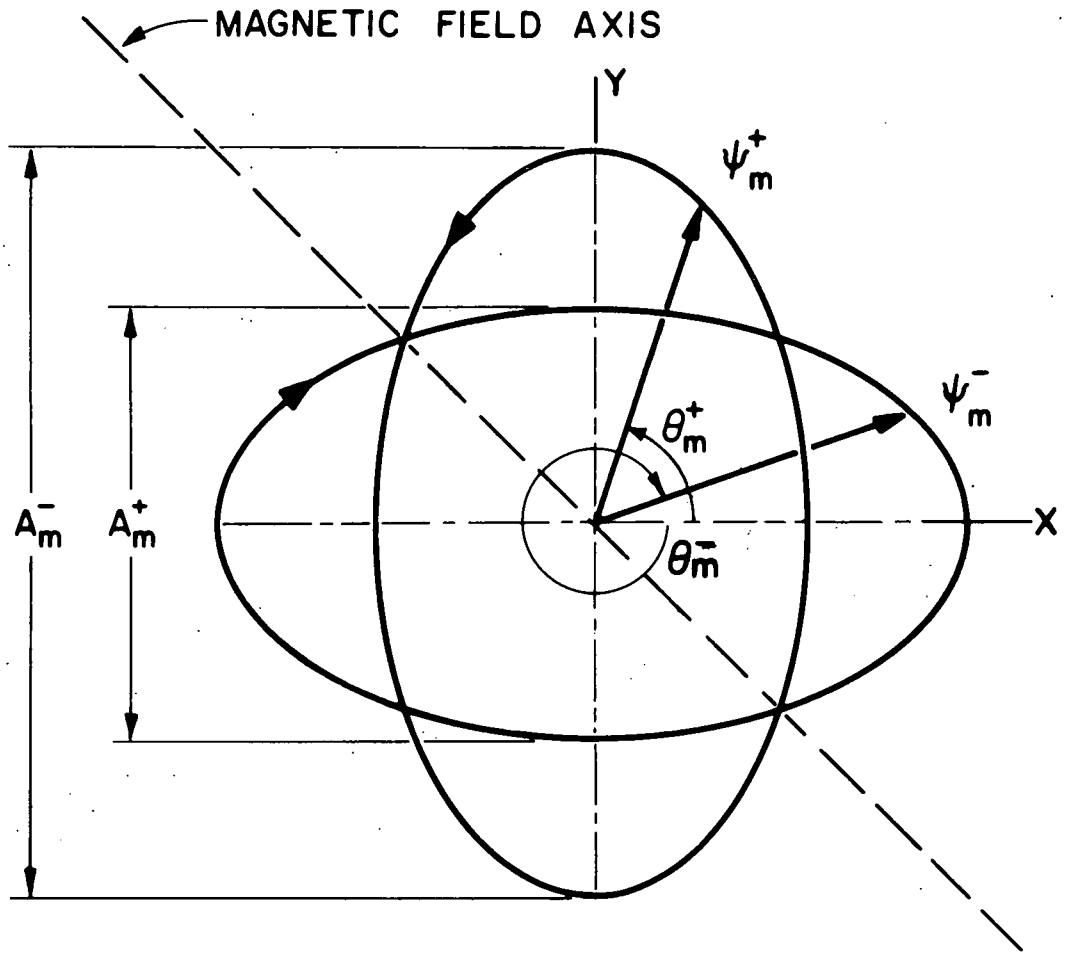

Figure 3. Elliptical Normal Modes of Vibrating Wire.

by the $m^{\underline{th}}$ pair of normal modes is

$$\mathcal{E}_m = - B \frac{d}{dt} \int_{-L/2}^{L/2} (\Psi_m^+ + \Psi_m^-)_p \, dz \, . \tag{85}$$

Here B is the magnetic field strength perpendicular to the wire. Again we let $f_{mo}(z) \cong g_{mo}(z)$. We also assume that $\lambda_m^+ \cong \lambda_m^- \cong \lambda_m$. Then using Eqs. (80), (83), and (84) we find that

$$\mathcal{E}_m \cong - \frac{Br_m}{2} \int_{-L/2}^{L/2} f_{mo}(z)dz \, \frac{d}{dt} \, e^{-\lambda_m t} (\cos \omega_m^+ t + \cos \omega_m^- t) \tag{86}$$

$$\cong \frac{Br_m}{2} \int_{-L/2}^{L/2} f_{mo}(z)dz \, \omega_{mo} \, e^{-\lambda_m t} (\sin \omega_m^+ t + \sin \omega_m^- t) \tag{87}$$

$$\cong Br_m \int_{-L/2}^{L/2} f_{mo}(z)dz \, \omega_{mo} \, e^{-\lambda_m t} \sin \omega_{mo} t \cos \frac{\Delta\omega_m t}{2} \, . \tag{88}$$

In going from Eq. (86) to (87) we have discarded corrections in $\mathcal{E}_m$ of order λ_m/ω_{mo} and $\Delta\omega_m/\omega_{mo}$. When displayed on an oscilloscope $\mathcal{E}_m$ is a decaying beat pattern. The angular frequency of the carrier wave is ω_{mo}; the angular beat frequency is $\Delta\omega_m/2$. The period between successive nodes of the beat pattern is $2\pi/\Delta\omega_m$.

G. Detecting the Sign of the Circulation

If μ, ρ_s, and the intrinsic beat frequency $\Delta\omega_{mo}$ have already been measured, then a measurement of $\Delta\omega_m$ determines the absolute value of $\bar{\kappa}_m$. It is possible in addition to determine the sign of $\bar{\kappa}_m$ by introducing an arbitrary constant of known sign into the phase difference between Ψ_m^+ and Ψ_m^-. The beat

pattern of (88) results from the constantly changing phase difference between Ψ_m^+ and Ψ_m^-: the phase of Ψ_m^+ advances relative to the phase of Ψ_m^- at a rate $\Delta\omega_{m\mu}$. Furthermore, we have seen that Ψ_m^+ always rotates in the direction of the circulation. Suppose now that the wire is initially displaced in a plane rotated slightly with respect to the plane which is perpendicular to the magnetic field. Then the phase of each normal mode is shifted from what it is in Figure 3. If the plane is rotated in the direction of the circulation, that is, in the direction in which Ψ_m^+ is rotating, the phase of Ψ_m^+ is advanced and the phase of Ψ_m^- is retarded. Therefore their phase difference is increased. If the plane is rotated in the direction opposite to the circulation the phase of Ψ_m^+ is retarded and the phase of Ψ_m^- is advanced, so that their phase difference is decreased. A shift in the phase difference of Ψ_m^+ and Ψ_m^- is observed on the oscilloscope as a shift in the time interval between the initial excitation of the wire and the appearance of the first node. If the phase difference is increased the time interval is decreased, and vice versa. The interval between successive nodes is not affected.

A simple example of this principle is the case of a symmetric wire with uniform circulation. We have seen in (78) that in this case the wire vibrates in a plane which precesses in the same sense as the circulation with angular frequency $\Delta\omega_\mu/2$.

If the wire is initially excited in a plane perpendicular to the magnetic field its plane of vibration will precess until it is parallel with the magnetic field in a time $|\pi/\Delta\omega_\mu|$. At that time the beat pattern will have its first null. If instead the wire is initially excited in a plane rotated from the perpendicular to the magnetic field by an angle δ, then the plane of vibration will precess until it is parallel to the magnetic field in a time $|\pi/\Delta\omega_\mu| - 2\delta/\Delta\omega_\mu$. If δ has the same sign as the circulation the first null of the beat pattern is advanced in time. If δ has the opposite sign from the circulation the first null of the beat pattern is retarded.

In practice it was possible to rotate the initial plane of excitation of the wire by superimposing the field of a small electromagnet on the permanent magnetic field at right angles to the permanent field and the wire. The electromagnet was turned on for the duration of the current pulse in the wire, then turned off in order to observe the e.m.f. induced by the permanent field alone. In addition to shifting the phase difference between the two members of a pair of normal modes, this method also changed their relative amplitude, so that the nodes of the beat pattern were no longer perfect nulls. However, it was still possible to tell whether the nodes were advanced or retarded in time.

H. Figure of Merit for the Wire

If we ignore the effects of asymmetry in the wire the principal measurement in this experiment is of a time interval proportional to $1/\Delta\omega_\nu$. The time available for this measurement is proportional to the decay time constant $1/\lambda$. An appropriate figure of merit for the wires used in the experiment is the ratio of these two times, equal to $\Delta\omega_\nu/\lambda$. Combining (40), (31) and (73) we find that for the low modes of a symmetric wire with uniform circulation the figure of merit for the $m^{\underline{th}}$ pair of modes is approximately

$$F_m \cong \frac{\rho_s \nu}{\pi a \sqrt{2\eta_n \rho_n \omega_m}} \quad . \tag{89}$$

For a given temperature and circulation the figure of merit is approximately proportional to $1/a\sqrt{\omega_m}$, where a is the radius of the wire. Therefore in principle the sensitivity of the experiment to a given level of circulation is enhanced by using thin wires at low frequencies. However, an opposing consideration is that in practice it was found that larger and more stable circulations tended to appear around the thicker wires. It is interesting to observe that the figure of merit is independent of the mass density of the wire. Values for the figure of merit of several wires are given in Tables 1a-d.

III. MECHANICAL APPARATUS

A. Basic Elements

The basic elements of the apparatus are shown in perspective in Figure 4 and in cross-section in Figure 5. The wire is 5 cm long and from 10 μ to 100 μ in diameter. It is stretched vertically down the center of a Pyrex tube and is attached at each end to a steel post. The tube, within which the observed circulation takes place, has a 3 mm inner diameter. The lower post is fixed, while the upper post can be moved up and down to control the tension in the wire and rotated to twist the wire. A brass can encloses the tube and wire, and the whole assembly of can, tube, and wire can be put into steady rotation around a vertical axis at speeds up to 80 rad sec^{-1}. A stationary permanent magnet provides an average transverse field of 1.35 kG at the wire. The electromagnet, which is shown in Figure 7, consists of two coils placed just outside the can on opposite sides of the wire, oriented in such a way as to produce a field which is perpendicular to the field of the permanent magnet and to the wire.

B. Wire Materials and Mounting

During the early stages of this work attempts were made to use wires made of tungsten and platinum. It was found that the tungsten wires, when oscillating at frequencies low enough to keep

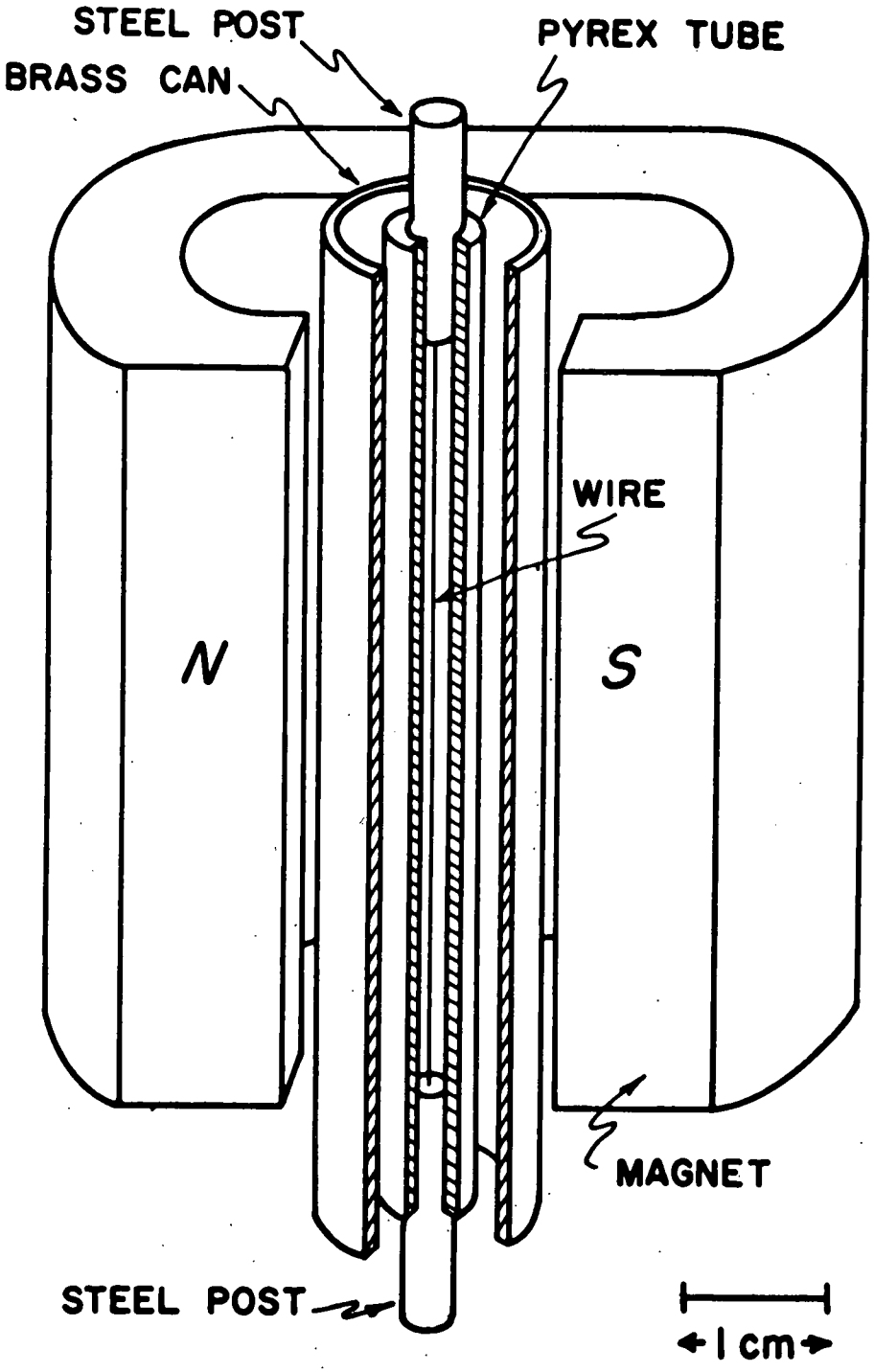

Figure 4. Basic Elements of Apparatus. Liquid helium surrounds these elements and fills the spaces between the can, tube, and wire.

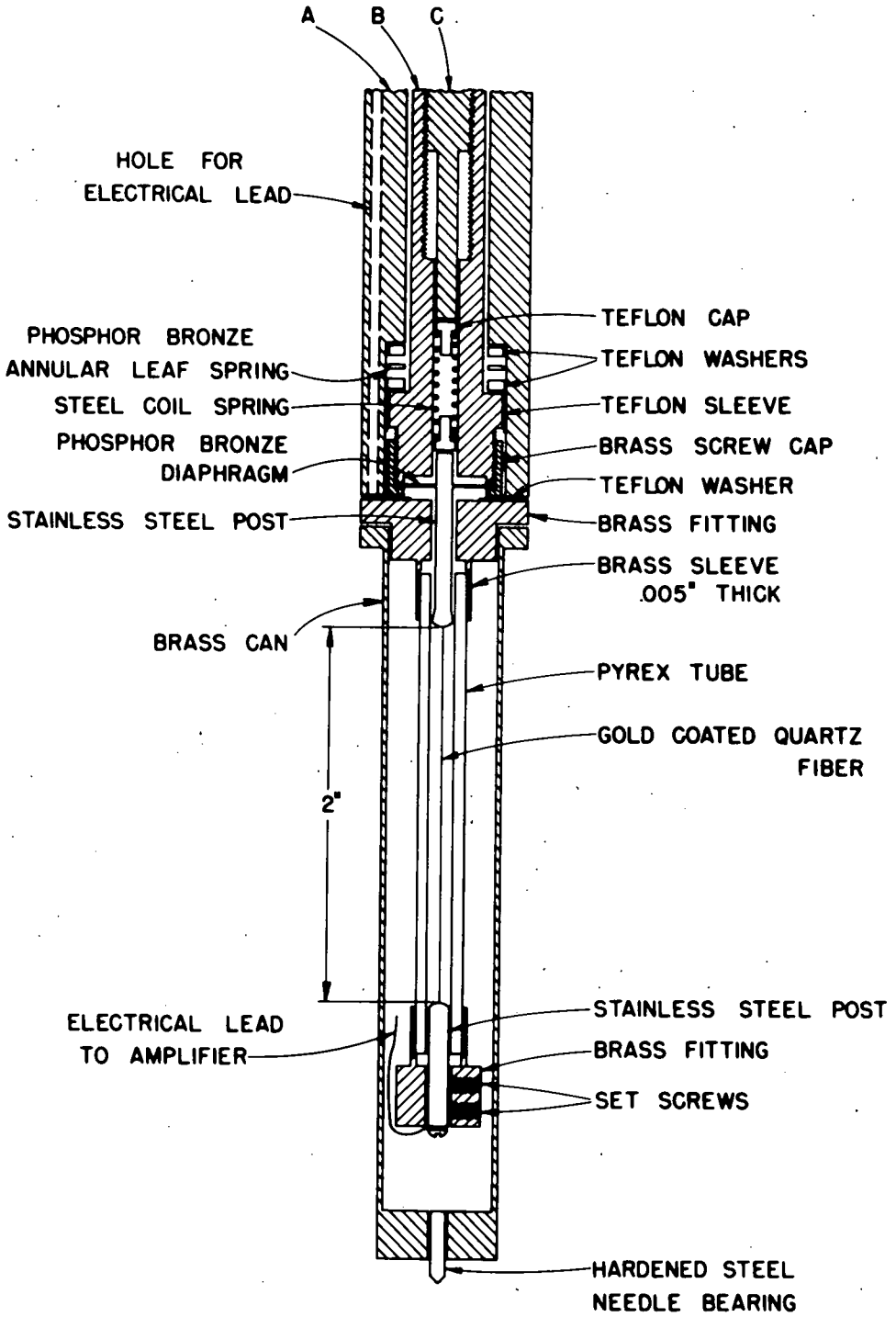

Figure 5. Details of Rotating Assembly.

the damping small, produced beat patterns even in the absence of liquid helium which were not the result of two perpendicular plane-polarized modes. The platinum wires, although satisfactory in other respects, were easily kinked and broken. It was found that quartz fibers could be depended on to last through many experimental runs and to behave in the predicted way. When coated with a conducting layer of gold they made very satisfactory "wires".

Fibers with diameter 25 μ and less were purchased commercially, while larger ones were drawn by hand from heated quartz rod.[36] All the fibers were coated by exposing them to vaporized gold under high vacuum. The thickness of the gold layer deposited on a fiber could be computed two ways, either from the electrical resistance of the fiber or by estimating the fraction of the total amount of gold evaporated which is deposited on the fiber. According to the first computation, which assumes that the gold coating is perfectly uniform and continuous, the thickness of a layer was typically 400 Å. According to the second, which assumes that all the gold which reaches the fiber adheres to it, the thickness of a layer was typically 4000 Å. The reason for the discrepancy is not known. Presumably one or both of the assumptions above is unrealistic.

The mass per unit length of a fiber was found by weighing it on a microbalance, then measuring its length with a steel ruler. The mass of fluid displaced by a unit length of the fiber was

found using the average of the diameters measured at each end of the fiber with a micrometer caliper, and the known density of liquid helium. All these measurements were made before the fiber was installed in the apparatus, in order to estimate the frequency splittings that circulation would produce, then repeated after the fiber had been removed from the apparatus on just that part of the fiber which had actually been exposed to liquid helium.

The diameter and effective mass per unit length of the fibers with which interesting experimental runs were made are listed in Tables 1a-d. The effective mass per unit length is the mass per unit length of the fiber plus the fluid displaced. In addition to runs with these fibers some earlier runs were made with quartz fibers about 10 μ in diameter and with platinum wires 25 μ in diameter.

Figure 6 shows in detail how a fiber was joined at each end to a steel post. The fiber was inserted into a .014" diameter hole drilled down the center of the post. A stainless steel capillary served as a spacer between the fiber and hole wall. (The spacer was cut from a long capillary using a die cutter and a tungsten wire filler to keep the hole in the capillary from closing.) The end of the fiber extended into a larger hole drilled into the post from the side, where electrical contact between the fiber and post was made with silver paint. The paint was dried by baking it overnight at about 120^{o}C. When it had

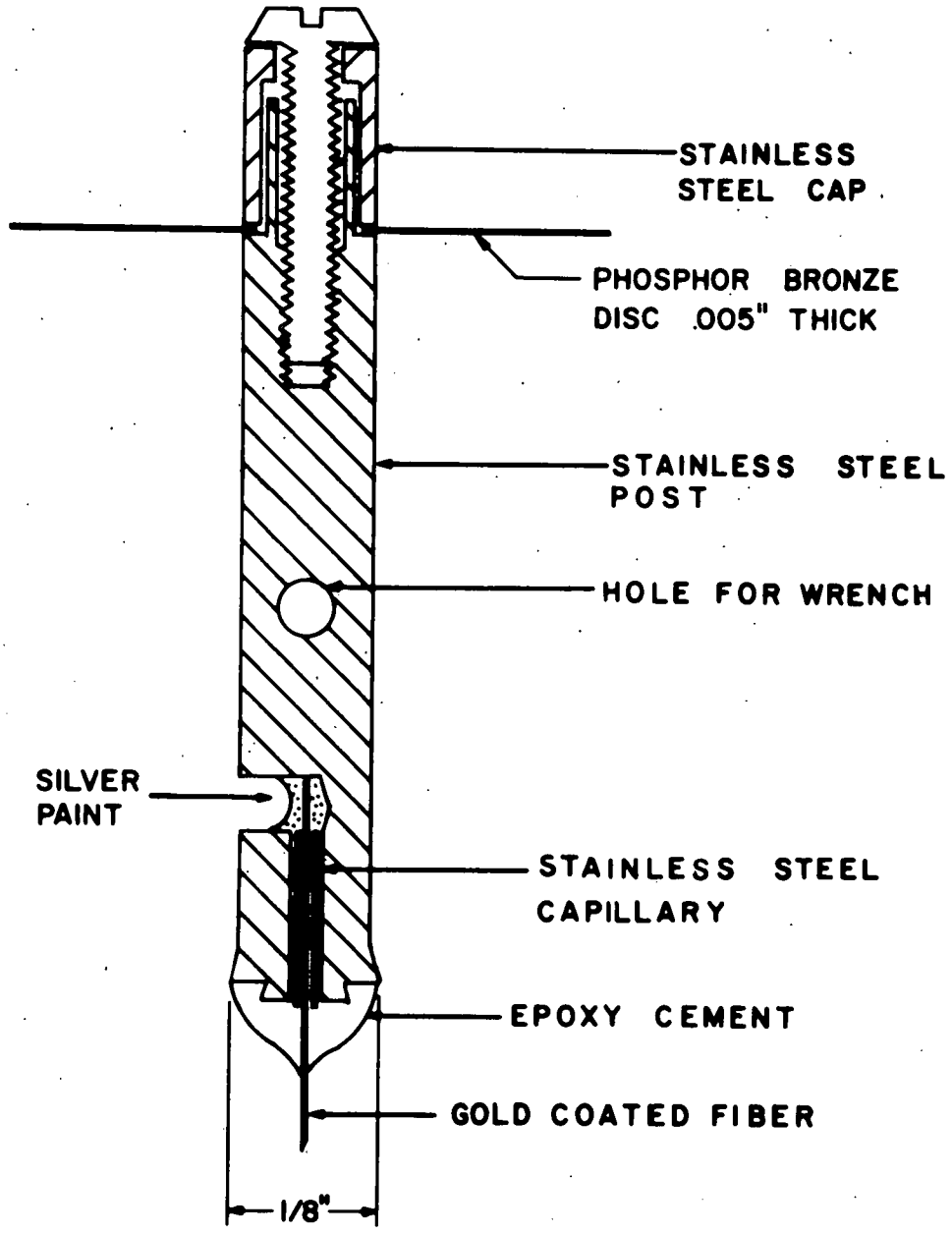

Figure 6. Details of Upper Post and Mounting.

dried it was a strong enough cement that the fiber could be suspended vertically from the upper post under tension from the weight of the lower post. Then epoxy cement was applied to the end of each post, enveloping the fiber with a cylindrically symmetric fillet as shown in Figure 6. The epoxy was baked overnight at about 100°C to a very hard smooth finish. The end of each post had been shaped in such a way that when during cooling the epoxy shrank in size compared to the post it would grip the post more tightly and not break away from it.

Care had to be taken while mounting the fiber to clean the cylindrical sides of the posts of paint and epoxy before baking them, so that the posts would fit freely into the Pyrex tube. The actual manipulations of the fiber and posts were all performed under a microscope, and it was found that the fiber could be handled without rubbing off any of the gold coating by using tweezers whose tips had been covered with latex tubing.

The last fiber, fiber H, was mounted using a silver-impregnated epoxy instead of silver paint.[37] This epoxy seemed to be as good a conductor as the silver paint, and has the advantage that it cures without tending to pull away from the fiber and break electrical contact as the silver paint tends to do. Unsilvered epoxy, since it flows much better than the silver-impregnated epoxy, was still used to finish the end of each post.

C. Installing the Fiber

The upper post which holds the fiber is fitted with a thin phosphor bronze disc, as shown in Figure 6, and is attached to the rest of the apparatus by clamping the disc at its perimeter to the lower end of a brass tube, labeled B in Figure 5. The actual clamp is a brass cap threaded to screw over the end of the tube. The post extends down through a brass fitting which holds the Pyrex tube, into the bore of the Pyrex tube itself. The lower end of the post is flared to fit the inner diameter of the tube, at the same time allowing the post to rotate and move vertically, free of any friction with the brass headpiece. The bottom post is a straight cylinder matched to the inner diameter of the Pyrex tube, and anchored with set screws to another brass fitting at the lower end of the tube.

It takes careful machining to make the flared end of the upper post fit properly to the inner diameter of the Pyrex tube. The fit must be loose enough so that the post can turn freely in the tube. On the other hand it must not be so loose that it permits lateral motion of the post when the fiber is vibrating, because this motion very quickly damps the vibrations.

Even after the fiber had been mounted in the steel posts it was a delicate operation to install it in the apparatus without breaking it. The two posts were held rigidly in a special jig with the fiber stretched between them, the same jig in which the fiber had been prepared. The brass cap was already in place on

the diaphragm, put there before the fiber and posts were joined together. Then the cap was screwed on over the end of tube B and tightened with a special wrench. The Pyrex tube with its fittings was suspended from the bottom of tube A, a larger coaxial tube surrounding tube B, by means of three slender rods four inches long which extended up through the headpiece holding the Pyrex tube into screw holes in the bottom end of tube A. With the rods screwed in place the two steel posts holding the fiber were released from the jig, first the lower post then the upper one. The Pyrex tube was slipped up around the posts and fiber, guided by the slender rods. The rods were removed and the headpiece fastened to the base of tube A with screws. Then the lower post could be secured with set screws. It was important that the Pyrex tube be thoroughly cleaned before installing it to ensure that the lower post slid through it freely.

D. Tension Control

With the bottom post anchored in place, the tension in the fiber is controlled by means of the elastic phosphor bronze diaphragm fitted to the upper post. The diaphragm is clamped around its edge to the base of tube B, so that the top end of the post extends up into the hollow bore of the tube. A brass rod labeled C in Figure 5 extends down from outside the helium dewar through the bore of the tube, to press against a coil spring which presses against the top end of the post. The rod

and tube are threaded so that the rod can be screwed up and down inside the tube, deflecting the diaphragm and changing the tension in the fiber.

It was important during an experimental run to be able to regulate the tension accurately, because it was found that small changes in wire frequency brought on measurable changes in the intrinsic beat frequency $\Delta\omega_o$. For example, a measurable change in the intrinsic beat frequency of the 25 μ diameter fiber resulted from a shift in the carrier frequency of about 1 part in 300. At 300 cps this frequency shift represented a change in tension of about 1 dyne. On the other hand, when at the beginning of an experimental run it was necessary to select a suitable value for $\Delta\omega_o$, it was very useful to be able to vary the carrier frequency over a range of several hundred cps, representing a tension change of perhaps 10^3 dynes. Both of these requirements on the tension control were well satisfied by the arrangement described above, when the diaphragm used was .005" thick and the coil spring was wound from .015" diameter steel piano wire.

As long as the apparatus was immersed in liquid helium and left undisturbed except for circulation measurements, the wire frequency was very stable, usually requiring no adjustment for many hours. Sometimes, however, the frequency would shift during rotation of the apparatus and require correction after the rotation had been stopped. There was always some hysteresis in the tension control, probably caused by friction between the coil

spring and the walls containing it. Hysteresis could be reduced by rapping sharply on the metal frame which held the dewar each time after the tension control rod had been turned.

Another problem in connection with tension control arose when the apparatus was cooled from room temperature. Those parts of the apparatus which support the fiber shrank more than the fiber itself, so that the fiber tended to go slack. As originally designed, the tube which encloses the fiber and holds the lower post was made of brass, with a Pyrex lining held in place with a coil spring to present a smooth surface to the liquid helium. This tube worked well with platinum wires, but a quartz fiber when cooled went slack beyond all power of the diaphragm to tighten it again. For this reason a new tube was made entirely of Pyrex, except for the brass fittings at either end. These fittings were joined to the Pyrex tube with an epoxy cement which was elastic enough so that the thermal contraction of the brass did not break the Pyrex.[38] The tube was inserted into sleeves which had been machined to a thickness of only .005", also in order to prevent the thermal contraction of the brass from breaking the Pyrex. Even with the Pyrex tube care had to be taken in advance of cooling to set the maximum tension high enough so as to leave the fiber taut at low temperatures. For example, the frequency of the 25 μ diameter fiber, if set at 2000 cps at room temperature, fell to 1000 cps at 1.2^{o}, representing a tension change of 7×10^{3} dynes.

E. Twist Control

Vinen found that the intrinsic beat frequency $\Delta\omega_o$ could be regulated by twisting the wire. Provision for doing this was made in the way shown in Figure 5. The brass tube B which holds the upper post is free to rotate inside the larger, co-axial tube A. Tube A is attached rigidly, through the Pyrex tube, to the post which holds the lower end of the wire, so that the wire is twisted by rotating tube B by hand from outside the dewar without rotating tube A. Rod C, which controls the tension in the wire, rotates along with tube B, so that the tension remains nearly constant as the wire is twisted. Vertical motion of tube B is prevented by an annular phosphor bronze leaf spring which rides against a shoulder machined in tube A and presses tube B firmly down against the brass fitting which holds the Pyrex tube. Brass surfaces which would otherwise rub together as tube B is turned are protected with teflon. Once the wire has been twisted by the right amount, unwanted changes in $\Delta\omega_o$ can be prevented by locking tubes A and B together with set screws at the top of the apparatus, outside the dewar.

F. Rotation

When tubes A and B are locked together, the whole assembly shown in Figure 5 can be rotated as a unit by applying a torque to tube A. The vertical axis of rotation is defined by three bearings shown in Figure 7. There are two bearings near the top

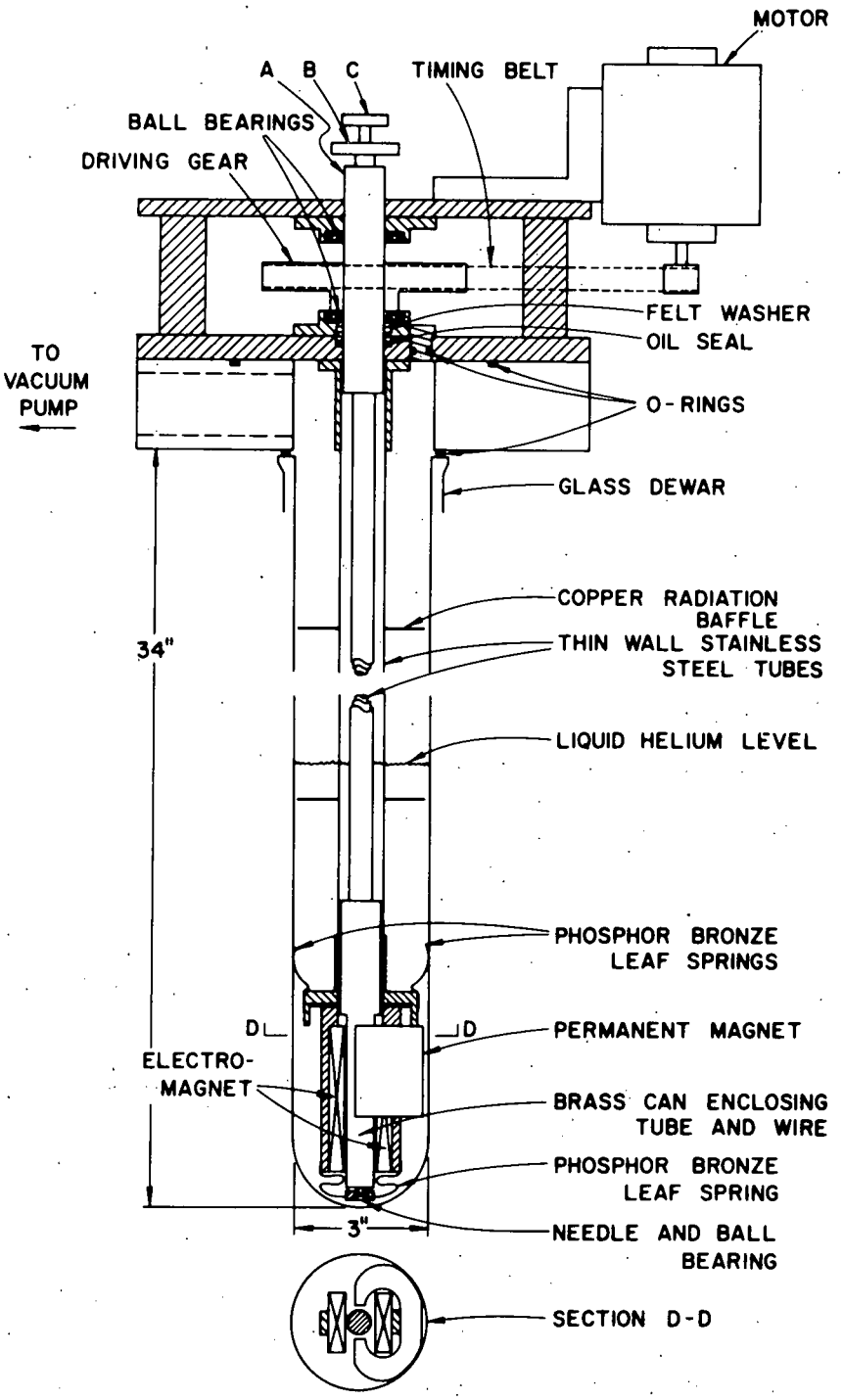

Figure 7. Overall View of Apparatus.

of the apparatus, outside the dewar. They are ball bearings, friction fitted to tube A, and held in place one 1½" above the other by two heavy horizontal brass plates. The plates are bolted together through four heavy brass posts, and the lower plate is bolted to the aluminum head block which supports the helium dewar. A driving gear encircles tube A between the two bearings and is connected through a timing belt to the drive shaft of a motor bolted to the upper plate. The two bearings keep the rotating assembly aligned to a vertical axis despite the tension in the timing belt.

The third bearing is a needle-and-ball bearing at the very bottom of the apparatus, the needle supported by the brass can which encloses the Pyrex tube, the ball bearing held in place by a phosphor bronze leaf spring attached to the frame which supports the electromagnet. This frame is in turn attached to the lower end of a large tube, co-axial with the rotating assembly, which extends the length of the dewar and is bolted at its top end to the bottom of the lower brass plate. This stationary tube also supports the permanent magnet, several copper radiation baffles, and three phosphor bronze springs which press against the walls of the dewar and prevent the apparatus from going into transverse oscillation when it is rotating.

A vacuum seal between the rotating assembly and the lower brass plate is provided by an oil seal, which generates less

friction than an O-ring and still keeps a seal which was good enough for this experiment.[39] A felt washer which encircles the rotating assembly just above the oil seal is soaked with oil to wet the rotating shaft and lubricate the seal.[40] Two rubber O-rings, which are not shown in Figure 7, make vacuum seals between tubes A and B, and tubes B and C, near the top of the dewar.

The rotating assembly was mounted in the stationary part of the apparatus by inserting it from below, then securing it to the driving gear with set screws. The gear rests on the rotating frame of the bearing held by the lower brass plate, so that this bearing takes the weight of the rotating assembly. The needle and ball bearing at the bottom of the apparatus were mated under tension from the phosphor bronze spring, enough tension to keep them mated when the apparatus was cooled with liquid helium. It was necessary when handling the rotating assembly to be careful not to bend it, since the long shafts of all three rotating tubes were made of thin-wall stainless steel. It was possible to align the assembly to a vertical axis well enough so that the excursion of the axis of the wire from the axis of rotation was probably less than $\pm$ 50 μ. A 1/50 hp direct current motor, with several gear ratios, provided steady rotational speeds from 3 to 80 rad sec^{-1}.[41] A synchronous motor was also used for speeds close to 0.1 rad sec^{-1}.[42] The speed of the direct current motor was regulated by a motor control.[43]

G. Electromagnet

The electromagnet consists of two coils wound from Supercon 75% Nb-25% Zr superconducting wire.[44] The wire has over-all diameter .014", including layers of copper and formvar each .001" thick. The reason for making the magnet superconducting was to keep the power dissipation low in the helium bath. The coil forms and supports were made of a magnesium alloy which is a normal metal at the temperatures used, so does not support persistent eddy currents which would distort the magnetic field. The presence of the permanent magnet tends to weaken the field of the electromagnet at the wire. Nevertheless, with 1A of current the coils produce a measured field of about 250 G at the wire with the permanent magnet present.

H. Electrical Connections

The e.m.f. induced in the oscillating wire is picked up at the bottom steel post by an electrical lead brought down through tube A from the top of the dewar. Where the lead wire passes through the field of the magnet it is taped down to the outside of the Pyrex tube, to prevent it from vibrating in the field and producing a spurious induced e.m.f. It is also wound around the Pyrex tube in a helix, in order to prevent the induction of a large e.m.f. when the electromagnet is turned on and off. The top end of the oscillating wire is grounded to the main body of the apparatus through tube B. Electrical connections are

made from the rotating assembly at the top of the dewar to instruments in the room with sliding phosphor bronze contacts.

I. Cryogenics

The entire liquid helium dewar is insulated from the room by a liquid nitrogen bath contained in a larger dewar. The dewar pair is of conventional design, each dewar having a double glass wall with silvered surfaces.[45] The long shafts of the four tubes in the apparatus which extend the length of the helium dewar are made of thin-wall stainless steel to reduce heat conduction into the helium bath from the room. The two inner tubes have wall thickness .006", the two outer tubes, .010". The outermost, stationary, tube is fitted with eight copper baffles to intercept radiation and for heat exchange. Electrical leads are 36 gauge copper wire, fine enough to keep their heat conduction small compared to other sources.

The helium bath was cooled from 4.2°K by pumping down along its vapor pressure curve with a mechanical vacuum pump.[46] The lowest temperature that could be reached with this system was 1.1°K, although 1.2°K was the lowest temperature customarily used. The pressure in the pump manifold was monitored by an octoil-S manometer for the purpose of regulating the rate at which the helium bath was cooled. It was found, for example, that if the pressure in the pumping line was maintained at 0.9 mm Hg the apparatus and helium bath would be cooled from 2.2°K, just above T_λ, to 1.2°K in about 90 minutes.

The liquid helium loss rate at 1.2°K was about 70 cm^3 hr^{-1}, which was small enough, with the large capacity of the dewar, to allow experimental runs to continue for more than 24 hours without a second transfer of liquid helium. Helium gas was recovered from the output of the mechanical pump and stored for another liquefaction.

The pressure over the helium bath was read by eye on an octoil-S manometer, and the temperature of the bath determined from its vapor pressure curve. This method gives a resolution of about 5 millidegrees, which was ample for this experiment. The pressure readings could also be used to calibrate an Allen-Bradley 0.1 watt, 68 ohm carbon resistor immersed in the helium bath, a more convenient thermometer to use when the temperature had to be changed several times during a run.[47]

The temperature was stabilized against small fluctuations with an electronic control system. The Allen-Bradley resistor is one arm of a Wheatstone bridge. An alternating signal at 225 cps is applied to the bridge, and any imbalance in the bridge is detected by a phase-sensitive detector. The direct current output of the phase-sensitive detector is used to regulate the current in a small heating coil placed in the helium bath. With the bridge in balance the power dissipation in the Allen-Bradley resistor was about 25 μW for regulation at 1.2°K.

J. Shock Mounts

The large aluminum frame which supports the helium and nitrogen dewars is shielded from vibrations in the laboratory floor by coil spring shock mounts. Heavy lead bricks were piled onto the aluminum frame near its base to reduce the resonant frequency of the suspension. Most of the noise in the liquid helium seemed to come from boiling in the nitrogen bath and from sound vibrations carried by the air in the room.

IV. ELECTRICAL APPARATUS

A. General Layout

The electrical apparatus is laid out in a block diagram in Figure 8. The chain of events which go into a single measurement of circulation starts with a signal from a waveform generator.[48] At designated intervals this generator puts out simultaneously a short positive pulse and a negative-going sawtooth. The positive pulse triggers a pulse generator which puts out a positive square pulse of variable amplitude and duration.[49] This square pulse will turn on the power to the electromagnet provided that a manual switch inserted in the line has been closed. Most measurements were made with the switch open and the magnet off. The negative-going sawtooth, after a certain time delay, triggers a pulse generator which sends a current pulse of variable size and duration through the detecting wire immersed in liquid helium.[50] The time delay is introduced in order to let the current in the magnet build up to its steady state value before the detecting wire is excited.

The detecting wire is one arm of a Wheatstone bridge as shown in Figure 11, and the current pulse which excites it is supplied to two opposite terminals of the bridge. The other two terminals are connected by way of a transformer to a selective amplifier, and the bridge is balanced so that there is no potential difference across the output terminals due to the current

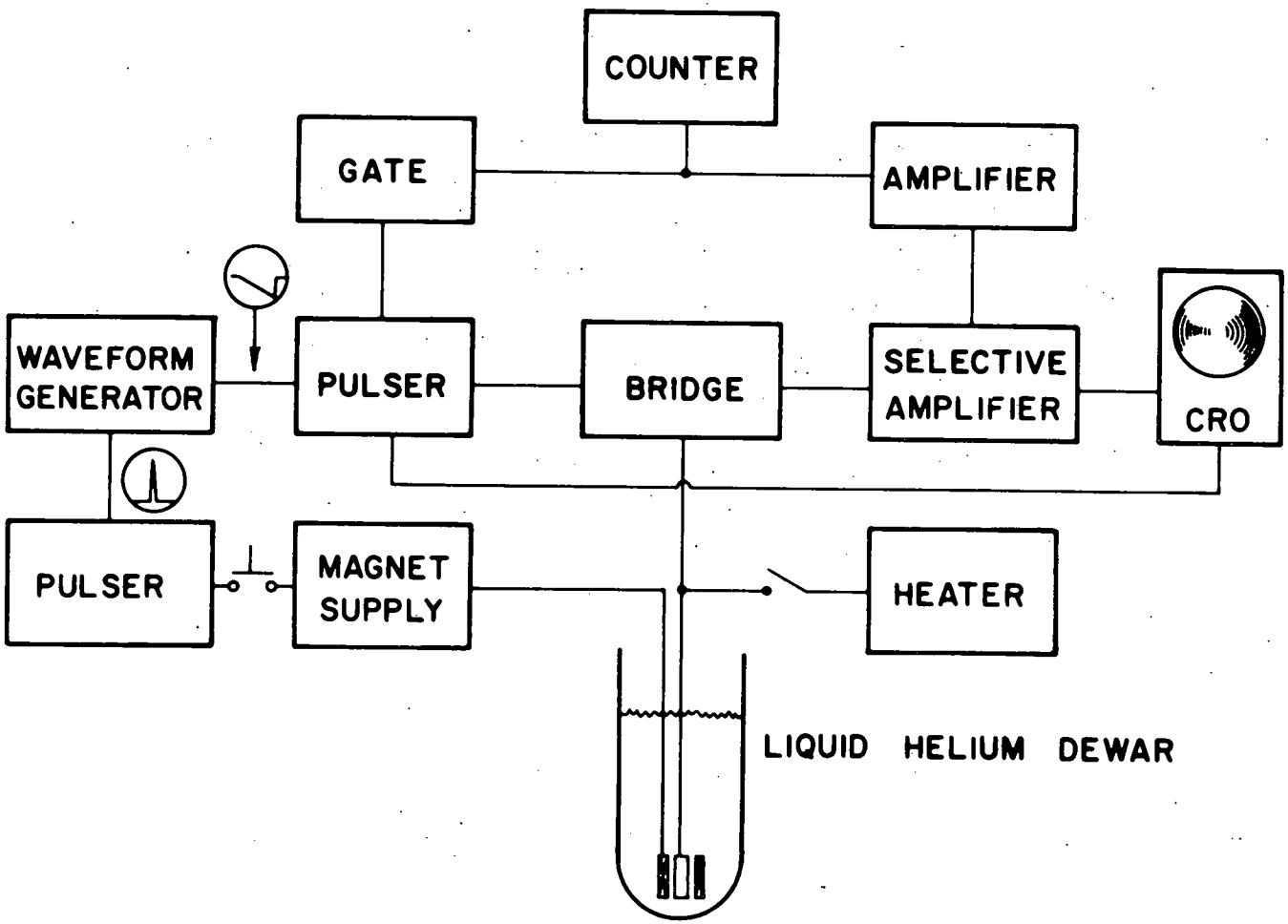

Figure 8. Block Diagram of Electrical Apparatus.

pulse. However, once the wire has been excited its oscillations induce a small current in the primary coil of the transformer which is detected and amplified by the selective amplifier.[51]

The output signal from the selective amplifier is applied to the vertical sweep of the oscilloscope[52] through an amplifier plug-in unit.[53] The horizontal time base of the oscilloscope is triggered by the onset of the current pulse which excites the wire.[54] The beat period of the wire is measured by observing visually the location of the first node of the beat pattern on the screen of the oscilloscope.

Once the beat period of the wire has been recorded the circulation measurement is finished. However, it was also necessary to measure the resonant frequency of the wire continually during a run, just to make sure that it had not changed. Figure 8 includes the apparatus used for this measurement. An electronic counter measures the period of the oscillating e.m.f. induced in the wire, averaged over ten cycles.[55] The oscillating signal is taken from the output of the selective amplifier and amplified again[56] to a high enough level to operate the counter. However, the vibration of the wire is distorted by the driving current pulse in the wire, so in order to get an accurate measurement the oscillating signal is gated off for a period of time somewhat longer than the current pulse lasts. This is done with a

negative square pulse supplied by a pulse generator triggered by the current pulse to the wire.[57]

B. Current Pulse

The current pulse controls the amplitudes of the normal modes of the wire. It is important to keep the amplitudes small compared to the penetration depth of the normal fluid in order to satisfy the assumptions which were made in analyzing the effect of the normal fluid on the wire. In addition, it was thought desirable to keep the amplitudes small compared to the radius of the wire in order not to disturb the superfluid unnecessarily. In order to know what the amplitudes are it is necessary to analyze the response of the wire to a current pulse.

For this purpose no generality is lost by assuming that the wire is symmetric and the circulation is zero. Then the equations of motion (38), with $\varkappa = 0$, are identical. With the current off the wire vibrates freely in a fixed plane with displacement r(z,t) given by Eq. (78).

$$r(z,t) \cong \sum_{m=1}^{\infty} 2A_m f_{mo}(z) e^{-\lambda_m t} \cos(\omega_{mo} t + \phi_m) \qquad (90)$$

When the current is turned on Eqs. (38) are modified by the addition of a driving term. We assume a steady current I and a uniform transverse magnetic field B. Then the magnetic force per unit length on the wire is BI. The equations of motion have

the form

$$\mu\frac{\partial^2 x}{\partial t^2} = T\frac{\partial^2 x}{\partial z^2} - S\frac{\partial^4 x}{\partial z^4} - 2\mu\lambda\frac{\partial x}{\partial t} + BI \ . \qquad (91)$$

The boundary conditions are not changed. The initial conditions for $x(z,t)$ are

$$x(z,t)\Big|_{t=0} = 0, \ \dot{x}(z,t)\Big|_{t=0} = 0 \ . \qquad (92)$$

There are an identical equation and set of initial conditions for $y(z,t)$. Solutions to (91) have the form

$$x_m(z,t) = f_{mo}(z)\ \theta_m(t) \ . \qquad (93)$$

We shall use the approximation that for low modes a stiff wire of length L is equivalent to a flexible wire of length $L^* = L - 2\sqrt{\frac{S}{T}}$. With the wires used in this experiment the error involved in this approximation is at most 1%. Then the solution for the sum of the $m^{\underline{th}}$ pair of normal modes is

$$r_m(z,t) \cong (-1)^{\frac{m-1}{2}} \frac{4BI}{m\pi\mu\omega_m^2}\cos\frac{m\pi z}{L^*}\ (1-e^{-\lambda_m t}\cos\omega_m t) \qquad (94)$$

$$\dot{r}_m(z,t) \cong (-1)^{\frac{m-1}{2}} \frac{4BI}{m\pi\mu\omega_m}\cos\frac{m\pi z}{L^*}\ e^{-\lambda_m t}\sin\omega_m t \ , \qquad (95)$$

where $m = 1,3,5,\ldots$. We note that only the even normal modes are excited when the magnetic field is uniform.

Suppose now that the current is turned off at time t'. Thereafter the wire vibrates freely again, but with initial conditions given by evaluating (94) and (95) at $t = t'$. In these

circumstances the solution for the sum of the $m^{\underline{th}}$ pair of normal modes is

$$r_m(z,t) \cong (-1)^{\frac{m-1}{2}} \frac{4BI}{m\pi\mu\omega_m^2} \cos\frac{m\pi z}{L^*} e^{-\lambda_m t}\left[e^{-\lambda_m t'} \cos[\omega_m(t-t')] - \cos\omega_m t\right]. \tag{96}$$

If t' is small, so that $e^{-\lambda_m t'} \cong 1$, then r_m has a local maximum in time when $\omega_m t' = \nu\pi$, where ν is an odd integer. In order to obtain the largest possible excitation of r_m for a given current we set $\nu = 1$. This means that the current is turned off after one half-period of vibration of the $m^{\underline{th}}$ pair of normal modes. Thereafter, setting $e^{-\lambda_m t'} \cong 1$, we have

$$r_m(z,t) \cong (-1)^{\frac{m+1}{2}} \frac{8BI}{m\pi\mu\omega_m^2} \cos\frac{m\pi z}{L^*} e^{-\lambda_m t} \cos\omega_m t \tag{97}$$

$$\dot{r}_m(z,t) \cong (-1)^{\frac{m-1}{2}} \frac{8BI}{m\pi\mu\omega_m} \cos\frac{m\pi z}{L^*} e^{-\lambda_m t} \sin\omega_m t \tag{98}$$

where $m = 1,3,5,\ldots$. Of course r_m and $\dot{r}_m$ are not directly observed in the experiment. The quantity measured is the induced e.m.f. The e.m.f. corresponding to the $m^{\underline{th}}$ pair of normal modes is

$$\mathcal{E}_m(t) \cong -B\int_{-L^*/2}^{L^*/2} \dot{r}(z,t)\,dz \tag{99}$$

$$\cong -\left(\frac{4B}{m\pi}\right)^2 \frac{IL^*}{\mu\omega_m} e^{-\lambda_m t} \sin\omega_m t \tag{100}$$

Equation (100) shows that the maximum e.m.f. induced by the $m^{\underline{th}}$ pair of normal modes is proportional to $1/m^3$, since $\omega_m \cong m\omega_1$. Since only the odd-numbered modes are excited $1/m^3 = 1$, 1/27, 1/125,...; the e.m.f. induced by the higher modes is very much smaller than $\mathcal{E}_1$. There are two reasons for this. One is that the higher modes are less strongly excited: at a given time $\dot{r}_m$ is proportional to $1/m^2$. The other is that $\dot{r}_m$ changes sign m - 1 times on L*, so the e.m.f., which is proportional to the integral of $\dot{r}_m$, is reduced by another factor of 1/m. Furthermore, the higher modes are damped more rapidly than the lower modes. The overall reduction is so large that only the lowest pair of modes was actually observed during the experiment. This fact justifies the use of the low-mode approximation for $f_{mo}(z)$ and $g_{mo}(z)$. Furthermore, r_1 and $\dot{r}_1$ can be properly thought of as the actual displacement and velocity of the symmetric wire with zero circulation, and $\mathcal{E}_1$ as the e.m.f. induced by the wire. With this understanding we shall consider only the lowest pair of normal modes from now on and omit the subscript m. r and $\dot{r}$ are plotted as functions of time for the first two cycles in Figure 9, along with the current pulse for reference. The duration of the current pulse is one half-period of vibration of the wire.

In order to compute r, $\dot{r}$, and $\mathcal{E}$ the induction of the permanent magnet has to be measured. This measurement was made

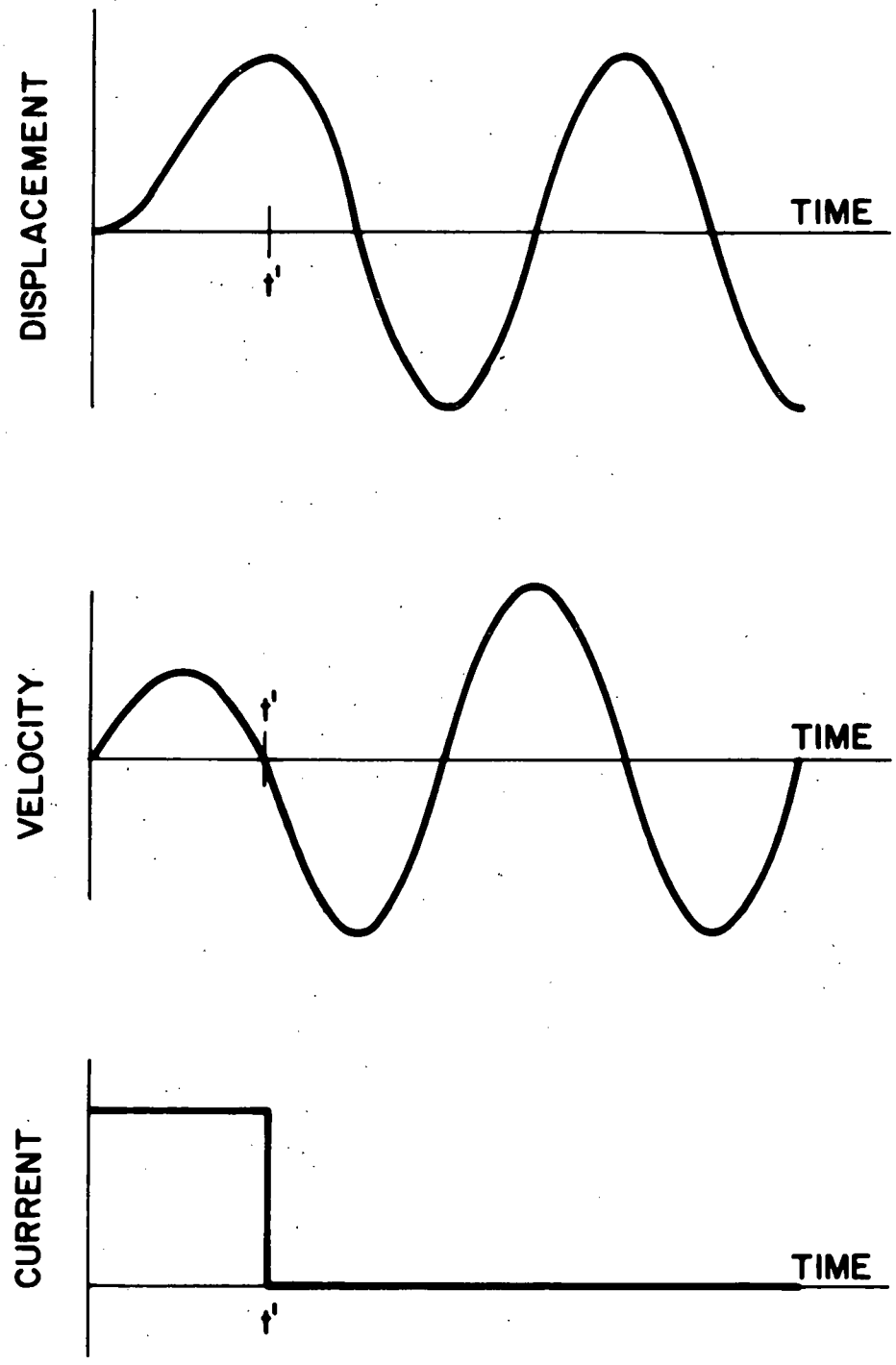

Figure 9. Wire Displacement, Velocity, and Driving Current as Functions of Time.

with a Hall-effect probe. The induction perpendicular to the wire measured along the axis of the wire had the profile sketched in Figure 10. The average of B over the length of the wire was 1.35 kG. The profile shows that B was not quite uniform over the length of the wire. As a result the relative amplitudes of the normal modes must have been slightly different in reality from the relative amplitudes given by (97).

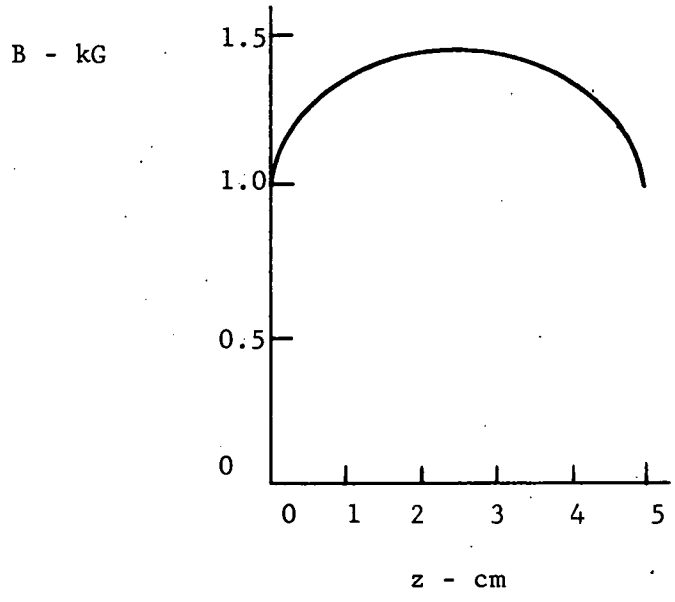

Figure 10. Profile of Stationary Magnetic Field Strength. B is the field strength perpendicular to the wire measured along the axis of the wire.

Values of the maximum displacement of the wire, which we call r_o, are tabulated for most of the experimental runs in

Tables 1a-d. Values of $\dot{r}_o$, the maximum velocity of the wire, are given by ωr_o; values of $\omega/2\pi$ are also listed in Tables 1a-d.

In addition to the requirement that the maximum displacement be small, another requirement which might be placed on the excitation of the wire in order not to disturb the circulation is that the maximum velocity of the wire be small compared to the superfluid velocity at the surface of the wire when the circulation is one quantum unit. In that case $\omega r_o \ll \frac{h}{m}\frac{1}{2\pi a} \simeq \frac{10^{-3}}{2\pi a}$. It proved to be impossible to satisfy this condition with the technique used in this experiment. That is, it was impossible to reduce the current pulse enough to satisfy this condition on the velocity, and still produce a large enough signal from the wire so that accurate measurements of the beat period could be made before the signal decayed below noise level. For example the smallest current pulse that could be used with fiber D, the 40 μ fiber, resulted in a maximum velocity at 500 cps of about 1.6 mm sec^{-1}, twice the fluid velocity at the surface of the wire for one quantum of circulation.

However, an observation was made which tends to cast doubt on the importance of the velocity criterion. It was found that even if the current was increased ten times from its lowest practical value the behavior of the apparent circulation did not change. That is, stabilities occurred at the same quantum levels as before, and, qualitatively, circulation changed with time in the same way. With this observation in mind it was

customary to use a fairly large current pulse, such that the maximum wire velocity was about twenty times the fluid velocity at the wire with one quantum of circulation. It should be noted that Vinen customarily used current pulses of this same size, applying the velocity criterion to his apparatus.

There is still a third criterion which might be applied to the amplitude of the current pulse, namely that the power dissipated in the wire due to Joule heating be small enough not to disturb the circulation. Values of the power I^2R are also listed in Tables 1a-d; R is the resistance of the wire when immersed in liquid helium. It is not known a priori what a suitable power limit might be. However, it can be seen in Tables 1a-d that the power dissipated in runs with wire G far exceeded the power required for runs with other wires, and that circulation observed with wire G was less stable than with other wires, and much less stable than with other wires of about the same diameter. In view of this fact it would seem to be a good rule to keep the power below 1 mW. Of course it is possible to reduce the power dissipation by evaporating more gold onto the fiber, reducing its electrical resistance.

Finally, it should be added that the time interval between successive current pulses used to excite the wire was 5.0 sec during those periods when circulation measurements were being made. This time interval was short enough to make possible a

detailed record of changes of circulation with time, yet long enough so that vibrations of the wire due to one current pulse had damped below noise well before the onset of the next pulse.

C. Bridge

A diagram of the Wheatstone bridge circuit appears in Figure 11a where the resistances in the arms of the bridge are those used with the 100 μ diameter fiber, fiber G, which had resistance 25 ohms at 1.2°K. The reason for using the bridge was to protect the selective amplifier from the current pulse which excites the wire. If the amplifier were just connected across the wire, for example, the current pulse would overload the amplifier so badly as to spoil its linear response to the oscillating e.m.f. from the wire. The transformer is introduced in order to isolate the output terminals of the bridge from ground, and to improve the impedance match to the amplifier.

Under normal operation the current pulse which excites the wire enters the circuit either at terminal #1 or #2. These two channels differ in their input impedance and in the fraction of the power drawn from the generator which each delivers to the wire. Terminal #2, with the high impedance, was used for most wires. However it was useful to have a low resistance channel available to admit very energetic pulses to the wire. These pulses, at current levels perhaps ten times the level of the pulses used to measure circulation, were sometimes used with the

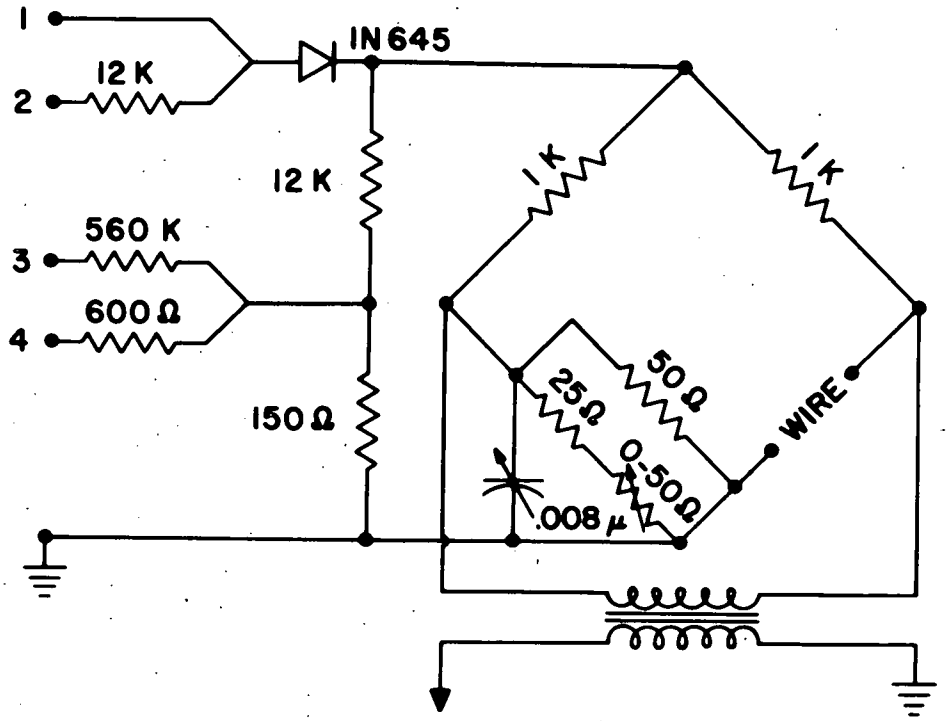

Figure 11a. Circuit Diagram of Bridge.

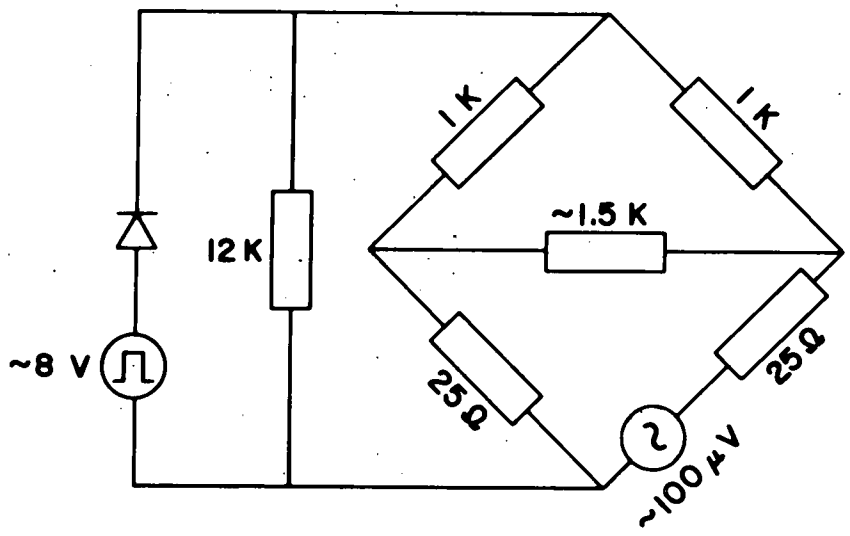

Figure 11b. Equivalent Circuit Diagram of Bridge.

deliberate intention of disturbing the apparent circulation with violent motion of the wire.

There are two other input channels to the bridge. Terminal #4 is suitable for use with an oscillator, should one wish to excite the wire with a continuous wave instead of a pulse. Terminal #3 was used with the regular current pulse when the wire had been manually switched out of the circuit, leaving that arm of the bridge open. In that case a current pulse appears across the transformer primary and excites the selective amplifier. The amplifier rings at its tuned frequency with oscillations which decay rapidly in time. These oscillations appear on the oscilloscope screen and permit a direct measurement of the time-constant for their decay. They also drive the frequency counter and permit a direct measurement of the frequency to which the amplifier is tuned. Both of these measurements were very useful for the experiment, for reasons which will become apparent, and were made often during the course of a run. Input channel #3 was provided so that the same current pulse could be used for these measurements as for the circulation measurements without overloading the amplifier.

The resistors which go into the arms of the bridge itself must be chosen so that the bridge can be balanced with the wire in place in the circuit. The resistance of the wire changes radically with temperature. For example, the resistance of

fiber G fell from 110 ohms at room temperature to 25 ohms at 1.2°K. The resistors shown in Figure 11a are appropriate for balance with fiber G at 1.2°K. It was also necessary to balance stray capacitance in the leads to the wire, which could be quite large. The balance conditions for the bridge are independent of frequency, so should hold true for any pulse. Nevertheless, in practice it was impossible to eliminate small transient currents from the transformer whenever the pulse was turned on or off. However, with good capacitive balance these currents could be reduced to a level comparable to the currents induced by the vibrating wire.

Once excited by the current pulse the vibrating wire acts as an ac generator in the circuit shown schematically in Figure 11b. Figure 11b includes just those circuit elements needed to compute impedances. One requirement of this circuit is that enough power from the wire be delivered to the transformer to provide an output signal to the selective amplifier which is well above electrical noise. The turns ratio of the transformer was 1:17.7.[58] Its input impedance reflected from the selective amplifier was about 1.5 K. The resistance in the two upper arms of the bridge must be about as large as 1.5 K in order to prevent them from shunting power away from the transformer.

In addition to the bridge itself there are two other branches in the circuit, parallel to the bridge, which draw current from

the wire and should have high impedance. One of these branches is the pulse generator itself, which has an output impedance which can be as low as a few ohms. In order to prevent it from loading the wire a solid state diode was inserted between the generator and bridge. This diode presents a low resistance to positive pulses from the generator, when the pulse height is a few volts. However it presents a very high resistance in both directions to the e.m.f. generated by the wire, which is of the order of 100 μV.

With all these safeguards built into the circuit the power delivered to the selective amplifier by the vibrating wire was large enough so that electrical noise was not a serious limitation on the experiment. The noise which limited the sensitivity of the experiment was acoustic noise in the liquid helium. The electrical signal to the oscilloscope was much noisier when the wire was immersed in liquid helium than when it vibrated in air or in vacuum.

Since electrical noise was not a serious limitation it was important that electrical damping of the wire be kept small compared to the viscous damping. The damping time constant of the wire is equal to Q/ω, where ω is the angular frequency of the wire and Q is the ratio between the energy stored in the wire and the energy it loses per radian of vibration. To evaluate the electrical damping we consider a symmetric wire with no circulation. Let the maximum velocity of the wire during any one cycle

of vibration be represented by $\dot{r}(z,t) \cong \dot{\theta}(t) \cos \frac{\pi z}{L^*}$. Then the energy stored in the wire, neglecting damping during the cycle, is

$$E_s \cong \frac{1}{2} \mu \dot{\theta}^2_{max} \int_{-L^*/2}^{L^*/2} \cos^2 \frac{\pi z}{L^*} \, dz \tag{101}$$

$$\cong \frac{\mu L^*}{4} \dot{\theta}^2_{max} . \tag{102}$$

The energy lost per radian due to electrical dissipation is, using equation (99)

$$E_d = \frac{\mathcal{E}^2_{max}}{2R\omega} \cong \frac{B^2}{2R\omega} \dot{\theta}^2_{max} \left[\int_{-L^*/2}^{L^*/2} \cos \frac{\pi z}{L^*} \, dz \right]^2 \tag{103}$$

$$\cong \frac{2L^{*2}B^2}{\pi^2 R\omega} \dot{\theta}^2_{max} . \tag{104}$$

Here R is the total resistance which loads the wire. Then the Q of the wire, considering only electrical dissipation, is

$$Q_e \cong \frac{\pi^2}{8} \frac{\mu R\omega}{L^* B^2} . \tag{105}$$

The time constant for electrical damping is

$$\frac{Q_e}{\omega} \cong \frac{\pi^2}{8} \frac{\mu R}{L^* B^2} . \tag{106}$$

The resistive load on fiber G can be estimated from Figure 11b to be about 1 K. Then Eq. (106) with the measured characteristics of the wire and magnet gives $\frac{Q_e}{\omega} \cong 30$ sec. The damping time constant of fiber G as actually measured in liquid helium at 1.2°K was about 0.5 sec, very close to the time constant

calculated from viscous damping alone. It is clear that the electrical load on the wire was a negligible source of damping for this fiber, as indeed it was for all the others. This conclusion was verified by the observation that the damping time constant for the wire oscillating in vacuum was very much larger than in liquid helium.

D. Selective Amplifier

The selective amplifier consists of three stages, a pre-amplifier, a frequency-selective amplifier, and a second linear amplifier. Only the first two stages were used in these measurements. The frequency selection of the second stage is accomplished using a linear amplifier with negative feedback through a null network. The network is tuned to transmit no signal at the chosen operating frequency of the amplifier. Since negative feedback occurs at all other frequencies the over-all response of the amplifier peaks at the frequency selected. The response of the amplifier for frequencies not too different from the resonant frequency is nearly equivalent to that of a forced, damped harmonic oscillator with a Q of about 20. This was too high a Q for some measurements, and in those cases the Q was reduced by inserting a variable resistance in the null network's connection to ground.

It was nearly essential to use a selective amplifier in this experiment because of its noise rejection. However the

instrument did complicate the measurements in an important way, for the following reason. In principle the frequency splitting $\Delta\omega$ is found by measuring the period $2\pi/\Delta\omega$ between successive nodes of the beat pattern. However, in practice the damping of the wire is large enough to make it necessary instead to measure the time interval between the initial excitation of the wire, which corresponds to a beat maximum, and the appearance of the first node. For example, Table 1c shows that the damping time constant for fiber E at $1.20^{o}K$ and 500 cps was 350 msec. This means that if the signal from the wire decayed to noise level in three time constants, then in order to measure $\Delta\omega_o$ using two nodes of the beat pattern $\Delta\omega_o$ would have to be about as large as $3\pi/(3\times.350) \cong 3\pi$ rad/sec. For fiber E the frequency splitting $\Delta\omega_n$ with one quantum unit of circulation at $1.20^{o}K$ was 1.24 rad/sec. Even with three quantum units of circulation the total frequency splitting $\Delta\omega = \sqrt{(\Delta\omega_o)^2+(\Delta\omega_n)^2}$ would be only 10 rad/sec, and the period between nodes would shift because of circulation by only 7%. However, using just the first node $\Delta\omega_o$ could be set at πrad/sec. Then three quantum units of circulation would shift the measured time interval by 36%.

In order to understand the influence of the selective amplifier on the beat pattern, let us treat the incident signal as the sum of two sinusoidal signals of slightly different frequency. Being a resonant system the amplifier changes the

phase of each signal by an amount which depends on its frequency. Consequently the amplifier shifts the phase difference between the two signals, and, since it is the steadily changing phase difference which generates the beat pattern, it shifts the phase of the beat pattern. That is, it shifts the measured time interval between the current pulse to the wire and the appearance of the first node on the screen of the oscilloscope. The shift is always such as to increase this interval, and since the increase can be as large as 10% it is important to know it accurately. The amplifier would not affect the interval between successive nodes if in fact more than one could be observed.

Of course it was impossible to measure the time delay directly so long as liquid helium covered the wire. What was done was to assume that the amplifier behaves just like a damped harmonic oscillator, and then calculate the time delay in terms of something that could be measured, namely the Q of the amplifier and wire. As a check on its validity the same procedure was used when the wire was set vibrating in vacuum. In that case it was possible to measure the time delay directly, for example by comparing the time it took the first node to appear with the time interval between successive nodes. The calculated time delays were generally about 10% $\pm$ 5% smaller than the measured values. It was then assumed that the same calculation could be applied when helium covered the wire. If this assumption

is correct the error introduced into the circulation measurements by the amplifier was 1% or less except in a few cases.

In order to understand the criteria used in tuning the amplifier and selecting its Q, it is useful to go through the calculation of its time delay in some detail. Considered as a harmonic oscillator its response to a driving signal f(t) is proportional to the solution x(t) of the equation

$$\ddot{x}(t) + 2\gamma\,\dot{x}(t) + \omega_o^2\,x(t) = f(t). \tag{107}$$

Here $1/\gamma$ is the time constant for free decay of the amplifier and ω_o is the fictitious undamped frequency of the amplifier. The driving function f(t) is the e.m.f. induced by the two lowest normal modes of the vibrating wire. Once the current pulse to the wire has been turned off f(t) has the form, from Eq. (87),

$$f(t) \simeq \mathcal{E}_o\, e^{-\lambda t}(\sin \omega^+ t + \sin \omega^- t). \tag{108}$$

With this driving signal the response of the amplifier is proportional to

$$x \simeq \frac{\mathcal{E}_o}{2\omega(\gamma-\lambda)} \left\{ e^{-\gamma t}(\sin^2\alpha^+ + \sin^2\alpha^-)\, \frac{\sin(\omega_o t + \beta)}{\sin\beta} \right.$$
$$\left. -e^{-\lambda t}\left[\sin\alpha^+ \sin(\omega^+ t + \alpha^+) + \sin\alpha^- \sin(\omega^- t + \alpha^-)\right] \right\}. \tag{109}$$

Here $\omega = \frac{\omega^+ + \omega^-}{2}$ and the approximation has been made in factoring out the leading coefficient that $\omega^+ \simeq \omega^- \simeq \omega$. $\alpha^\pm$ and β are functions of the frequencies and damping constants. $\alpha^\pm$ are given by (110); β will not be needed in the discussion which follows.

The response of the amplifier is the sum of two terms which decay with different time constants. Since in practice $\gamma >> \lambda$ the first term is the transient part of the response, and the second term corresponds to the steady state of a resonator driven by a steady signal. In this case the second term is the slowly decaying beat pattern which is used to measure circulation. In order that the first term not interfere with the measurement it is essential that it decay to noise level before the first node of the beat pattern appears. Otherwise this first term would itself beat with the signal from the wire and produce a spurious effect. This is one condition on the Q of the amplifier, that the time constant for decay, which is $1/\gamma = Q/\omega_o$, be small enough to prevent interference with the measurement. For nearly all runs $1/\gamma \leqq 10$ msec even with the amplifier at its full Q of about 20, whereas the time interval to the first node was nearly always greater than 300 msec.

It is apparent from the second term of (109) that the two components of the driving signal from the wire are shifted in phase, each by a different amount. The phase shifts are

$$\alpha^{\pm} = - \tan^{-1} \frac{2(\gamma-\lambda)\omega^{\pm}}{\omega_o^2 - \omega^{\pm 2} - 2\lambda(\gamma-\lambda)} . \qquad (110)$$

The relation between phase shift and frequency is plotted in Figure 12. The slope of this curve is positive or negative depending on the sign of $\gamma-\lambda$. In practice $\gamma-\lambda$ is always positive and the curve has been drawn accordingly.

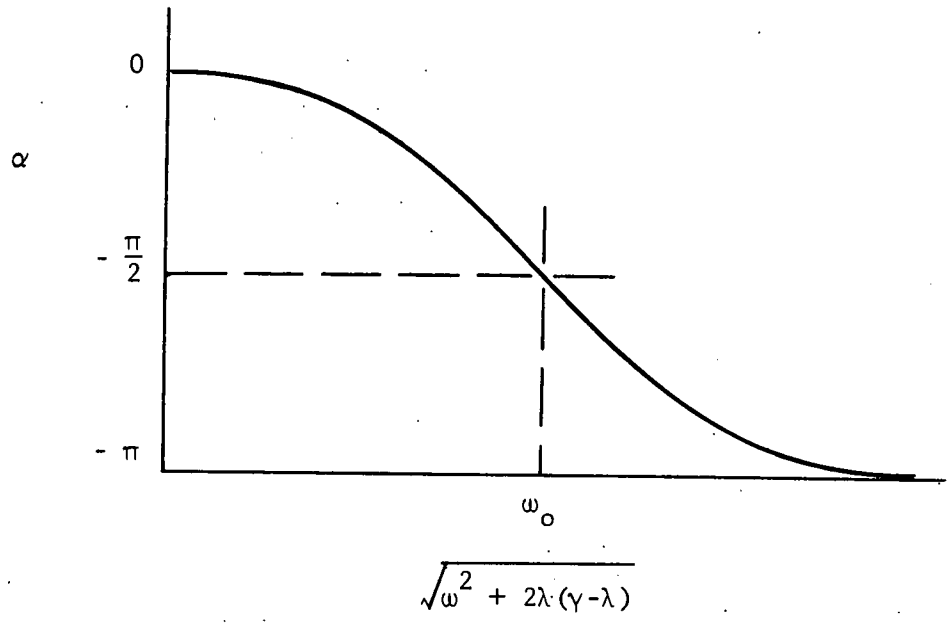

Figure 12. Phase Shift in Response of a Resonant System Relative to Driving Signal as a Function of Frequency

It is apparent from the plot that for a given frequency splitting $\Delta\omega$ between the two lowest normal modes of the wire the difference between the two phase shifts is largest in the neighborhood of $\alpha = -\frac{\pi}{2}$, where the curve has its steepest slope. If the difference between the phase shifts is $\Delta\alpha = \alpha^{+}-\alpha^{-}$ the first node of the beat pattern is shifted in time by $-\frac{\Delta\alpha}{\Delta\omega}$. From the plot $\Delta\alpha/\Delta\omega$ is negative, so the time shift is always positive; that is, the appearance of the node is delayed. The time delay is a maximum when $\alpha^{\pm} = -\frac{\pi}{2} \pm \frac{\Delta\alpha}{2}$. We recall that at resonance an oscillator shifts the phase of a single driving sine wave by

$-\frac{\pi}{2}$. The corresponding condition for resonance here is that the average phase shift equal $-\frac{\pi}{2}$, where the average phase shift is $\alpha = \frac{\alpha^+ + \alpha^-}{2}$. Then one test of whether or not the amplifier is at resonance with the wire is that the time delay should be a maximum.

The long-lived response from the amplifier can be written in the form

$$x_2 \cong \frac{\mathcal{E}_o}{2\omega(\gamma-\lambda)} e^{-\lambda t}\left[\sin^2\alpha^+ + \sin^2\alpha^- + 2\sin\alpha^+ \sin\alpha^- \cos(\Delta\omega t + \Delta\alpha)\right]\sin(\omega t+\alpha). \tag{111}$$

When $\alpha^{\pm} = -\frac{\pi}{2} \pm \frac{\Delta\alpha}{2}$ we have

$$x_2 \cong -\frac{\mathcal{E}_o}{\omega(\gamma-\lambda)} e^{-\lambda t} \cos\frac{\Delta\alpha}{2} \cos\left[\frac{\Delta\omega}{2}\left(t+\frac{\Delta\alpha}{\Delta\omega}\right)\right]\cos\omega t. \tag{112}$$

At resonance the long-lived response of the amplifier is a fully modulated beat pattern of angular frequency $\frac{\Delta\omega}{2}$, provided that the two normal modes of the wire are equally excited. Therefore another test of whether or not the amplifier is tuned for resonance is that the node of the beat pattern should be a true null. For comparison with (112) we note that (108), the e.m.f. from the wire, can also be written

$$f(t) \cong 2\mathcal{E}_o e^{-\lambda t} \cos\frac{\Delta\omega t}{2} \sin\omega t. \tag{113}$$

The condition for resonance that $\alpha \cong -\frac{\pi}{2}$ is satisfied when the amplifier is tuned so that

$$\omega_o^2 = \omega^+\omega^- + 2\lambda(\gamma-\lambda). \tag{114}$$

Then

$$\alpha^{+} = \tan^{-1} \frac{2(\gamma-\lambda)}{\Delta\omega} \tag{115}$$

$$\alpha^{-} = -\tan^{-1} \frac{2(\gamma-\lambda)}{\Delta\omega} \tag{116}$$

$$\frac{\Delta\alpha}{2} = -\tan^{-1} \frac{\Delta\omega}{2(\gamma-\lambda)} . \tag{117}$$

The first two terms in the Taylor expansion of $\tan^{-1}$ give

$$\frac{\Delta\alpha}{2} \cong -\frac{\Delta\omega}{2(\gamma-\lambda)} + \frac{1}{3}\left(\frac{\Delta\omega}{2(\gamma-\lambda)}\right)^{3} . \tag{118}$$

The time delay in the appearance of the first node, which we call $\Delta\tau$, is then given by

$$\Delta\tau = \left|\frac{\Delta\alpha}{\Delta\omega}\right| \cong \frac{1}{\gamma-\lambda}\left[1 - \frac{1}{12}\left(\frac{\Delta\omega}{\gamma-\lambda}\right)^{2}\right] . \tag{119}$$

Another condition on the Q of the amplifier was thought to be that it should be small enough so that the time delay was 10% or less of the measured time interval, which is roughly $\pi/\Delta\omega$. With this condition satisfied

$$\left|\frac{\Delta\alpha}{\Delta\omega}\right| \frac{\Delta\omega}{\pi} \cong \frac{\Delta\omega}{\pi(\gamma-\lambda)} \leq 10\% \tag{120}$$

$$\frac{\Delta\omega}{\gamma-\lambda} \leq \frac{1}{3} . \tag{121}$$

Then (119) shows that the time delay is equal to $\frac{1}{\gamma-\lambda}$ to 1% accuracy.

Therefore in order to compute the time delay in the approximation that the amplifier behaves like a harmonic oscillator it was necessary only to measure the time constants for decay of

the amplifier and wire. The time constant of the wire was measured from its decay pattern on the oscilloscope screen. To make an accurate measurement the wire had to be rotated so that only one of its lowest normal modes was excited by the current pulse. However for most wires the measurement had to be made only once at a given temperature and frequency. For most wires at the frequencies used the decay was so much slower than the amplifier that it had only a small effect on the computed time delay. It was safe to assume that the results of one measurement could be used for several experimental runs.

On the other hand it was important to know the time constant of the amplifier accurately, to 10% at least. Furthermore, it had to be measured periodically throughout a single run since it was capable of drifting in time. This measurement could be made in either of two ways, which gave results in good agreement with each other. One way was to excite the amplifier with an impulse then watch its free decay on the oscilloscope. The other way was to drive it with a continuous wave from an auxiliary oscillator at the frequency of the wire and measure the half-width of its response function near resonance. The half-width of the voltage resonance, defined as the difference between the two frequencies at which the output voltage from the amplifier falls to one-half its maximum value, is related to the decay rate γ as $\Delta\omega_{\frac{1}{2}} = \sqrt{12}\,\gamma$. Of the two methods, the first was easier and used more often.

The computation of the time delay using these measured time constants is correct only if the amplifier is at resonance, so it is important to tune the amplifier carefully. When corrections of order $(\Delta\omega/\omega)^2$ are neglected, the amplifier is at resonance when its frequency in free decay is equal to the carrier frequency of the e.m.f. from the wire. The carrier frequency from the wire is continually monitored throughout a run by the electronic counter, and the frequency of the amplifier in free decay can easily be measured by exciting the amplifier with an impulse and timing its period of oscillation with the same counter. The most convenient way to tune the amplifier was just to make these two frequencies equal, and it was verified even with the wire vibrating in vacuum, when the beat pattern could be very accurately observed, that this method gave a true resonance. That is, the beat pattern which resulted was fully modulated, with true nulls at the nodal points; the measured time to the first node was a maximum; and the over-all amplitude of the pattern was a maximum.

In principle it should have been possible to omit the use of the counter and determine whether or not the amplifier was tuned for resonance just by observing the beat pattern. However, this method proved to be difficult when the wire was immersed in liquid helium, because especially near the beginning of a run the beat pattern was continually changing because of changes in the circulation.

Another advantage of tuning with the frequency counter was that it made it easy to align the wire properly in the field of the stationary magnet. With the amplifier at resonance it was only necessary to rotate the wire until the amplitude of the beat pattern at the node went to zero, to be sure that the wire was aligned so that its two normal modes were excited with equal amplitude. It was easy to tell when the amplitude at a node went to zero, or at least fell below noise level, whatever the level of the circulation. However, it was not possible to use this observation in reverse, as a fool-proof determination that the amplifier was properly tuned. One could get a null even with the amplifier off resonance, if the normal modes of the wire were excited unequally. Of course such a null would not reflect the true time delay as computed above, and would lead to error in the measurement of circulation.

E. Magnet Control

The circuit which controls the current in the superconducting electromagnet is shown in Figure 13. The circuit is designed so that when a manual switch has been closed, a current pulse will gate on a large current in the magnet. The current stays on for the duration of the pulse, and the size of the current is determined to some extent by the pulse height. Currents used were about 1 A, for periods of a few milliseconds. The inductance of the magnet at 1.2^{o}K was 12.7 mH. The rise time of the current was

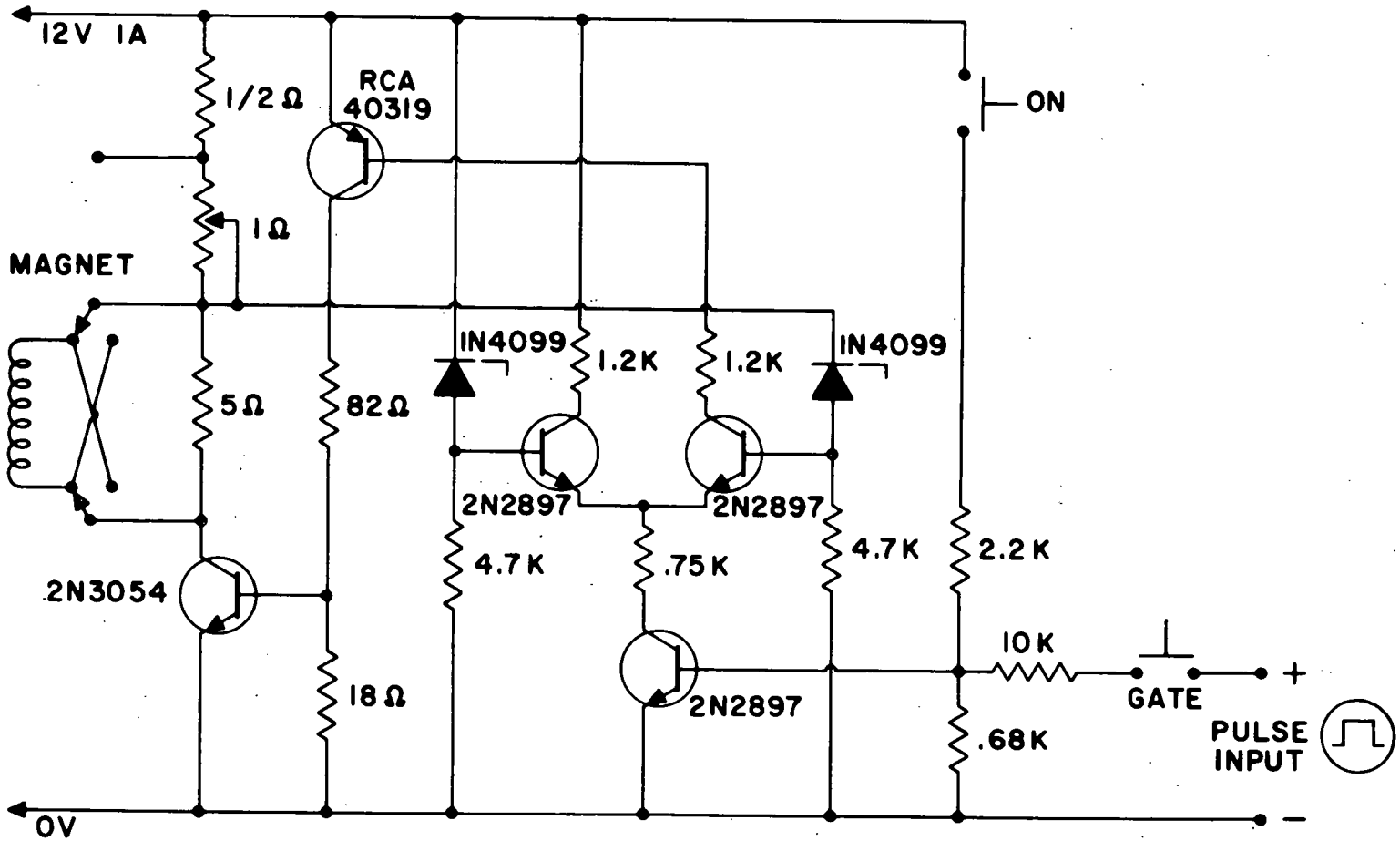

Figure 13. Circuit Diagram of Magnet Control.

about 2 msec. An auxiliary switch is provided for turning on the magnet at will. It is useful, for example, to be able to turn on the magnet before the vibrating wire is excited, and leave it on until after the appearance of the first node of the beat pattern. This is equivalent to rotating the stationary magnetic field through a small angle, raising the amplitude of the e.m.f. at the first node. Then if the polarity of the permanent magnet is known it is possible to determine the polarity of the electromagnet just by rotating the wire slightly to see which direction of rotation restores the amplitude at the first node to zero.

V. PROCEDURE

The procedure used to measure circulation during a typical experimental run was as follows. To begin, the apparatus and dewar were pre-cooled overnight with liquid nitrogen, then liquid helium was transferred into the dewar itself. The liquid flowed into the cylindrical vessel containing the wire and covered it to a depth of as much as 50 cm. The apparatus and helium bath were then cooled from $4.2^{\circ}K$ to $1.2^{\circ}K$ by pumping.

In some cases the assembly carrying the vessel and wire was rotated during cooling. The rotation and cooling were timed so that rotation would continue for several minutes at temperatures above T_{λ} to allow the fluid around the wire to come into equilibrium with the wall of the vessel. Calculations show that the longest time constant to be associated with the fluid's coming into rotation was 45 sec. The rate of cooling was controlled by regulating the pressure in the pump manifold. At $1.2^{\circ}K$ the rotation was stopped and the temperature stabilized by balancing the regulating bridge. If the pumping rate was adjusted properly the bridge would keep itself in balance at the chosen temperature. Then it was possible to start pulsing the wire and observing its beat pattern on the oscilloscope.

Measurements of the beat period were most accurately made when the beat pattern was 100% modulated, that is, when the amplitude of the induced e.m.f. fell below the acoustic noise

level at the observed node. In order to achieve this degree of modulation it was necessary for the axes of the elliptical normal modes of the wire to lie at an angle of 45^{o} to the direction of the magnetic field. In this orientation the normal modes were excited with equal amplitude by the current pulse. Ordinarily, on stopping rotation, the normal modes would lie at some other angle, and the wire assembly would have to be turned by hand to achieve full modulation.

If the position of the first node of the beat pattern on the screen of the oscilloscope was to shift under the influence of circulation by an amount which was large enough to measure accurately, it was necessary for the intrinsic frequency splitting $\Delta\omega_o$ to be about equal in size to the expected frequency splitting due to circulation, $\Delta\omega_\kappa$, or smaller. Usually, after cooling, a first examination of the beat pattern showed a value of $\Delta\omega_o$ which was too large, and the wire had to be twisted to reduce $\Delta\omega_o$ to a proper size. The angle through which the wire was twisted was carefully recorded each time, to prevent it from being twisted far enough to break. Generally the orientation of the normal modes would shift each time the wire was twisted, so that it was necessary to turn the wire assembly by hand to restore full modulation to the beat pattern.

In practice it was found that $\Delta\omega_o$ also depended strongly on the average frequency of the wire, ω, so that to some extent $\Delta\omega_o$ could also be controlled by changing the tension in the wire.

Usually $\Delta\omega_o$ was reduced by increasing ω, that is by tightening the wire. However, since the e.m.f. induced in the wire for a given driving pulse decreases as ω^{-1}, and its damping time constant decreases roughly as $\omega^{-\frac{1}{2}}$, it was advantageous when possible to fix ω at some small value, for example 500 cps, and rely on the twisting technique alone to reduce $\Delta\omega_o$. Unfortunately the frequency ω usually shifted uncontrollably each time the wire was twisted and had to be restored to its initial value before the effect of the twist on $\Delta\omega_o$ could be determined.

There were two other considerations which affected a choice of the wire frequency ω. It was found that if ω was made too small, even in the absence of circulation the wire no longer behaved in a way which could be described as the superposition of plane-polarized normal modes. For example the beat pattern might be only partially modulated but not depend on the orientation of the wire in the magnetic field; or the damping of the wire might even depend on orientation. A pattern which depended on orientation in the proper way could generally be restored by raising the tension in the wire. A second consideration was that at some frequencies the acoustic noise picked up by the wire was much larger than at others. Presumably at those frequencies the wire was tuned to a mechanical resonance in the apparatus, and it was imperative that they be avoided.

In order to establish a certain intrinsic frequency splitting $\Delta\omega_o$ on the wire, it was of course necessary to know when the circulation around the wire went to zero. This was by no means a trivial problem, since it was found that large amounts of circulation appeared spontaneously around the wire even when the apparatus was cooled to 1.2°K without rotation. It might be supposed that $\Delta\omega_o$ could be measured above T_λ, where the fluid was entirely normal and at rest, or at 1.2°K in helium vapor. However, at T_λ the damping of the wire was much too large to permit measurement of a suitable $\Delta\omega_o$, and it was found that $\Delta\omega_o$ was in general very different when the wire was immersed in liquid helium at 1.2°K than when the wire was surrounded by helium vapor at the same temperature. This last effect would be expected for a wire of elliptical cross-section, since the contribution of the liquid to the effective mass density of the wire would then be different in different directions.

Vinen found it to be a general rule in his experiment that the observed total frequency splitting $\Delta\omega$ always decreased to a well-defined minimum value "just before the helium drained out of the space surrounding the wire."[59] He took this value of $\Delta\omega$ to be equal to $\Delta\omega_o$. In the present experiment $\Delta\omega$ was observed to take on an unusually steady value during almost every run when the surface of the helium bath had fallen to a level about 1 cm above the top of the wire. However, except in a few cases this steady value was not the minimum value for that run. These

unusual levels were regarded as probably spurious effects of the apparatus. It was impossible to regard them as defining $\Delta\omega_o$.

There were two independent methods in this experiment of successfully determining the frequency splitting with zero circulation. One of them was just to excite the wire repeatedly and observe $\Delta\omega$ over a period of time. It was found that near the beginning of a run, during the first few hours after the liquid helium transfer, $\Delta\omega$ would decrease to a well-defined minimum value several times an hour. It was sometimes possible to drive $\Delta\omega$ to a minimum by heating the wire briefly with a direct current. This value of $\Delta\omega$ was taken, provisionally, to be equal to $\Delta\omega_o$. If later in the run $\Delta\omega$ fell to a lower minimum, then $\Delta\omega_o$ had to be revised to be equal to this new value. In practice such revisions as had to be made were very minor, amounting at most to 2% of the assumed value. What was striking was the reliability with which the assumed minimum would reappear throughout a run lasting as long as 22 hours. The small changes that did occur were usually brought on by warming and cooling the apparatus or by a fast rotation.

Early in the experiment, as a means of determining that the behavior of the wire had not changed during a run, and by inference that $\Delta\omega_o$ had remained stable, it was customary to transfer liquid helium twice during a run and each time let the liquid

drain completely away from the wire. Measurements of the frequency splitting in helium vapor were made each time, and compared. The measurements usually agreed to within 2%. After several runs of this kind the apparatus was felt to be reliable enough that this practice could be abandoned.

Another method of determining frequency splitting with zero circulation was provided by the superconducting electromagnet. The purpose of the electromagnet was to shift the position of the first node of the beat pattern on the face of the oscilloscope either to the left or right depending on the direction of the circulation around the wire. When the circulation was zero the electromagnet produced no shift in the node position. The reason for this is that a shift in the node position is the result of a shift in the relative phase of the two lowest normal modes of the wire. Having the electromagnet turned on at the time the wire is excited by the current pulse shifts the relative phase of the two normal modes from what it would be with the electromagnet off, provided that the normal modes are circularly or elliptically polarized. If they are plane-polarized, as is the case with zero circulation, the normal modes are excited with a phase difference of either 0° or 180° whatever the direction of the magnetic field. To be sure, they are excited with different amplitudes and the node of the beat pattern is smeared out. Nevertheless it does not shift in time, so its position on the screen of the oscilloscope is the same as

it is when the electromagnet is left off. This effect occurs only in the presence of zero circulation, so uniquely identifies $\Delta\omega_o$.

Once a suitable value of $\Delta\omega_o$ had been established on the wire at a suitable frequency ω, the twist control was locked with set screws and the frequency carefully measured with the electronic counter. The selective amplifier was carefully tuned to be in resonance with the wire, and the orientation of the wire in the magnetic field was adjusted for full modulation of the beat pattern. This orientation was then recorded, and subsequent measurements of the beat period were all made either with the wire assembly in this position or rotated through multiples of 90^o.

In preparation for the measurements the width of the current pulse was set to one-half the period of vibration of the wire, and the current amplitude was fixed at an appropriate level using the criteria discussed in chapter IV. The current was measured by measuring the resistance of the wire with an ohmmeter and the pulse voltage to the wire with the oscilloscope. The maximum signal to the oscilloscope generated by the wire was also measured and recorded as a check on the amplitude of vibration of the wire. The gain of the bridge and amplifier had been measured previously. Of course knowing the current and the voltage in the pulse it was easy to compute the power dissipated in the wire.

The stage was now set for careful measurements of the position of the first node of the beat pattern on the screen of the oscilloscope. The wire was excited once every five seconds by the current pulse. The position of the node was read by eye, and recorded by hand as a point on a roll of chart paper. The direction of the apparent circulation was measured by pulsing the wire several times with the electromagnet alternately on and off. Then the polarity of the magnet was reversed and the same procedure repeated. Measurements could be continued essentially without interruption for as long as the observer's stamina would permit or until the helium bath level fell to the top of the wire.

It was a good idea to check the beginning of the beat pattern periodically throughout a run to make sure that it coincided with the zero position on the graticule of the oscilloscope. It was quite possible for it to drift out of position during a long run. It was also a good idea to calibrate the sweep speed of the oscilloscope before and after a run using an audio oscillator and the frequency counter.

With these precautions the measured node positions could be converted into time measurements. However, before these time measurements could be used to compute the frequency splitting $\Delta\omega$, it was necessary to subtract the time delay introduced into the beat pattern by the selective amplifier. To know the time

delay it was necessary to measure the damping time constants of both the wire and amplifier. Again, it was a good idea to measure the time constant of the amplifier periodically, because it could drift by 10% during the course of a long run. The time constant of the wire had to be measured only once for a given wire at a given frequency and temperature.

Knowing the time delay it was then possible to use the measured node positions to compute the total frequency splitting $\Delta\omega$. Knowing the frequency splitting for zero circulation, $\Delta\omega_o$, it was possible to compute $\Delta\omega_\kappa$. Finally, knowing the effective mass density of the wire and the superfluid density ρ_s at the temperature used, it was possible to compute the apparent circulation at each point of the data record in units of h/m. Values for ρ_s were obtained from the tables of Reynolds et al.[60] In practice what was done was to calculate the apparent circulation at a few points covering the range of node positions observed, then to draw a calibration curve for each temperature of that particular run directly relating time at the appearance of the first node to apparent circulation. One such curve, for run E-7 at 1.20°K, is shown in Figure 14.

Although most measurements were made at 1.2°K some measurements were made at higher temperatures, up to 1.9°K. Measurements at higher temperatures were necessarily less accurate, because as the temperature increases $\Delta\omega_\kappa$ decreases in proportion

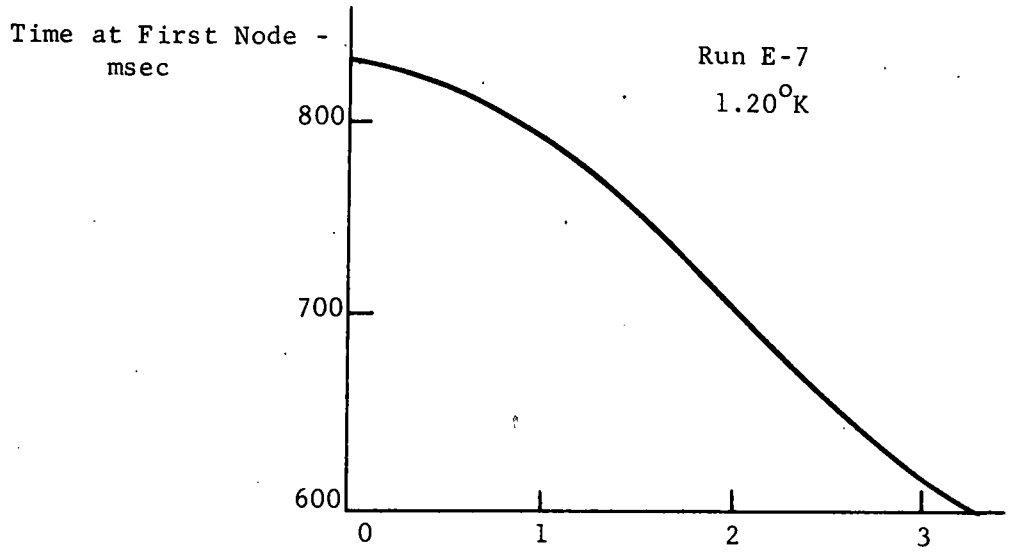

Figure 14. Time at First Node as a Function of Apparent Circulation for Run E-7 at 1.20°K

to ρ_s, and the damping gets larger as ρ_n increases. Also, the delay time of the amplifier increases with larger damping. At 1.9°K ρ_n/ρ is equal to 42%; above that temperature the damping is so large that no measurements were possible.

VI. RESULTS

A. Results

Two methods have been chosen to display the results of circulation measurements for a given experimental run. One is just to plot apparent circulation against time as the run progressed. The other is to compile a histogram of the total time the apparent circulation remained stable at each value of the circulation. Examples of both kinds of display appear in the following pages. No attempt has been made here to present an exhaustive record of results. Many runs are not represented by graphs at all. Instead the attempt has been made to present interesting features of the results, and runs are reported which exemplify those features.

Thirty-six runs were made in all. The first eight were made with a wide-band amplifier which had a much poorer signal-to-noise ratio than the narrow-band amplifier used later. Also, the beat period was determined during these early runs by measuring the time interval between the first two nodes of the beat pattern instead of the interval between the initial excitation of the wire and the first node, so that the shift in the beat period induced by circulation was very small. It was impossible to measure these small shifts accurately by eye. Instead the beat pattern on the screen of the oscilloscope was photographed with a Polaroid camera, and distance measurements were

made on the photographs with a travelling microscope after the run was finished.

Because of the effort required by this method the beat period was recorded on the average once every several minutes instead of once every five seconds as was done later. Apparent circulation was observed at values between zero and one quantum units, but otherwise the results, being so fragmentary, were not very interesting. Of these first eight runs the first five were made with platinum wires with diameter 25 μ, and the other three with quartz fibers with diameter about 12 μ. It is interesting that Vinen, although he used a narrow-band amplifier and just one node of the beat pattern, was forced to rely on photographs for his measurements.

All of the runs subsequent to these first eight are listed in Tables 1a-d, together with the important measured parameters for each run. The third row from the bottom of the table shows for each run the number of hours during which the apparent circulation was actually being measured, at the rate of one measurement every 5 seconds (every 10 seconds for runs C-1, C-2, and C-3). For runs which went to completion this time varied from 1 to 10 hours. The next-to-last row of the table shows for each run the ratio of the total time during which the apparent circulation remained stable to the total time during which circulation was observed. The criterion according to which

TABLE 1a. Experimental Parameters for Runs with Wire C

Wire				C			
Wire Diameter - μ				25			
Eff. Mass/Length - $\mu g\ cm^{-1}$				23			
$\Delta\omega_n$ (1.20°K, n=1)-rad sec^{-1}				6.1			
Decay time $1/\lambda$ (1.20°K, 500 cps)- msec				110			
Figure of Merit $\Delta\omega_n/\lambda$				.670			
Run Number	1	2	3	4	5	6	7
Wire Frequency $\omega/2\pi$ - cps	333	338	333	570	462	572	542
$\Delta\omega_o$ - rad sec^{-1}	10.3	4.6	8.9	9.8	8.7	8.7	8.4
Amplifier Time Delay (1.20°K)- msec	95	20	17	20	20	20	20
Power in Current Pulse - μW	16	16	16	16	16	16	16
Max. Wire Displacement - μ	8.4	8.4	8.4	2.9	4.2	2.9	3.2
Rotation Speed above T_λ - rad sec^{-1}	41	—	37	36	—	77	95
Total Observation Time - hrs	0.9	0.2	2.0	1.6	0.8	1.4	0.5
Time in Stable Levels/ Time of Observation	.33	0	.13	.41	.61	.70	.36
Quantum Levels Observed	0,1,2	—	—	0,1	—	0	0

TABLE 1b. Experimental Parameters for Runs with Wire D

Wire				D			
Wire Diameter - μ				39.4			
Eff. Mass/Length - $\mu g\ cm^{-1}$				40.1			
$\Delta\omega_{\mu}$ (1.20°K, n=1)-rad sec^{-1}				3.52			
Decay time $1/\lambda$ (1.20°K, 500 cps) - msec				190			
Figure of Merit $\Delta\omega_{\mu}/\lambda$				.670			
Run Number	1	2	3	4	5	6	7
Wire Frequency $\omega/2\pi$ - cps	482	503	499	502	502	501	519
$\Delta\omega_{o}$ - rad sec^{-1}	8.58	7.27	7.58	9.03	5.07	4.98	4.95
Amplifier Time Delay (1.20°K) - msec	37	40	16	45	45	55	55
Power in Current Pulse - μW	45	66	66	114	114	114	1.1
Max. Wire Displacement - μ	5.0	5.6	5.7	7.3	7.3	7.3	0.67
Rotation Speed above T_{λ} - rad sec^{-1}	21	19	19	25	6.3	32	32
Total Observation Time - hrs	3.7	3.6	4.6	4.0	3.1	2.7	1.5
Time in Stable Levels/ Time of Observation	.38	.30	.50	.74	.24	.28	.30
Quantum Levels Observed	0,2	0	0,2	0,1,2	0	0,2	0,2

TABLE 1c. Experimental Parameters for Runs with Wire E

Wire				E			
Wire Diameter - μ				75.0			
Eff. Mass/Length - $\mu g\ cm^{-1}$				113.2			
$\Delta\omega_n$ (1.20°K, n=1)-rad sec^{-1}				1.24			
Decay time $1/\lambda$ (1.20°K, 500 cps) - msec				350			
Figure of Merit $\Delta\omega_n/\lambda$				.435			
Run Number	1	2	3	4	5	6	7
Wire Frequency $\omega/2\pi$ - cps	498	595	612	580	503	500	504
$\Delta\omega_o$ - rad sec^{-1}	2.41	3.53	3.38	3.38	3.98	4.05	3.98
Amplifier Time Delay (1.20°K)-msec	45	40	35	40	45	45	43
Power in Current Pulse - μW	8.7	8.5	22	22	22	22	22
Max. Wire Displacement - μ	2.0	1.3	2.1	2.2	2.6	2.6	2.6
Rotation Speed above T_λ - rad sec^{-1}	25	9.5	——	——	6.3	6.3	3.0
Total Observation Time - hrs	5.6	0.8	5.4	5.7	8.7	10.1	10.1
Time in Stable Levels/ Time of Observation	.62	.56	.53	.29	.43	.69	.67
Quantum Levels Observed	0,3	0	0,2	0,3	0,3	0,1,2,3	0,2,3

TABLE 1d. Experimental Parameters for Runs with Wires G and H

Wire				G			H
Wire Diameter - μ				100			95.7
Eff. Mass/Length - $\mu g\ cm^{-1}$				217			179
$\Delta\omega_n$ (1.20°K, n=1)-rad sec^{-1}				.650			.787
Decay time $1/\lambda$ (1.20°K, 500 cps) - msec				480			500
Figure of Merit $\Delta\omega_n/\lambda$				.310			.394
Run Number	1	2	3	4	5	1	2
Wire Frequency $\omega/2\pi$ - cps	810	810	815	681	681	583	625
$\Delta\omega_o$ - rad sec^{-1}	1.87	1.80	1.76	1.81	1.94	3.43	1.93
Amplifier Time Delay (1.20°K) - msec	20	18	18	25	24	40	29
Power in Current Pulse - μW	{2200 113	2200	{2200 400	1500	1500	150	270
Max. Wire Displacement - μ	{7.7 1.8	7.7	{7.7 3.3	6.0	6.0	2.3	3.1
Rotation Speed above T_λ - rad sec^{-1}	9.5	—	{3.4 10	—	{14 9.5	{7.8 2.9	3.2
Total Observation Time - hrs	4.5	6.6	5.4	4.4	6.1	5.2	8.0
Time in Stable Levels/ Time of Observation	.26	.31	.19	.31	.23	.61	.59
Quantum Levels Observed	0,-2	0	0	0,3	0	0	0,±3

circulation was said to be stable or unstable is described below. The last row of the table indicates which quantum levels, if any, can be said to have been observed during each run.

Apparent circulation is plotted against time for three runs, E-6, E-7, and H-2, in Figures 16, 17, and 18. Because of the compressed time scale required to fit each curve on a single page it was necessary to plot averages of circulation made over intervals of about 60 seconds, instead of the actual apparent circulation point by point. An idea can be gained of how much information is lost in this averaging process by examining Figure 15. This figure presents data covering about 12 minutes of run E-7. The top panel is an actual point-by-point record of the time interval between the initial excitation of the wire and the appearance of the first node of the beat pattern on the screen of the oscilloscope. The second panel is a point-by-point transcription of these time measurements into values of apparent circulation, using the calibration curve of Figure 14. The third panel shows the average apparent circulation for this segment of the run. When the time scale for this panel is compressed to fit the time scale for Figure 17, which is the plot of the whole of run E-7, this segment occupies just the very small region between hours 1.3 and 1.5 near the beginning of the plot. It is evident that Figure 17 presents only the broad features of a very large quantity of information.

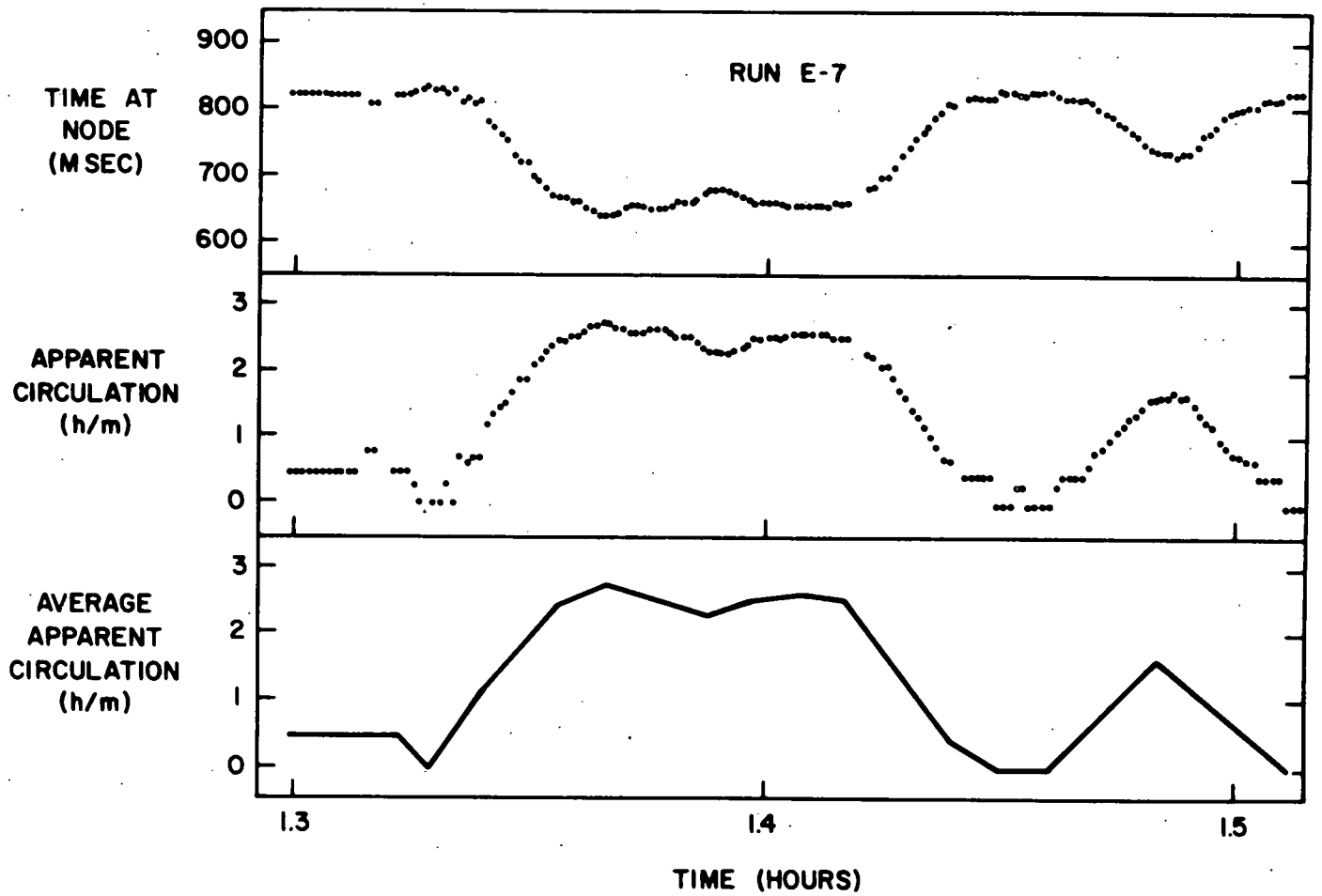

Figure 15. Comparison of Actual Data with Averaged Data for Part of Run E-7.

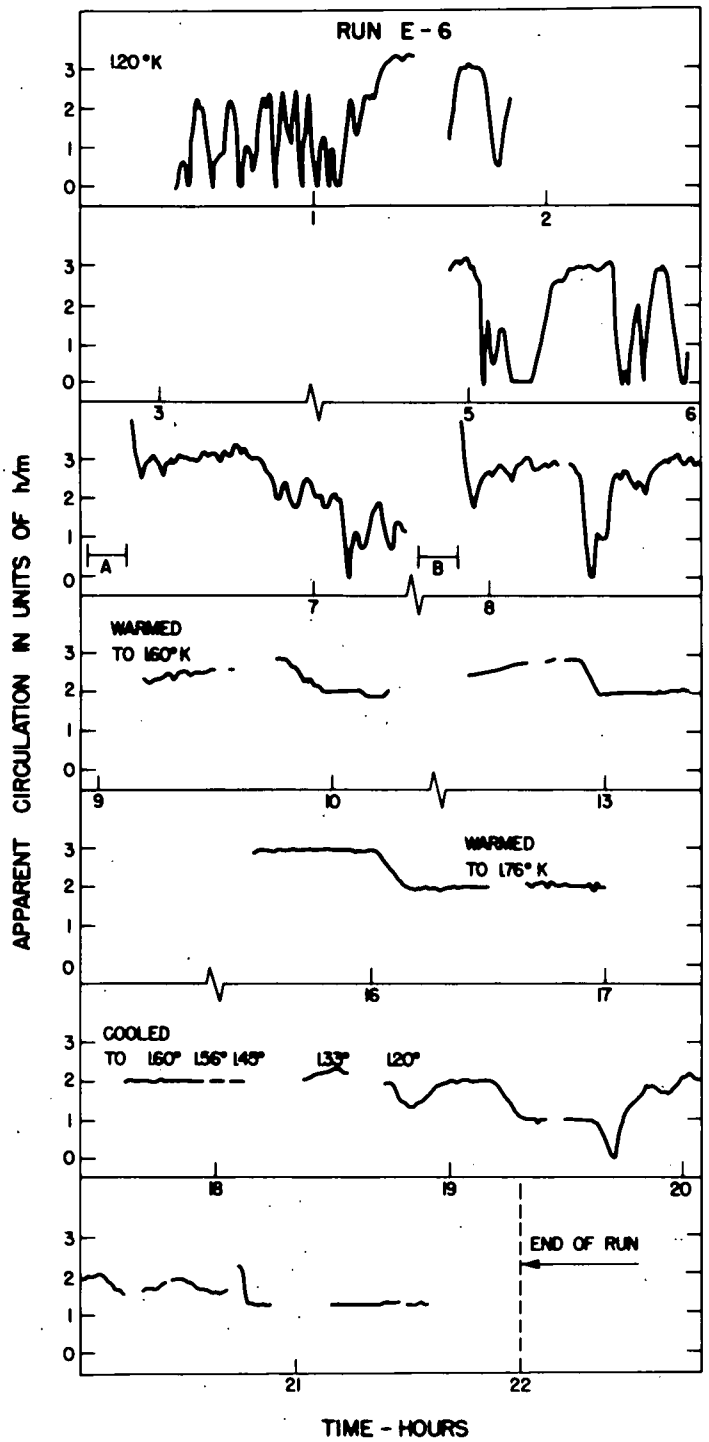

Figure 16. Apparent Circulation as a Function of Time during Run E-6. The lettered horizontal bars denote periods during which the assembly carrying the tube and wire was rotated at 6 rad sec^{-1} with the temperature constant at 1.20°K.

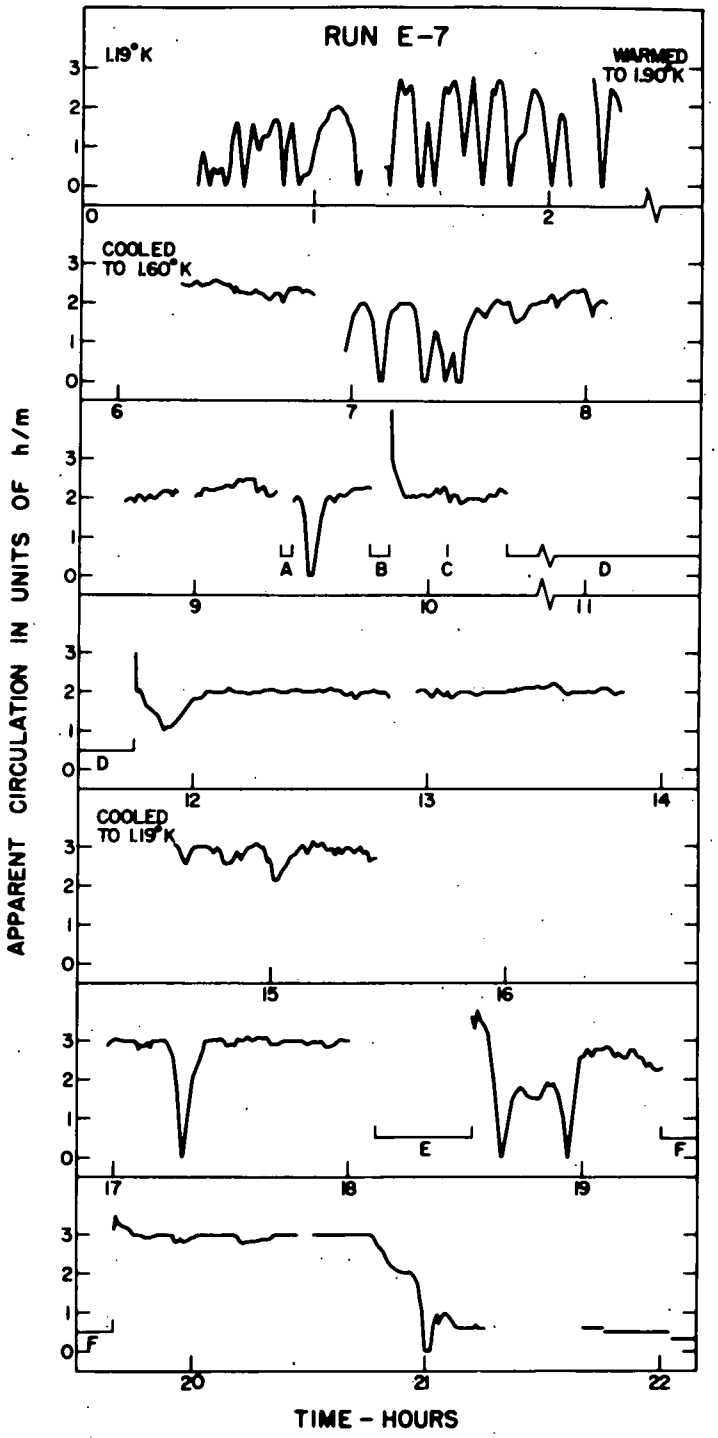

Figure 17. Apparent Circulation as a Function of Time during Run E-7. The lettered horizontal bars denote periods during which the wire was heated at the level of 3 mW by a direct current.

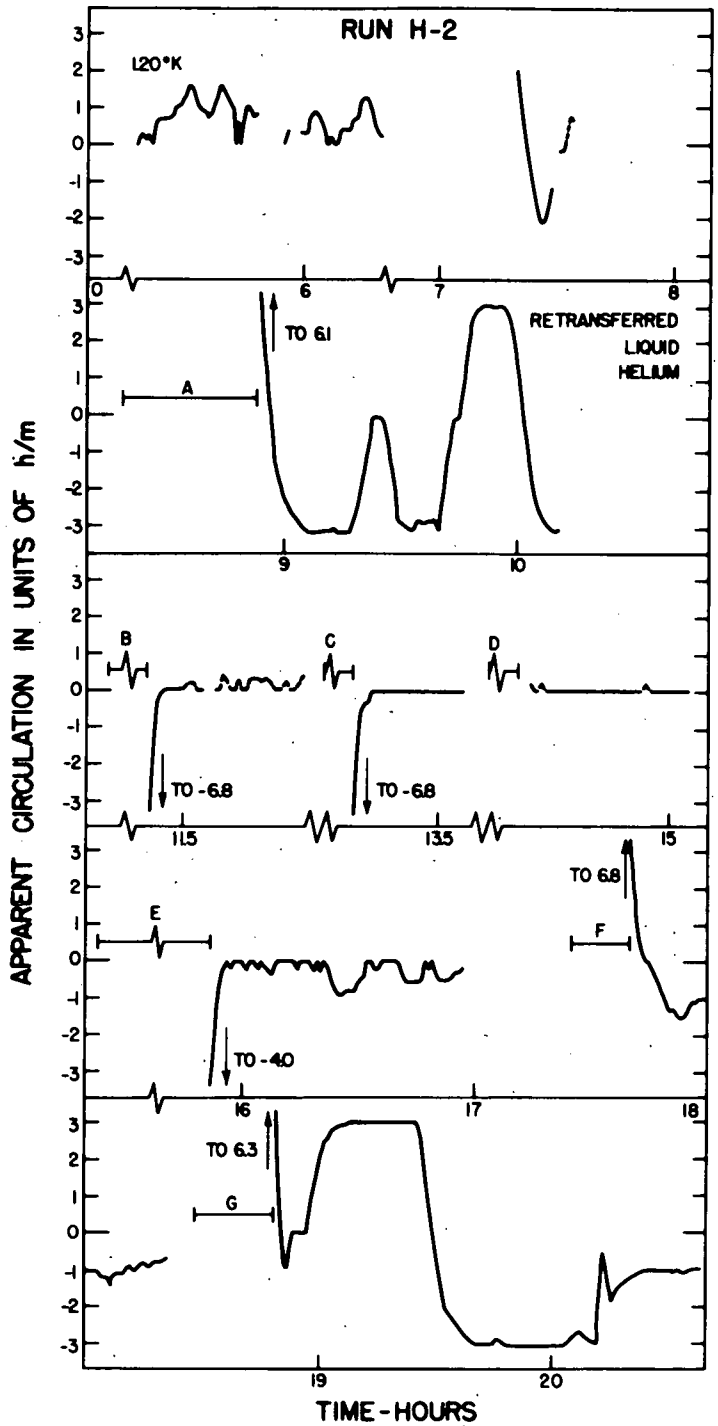

Figure 18. Apparent Circulation as a Function of Time during Run H-2. The lettered horizontal bars denote periods during which the assembly carrying the tube and wire was rotated at about 3.2 rad sec^{-1}. Except during period D the liquid helium was first warmed to a temperature above T_λ, then cooled in rotation to 1.20°K. Rotation was in the positive sense during periods A,D,F, and G, and in the negative sense during periods B,C, and E.

Nevertheless, even the broad features of the data have some very interesting properties. One of them, which is the first principal result of this experiment, is that motion of the superfluid around the wire can persist for long periods of time even though the assembly carrying the wire and surrounding tube is stationary. A good example of this effect occurs in run E-7. Previous to the beginning of this plot the apparatus was filled with liquid helium and the assembly carrying the tube and wire set into steady rotation at an angular speed of 3.0 rad sec^{-1} at a bath temperature above T_λ. While in rotation the apparatus was slowly cooled through T_λ to 1.19°K, where the rotation was brought to a stop. No further rotation was carried out during the run, which lasted until the helium bath level fell to the top of the wire. Circulation measurements were made only during those periods for which the curve is shown in Figure 17. The technique for measuring the direction of the apparent circulation was not in use by the time this run was made, so only the magnitude of the apparent circulation is plotted in this figure.

It is also apparent from Figure 17 that the persistent motion of superfluid around the wire is in general not steady. Smooth changes in apparent circulation take place spontaneously throughout the run. It may seem from the top panel of the figure that the spontaneous changes which occur there are rapid, noisy fluctuations. If so, this is an illusion created by the compressed time

scale of the drawing. Reference to the segment of the original data plotted in Figure 15 shows that on a realistic time scale the changes in circulation are smooth and gradual. The curve of Figure 17 represents actual circulation drifting in time. The noise level of the experiment is far below any variations which are plotted there.

Perhaps a still more striking example of the way in which the apparent circulation can spontaneously drift in time is provided by run H-2, plotted in Figure 18. By the time this run was made the electromagnet was in use, so the direction of the apparent circulation was measured as well as its magnitude. The sign convention used is that circulation directed counter-clockwise around the wire looking down along the wire is positive. Several times during run H-2 the apparatus and helium bath were warmed to a temperature above T_λ; the assembly carrying the tube and wire was set into steady rotation at about 3.2 rad sec^{-1}; then the apparatus and bath were cooled back through T_λ to 1.20°K where the rotation was brought to a stop. As in every other run performed in this experiment all measurements of the apparent circulation were made with the apparatus at rest.

Three separate times during run H-2 the apparent circulation drifted spontaneously from a level of three quantum units in one direction, through zero, to a level of three quantum units in the other direction. In each case the drift was smooth and monotonic,

and took about ten minutes. It is remarkable that although the apparent circulation was stable at both ends of each transition, at plus and minus three quantum units, there is no evidence of stability at the intervening quantum levels. In another case the apparent circulation drifted from a level of three quantum units to zero, then back to three units in the same direction. Again the circulation was stable at the end points of the transition and at zero, but not in between.

The second principal result of this experiment is that the circulation around the wire tends to show markedly greater stability at the anticipated quantum levels than at other values. It can be seen in Figures 16 and 17 that during runs E-6 and E-7 there were long periods of stability at the level of two and three quantum units, and during run E-6 stable circulation also occurred at the level of one quantum unit. During run H-2, which is plotted in Figure 18, there were long periods when there was no circulation around the wire, but there were other periods when the circulation was stable at the level of three quantum units in both the clockwise and counter-clockwise directions.

This stability is shown in another way by the histograms which have been compiled for several runs. The histograms for runs E-6, E-7, and H-2 are shown in Figures 24, 25, and 26 respectively. These histograms represent for a given run the total time the apparent circulation remained stable at each value of

the circulation. The criterion for stability was that during a period of at least 100 seconds the position of the first node of the beat pattern on the screen of the oscilloscope should not drift by more than ± 0.5 mm, which was the smallest displacement that could be estimated by eye. (The smallest division inscribed on the graticule of the oscilloscope was 2 mm.)

The drift in apparent circulation which this much drift in the node position represented depends both on the frequency splitting being measured at the time, $\Delta\omega$, and the frequency splitting with zero circulation, $\Delta\omega_o$. The reader can get an idea of how large a drift in circulation this was for each run by looking at the histograms. For every run except C-1, C-4, and D-1 the width of a vertical column corresponds to a change in the node position of 0.5 mm, the smallest displacement which it was possible to resolve on the screen of the oscilloscope. Therefore, in order to satisfy the stability criterion circulation was required not to drift further than the width of one column in either direction for a period of at least 100 seconds. For runs C-1, C-4, and D-1 the column width corresponds to node shifts of 1.0 mm. Roughly speaking, for most runs at 1.2°K the criterion for stability required that the circulation not drift by more than ± 5% of one quantum unit. Exception must be made for small circulation. For circulation of one quantum unit or less the allowed drift was more like 10% of one unit.

Histograms of stable circulation for some earlier runs than E-6, E-7, and H-2 are shown in Figures 19 through 23. In order to demonstrate that no serious injustice has been done to the data by selecting only certain points for display in these histograms, another kind of histogram has been compiled for runs C-1, C-4, D-1, and D-6, which is shown in Figures 19 and 20. These other histograms include all the data points for a given run, plotted as the number of points observed for each value of the apparent circulation. It is interesting to compare the two kinds of histogram for the same run, and it is evident that peaks at quantum levels, if they appear in the histogram of selected points, also appear in the histogram which includes all points. Only one histogram, which includes all the data points, has been compiled for run C-1, because the apparent circulation during this run was stable only at the zero level. Comparatively very few observations were made during this run, but it is interesting to see that even at this, in retrospect, primitive stage of the experiment the data suggested that quantized circulation exists.

It can be seen on the histograms which include all observations for a given run that some points fall to the left of zero circulation. These are all isolated points which do not qualify as stable circulation, and are thought to represent acoustic noise in the liquid helium.

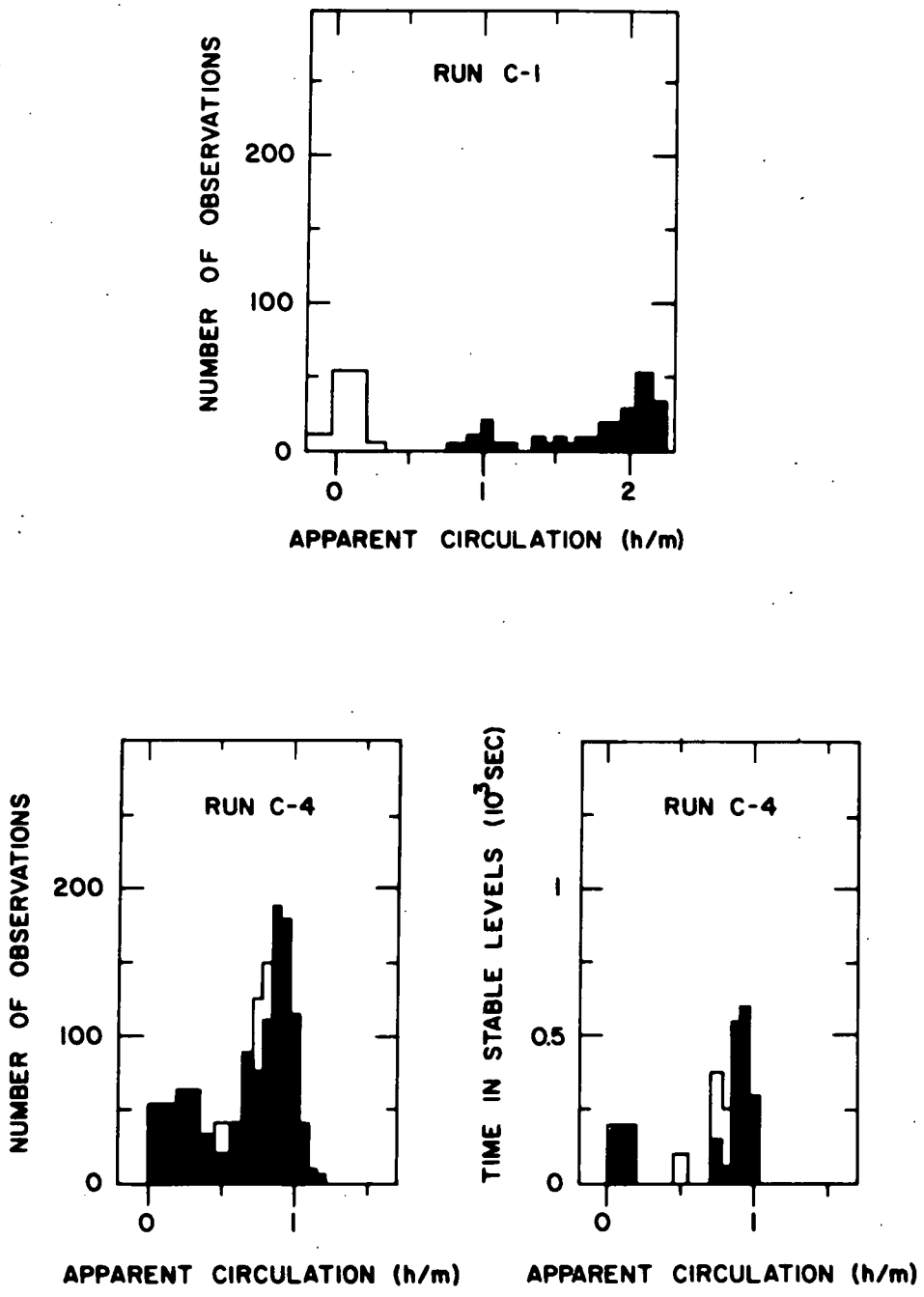

Figure 19. Number of Observations vs Apparent Circulation for Runs C-1 and C-4. Time in Stable Levels vs Apparent Circulation for Run C-4. The unshaded columns represent circulations observed during the last hour of each run.

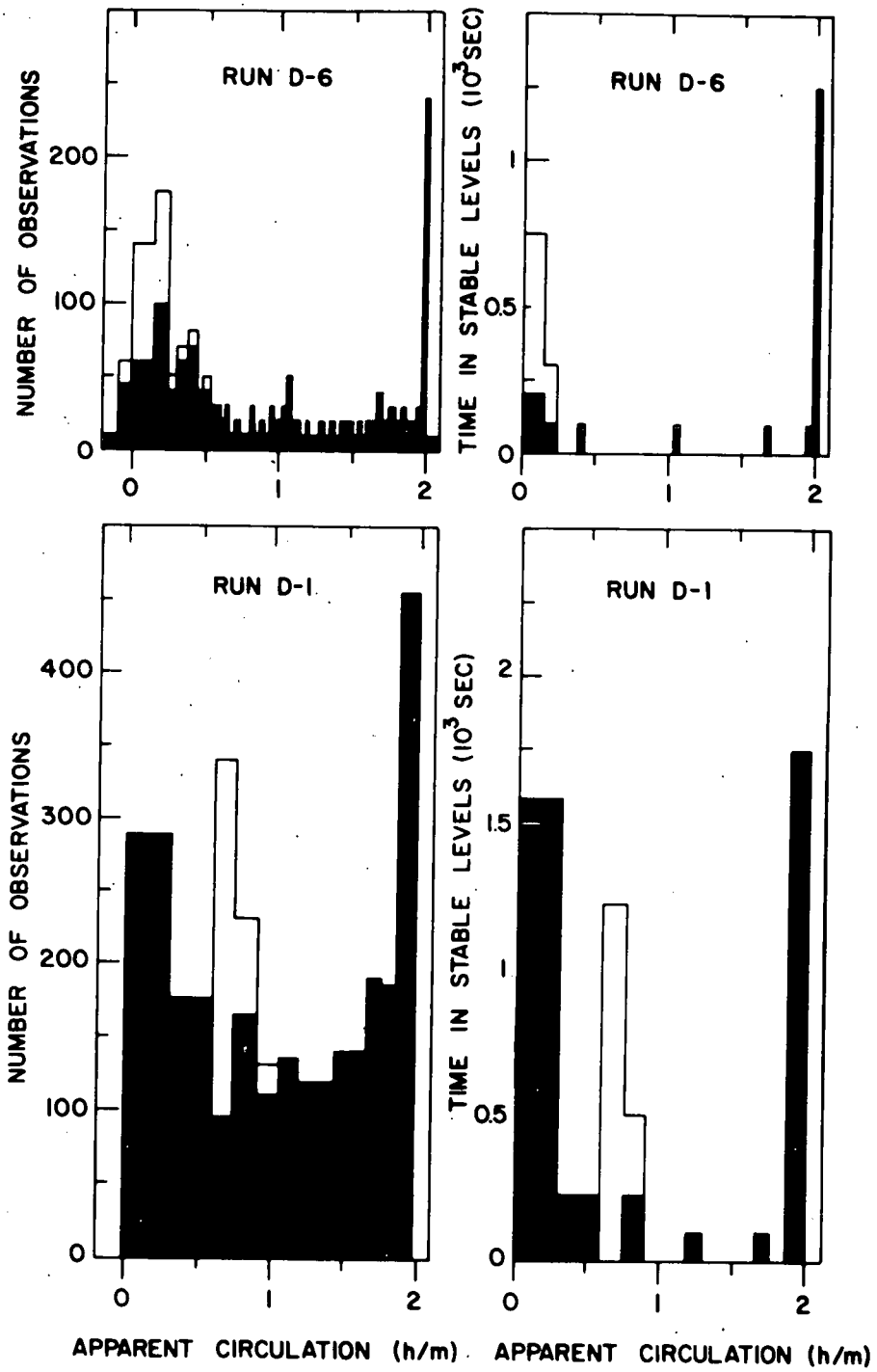

Figure 20. Number of Observations vs Apparent Circulation for Runs D-1 and D-6. Time in Stable Levels vs Apparent Circulation for Runs D-1 and D-6. The unshaded columns represent circulations observed during the last hour of each run.

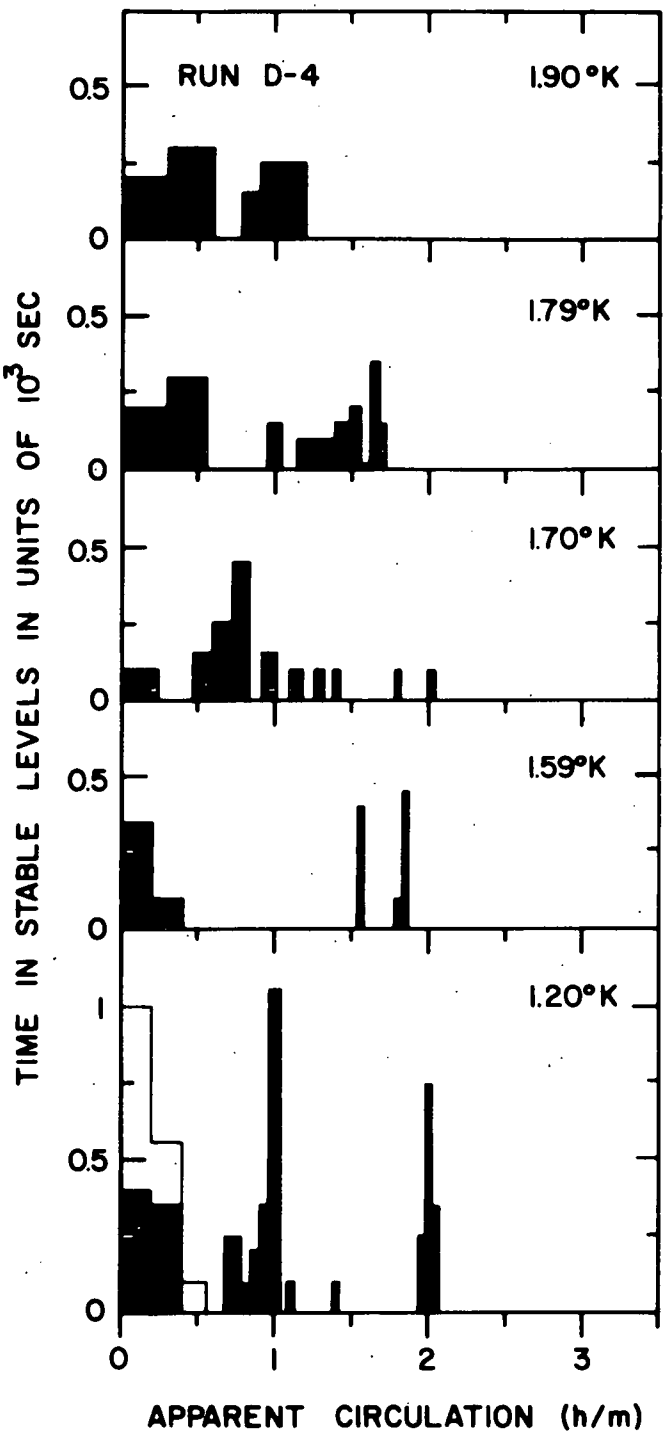

Figure 21. Time in Stable Levels vs Apparent Circulation for Run D-4. The unshaded columns represent stable circulations observed during the last hour of the run.

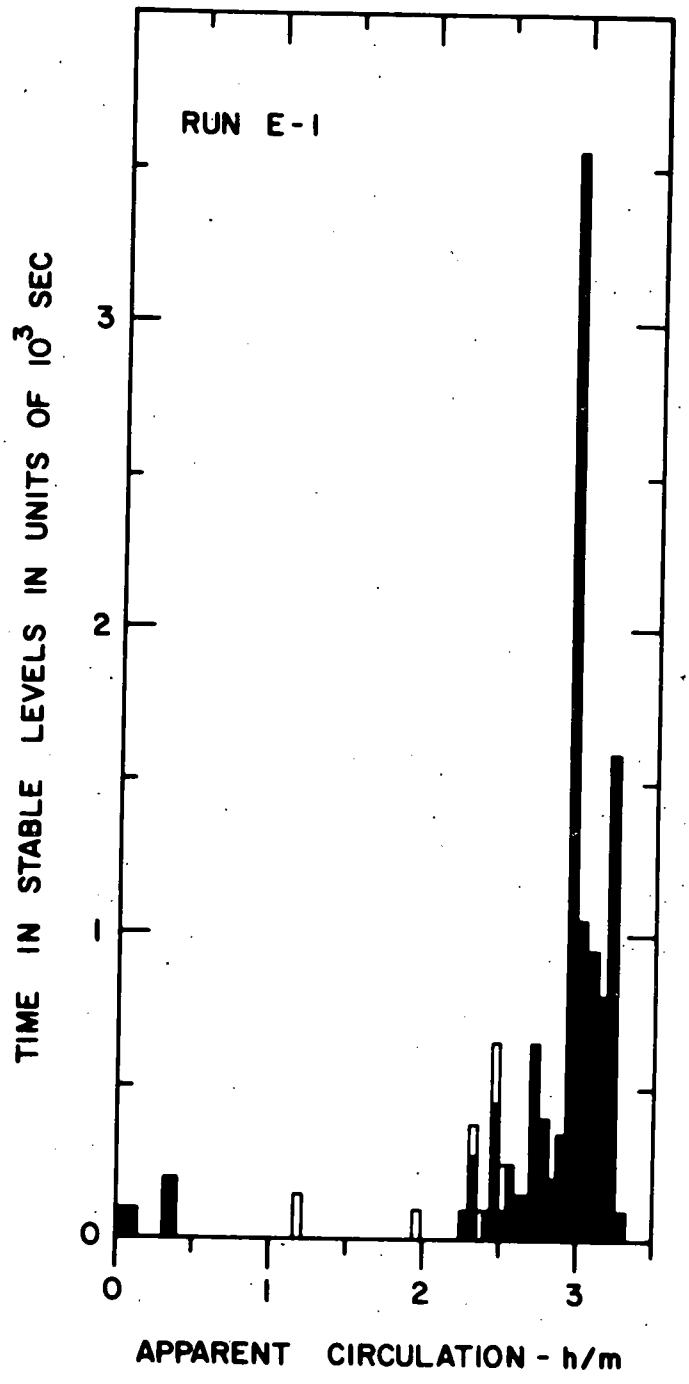

Figure 22. Time in Stable Levels vs Apparent Circulation for Run E-1. The unshaded columns represent stable circulations observed during the last hour of the run.

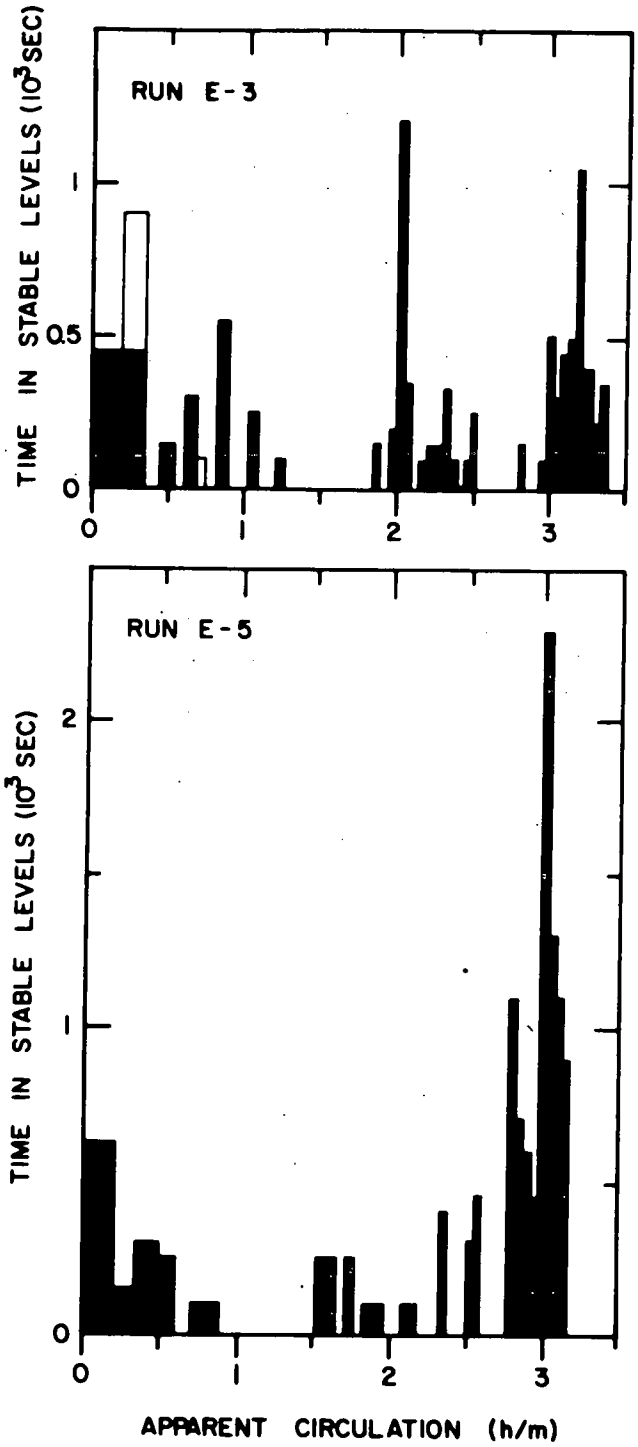

Figure 23. Time in Stable Levels vs Apparent Circulation for Runs E-3 and E-5. The unshaded columns represent stable circulations observed during the last hour of each run.

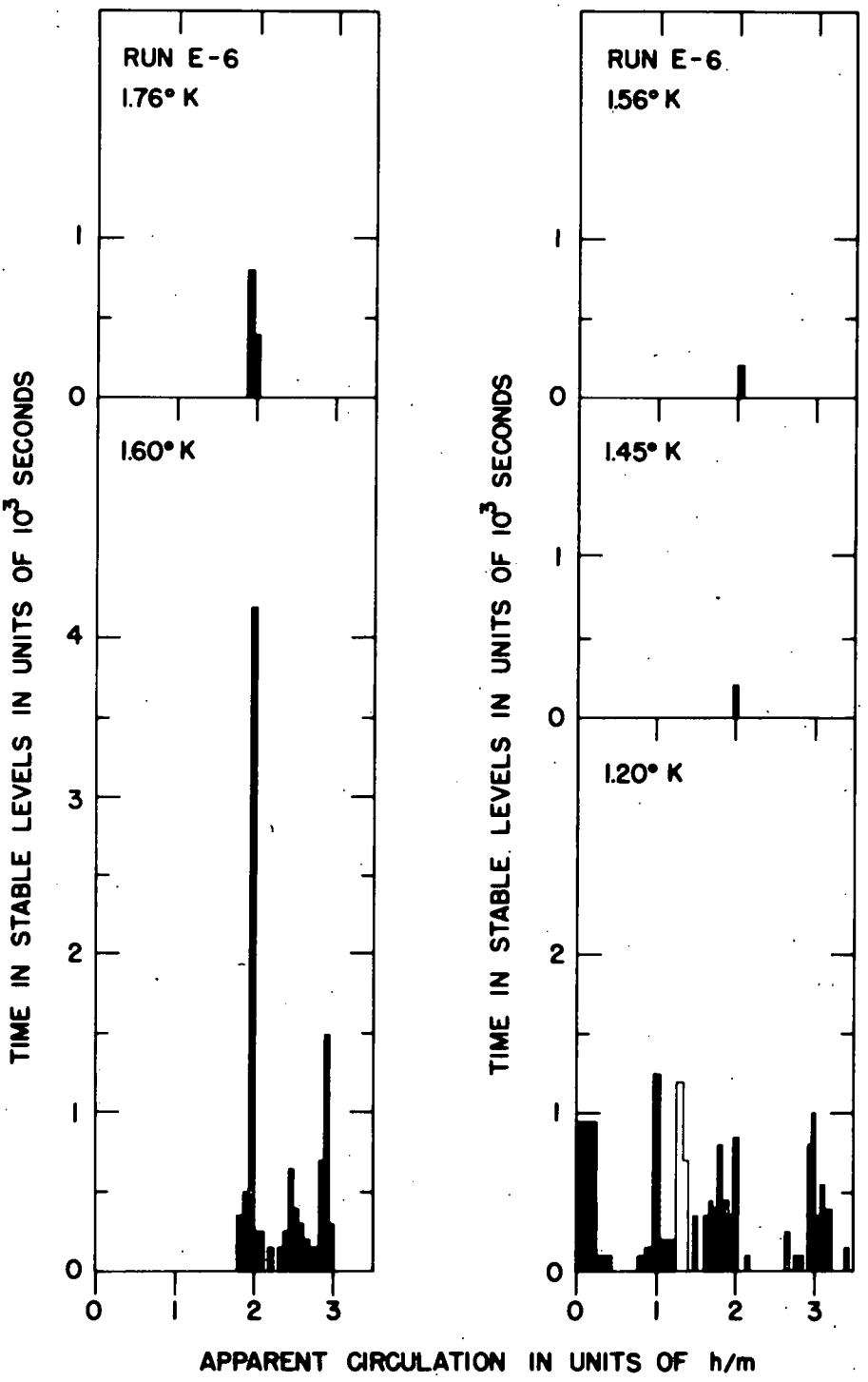

Figure 24. Time in Stable Levels vs Apparent Circulation for Run E-6. The unshaded columns represent stable circulations observed during the last hour of the run.

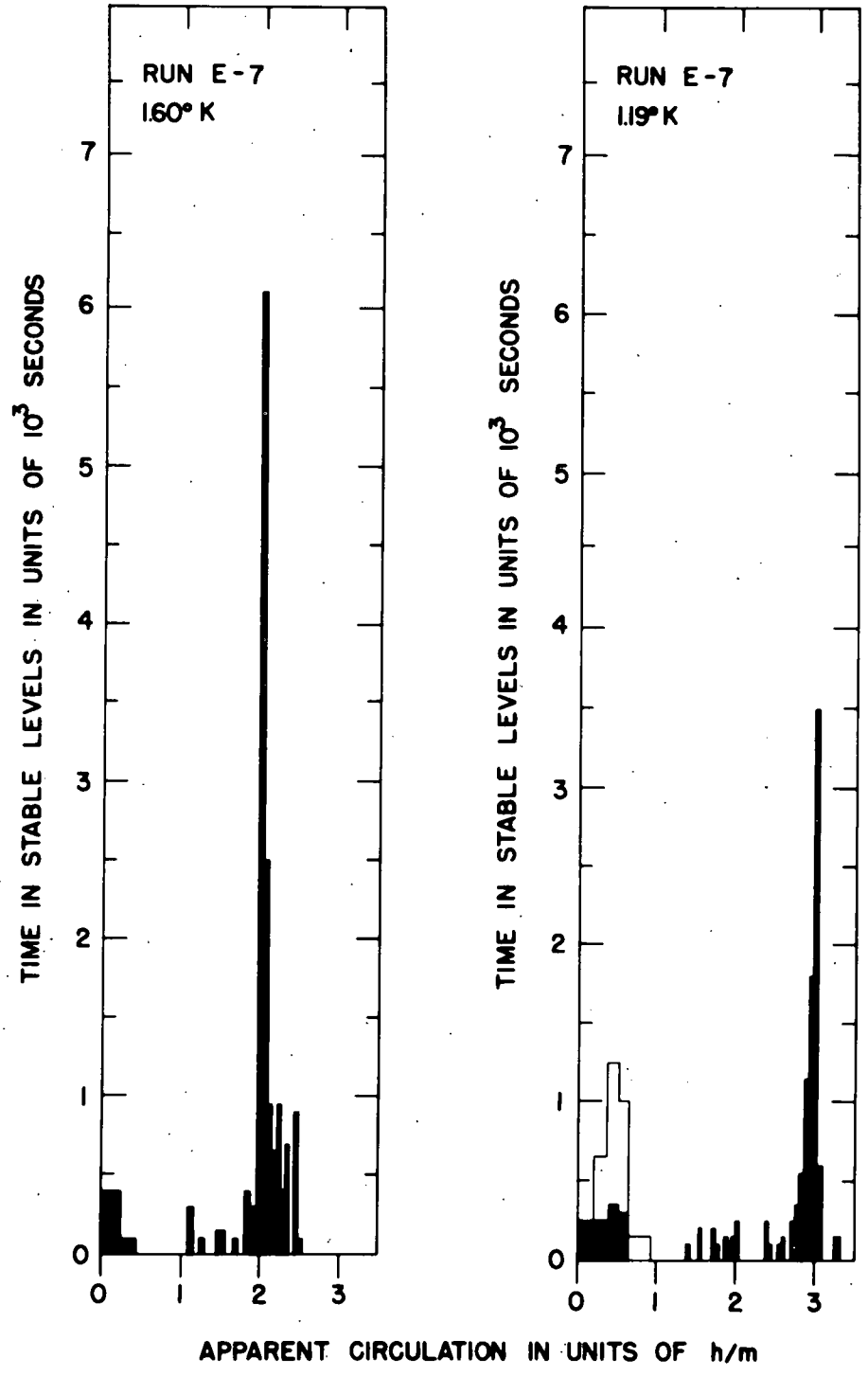

Figure 25. Time in Stable Levels vs Apparent Circulation for Run E-7. The unshaded columns represent stable circulations observed during the last hour of the run.

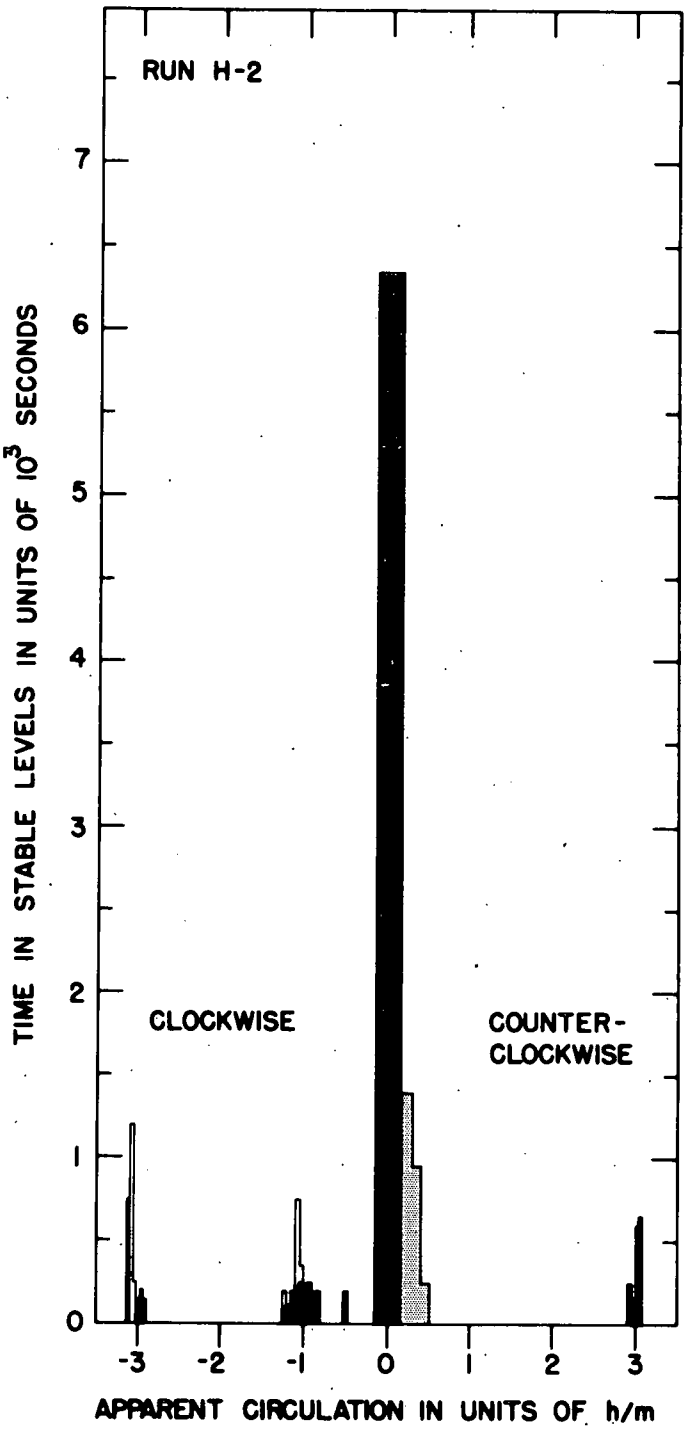

Figure 26. Time in Stable Levels vs Apparent Circulation for Run H-2. The unshaded columns represent stable circulations observed during the last hour of the run. The lightly shaded columns represent stable circulations of undetermined sign.

Not every peak in the histograms of stable circulation appears exactly at the quantum levels. However the experimental error associated with each peak is in most cases about 0.1 quantum units, so that within the accuracy of the experiment most of the peaks do coincide with integral multiples of h/m. There are exceptions. In run E-3 a distinct peak occurs at 3.2 h/m. In runs E-1 and E-5 peaks occur at 3.2 h/m and 2.8 h/m respectively, although in these cases still higher peaks occur at 3.0 h/m.

The reader will notice that there are columns in many of the histograms which are drawn only in outline instead of solid black. These columns represent circulations measured during the last hour of the run, when the surface of the helium bath was within 1 cm of the top of the wire. At some point during the last hour of nearly every run the apparent circulation was observed to shift rather suddenly to a very quiet, stable plateau, in general not a quantum level, and then slowly drift to smaller values. This kind of stability appears near the end of the circulation vs. time plots of runs E-6, E-7, and H-2. It seems not to be related to the stability at the quantum levels. As evidence, it was possible during these periods near the end of a run to shift the measured circulation to a different plateau, still not a quantum level, by heating the wire briefly with a direct current. It was not possible to manipulate circulation this way at the quantum levels.

In order to avoid bias in the observer, all periods of stable circulation which occurred during the last hour of a run have been plotted on the histograms as open columns, whether or not the circulation behaved in the peculiar manner described above. Because of this practice almost certainly some genuine quantum levels have been misrepresented as perhaps spurious. For example the negative circulation near the end of run H-2 which is stable at the level of minus three quantum units clearly deserves a solid column in Figure 26 but gets an open column because it occurred during the last hour of the run.

There are some other observations which support the conclusion that these measurements reveal the effects of quantized circulation. Measurements of apparent circulation have been made at temperatures higher than $1.2^{\circ}K$, notably during runs D-4, E-6, and E-7. Run D-4 presents no evidence of stable circulation at quantum levels for the higher temperatures, but during runs E-6 and E-7 stable circulation appeared at the anticipated quantum values over a range of temperatures from $1.19^{\circ}K$ to $1.76^{\circ}K$. This is to say that $\Delta\omega_n$ for the respective stable levels depends linearly on ρ_s as expected, as ρ_s/ρ_λ varies from 0.97 to 0.70. Here ρ_λ is the liquid density at T_λ. The evidence for this agreement appears in Figure 27, where $\Delta\omega_n$ is plotted as a function of ρ_s/ρ_λ for three different quantum

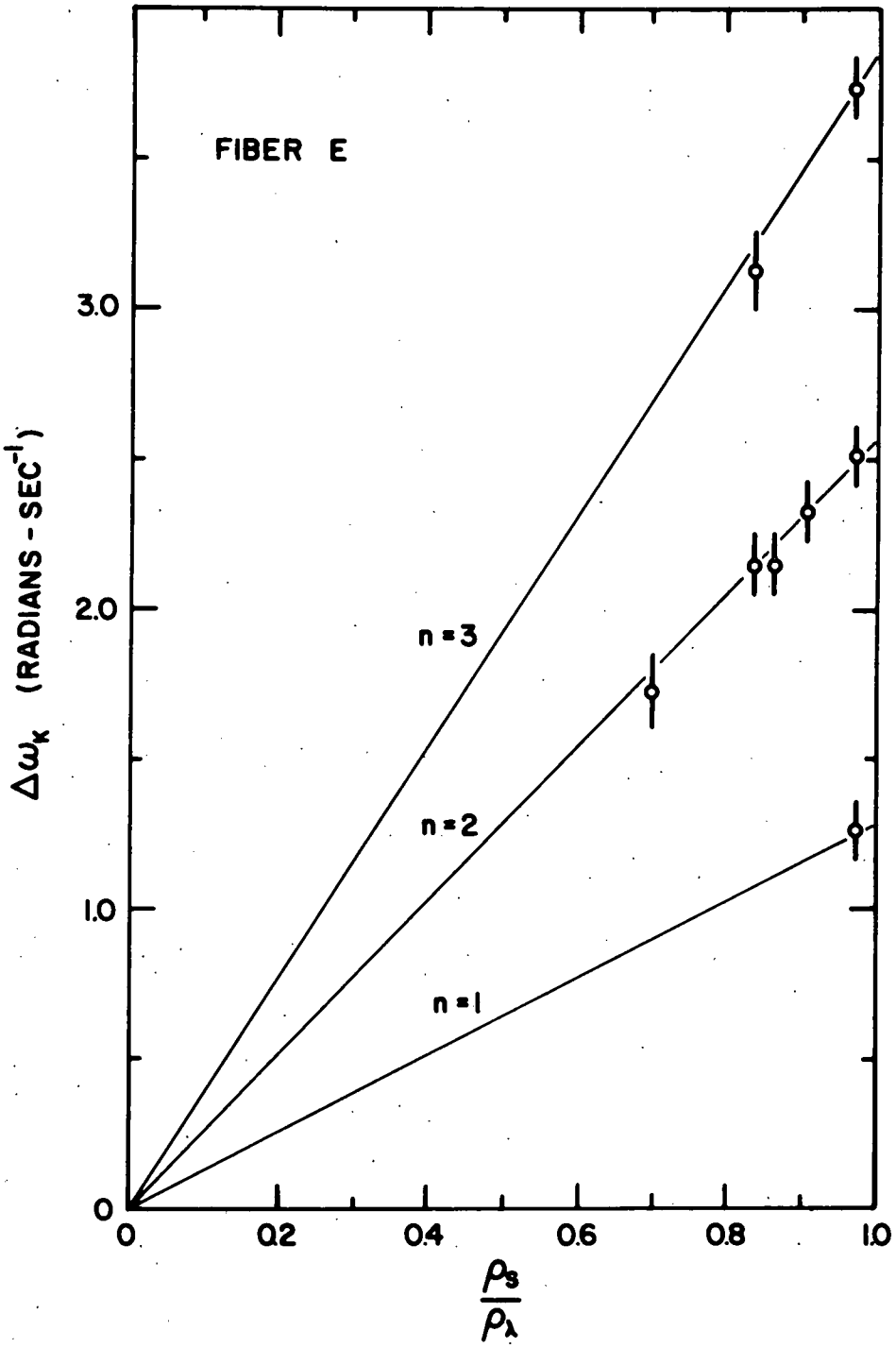

Figure 27. $\Delta\omega_\mu$ vs ρ_s/ρ_λ for Wire E.

levels observed with fiber E. The data points were taken from the histograms of runs E-6 and E-7. It can be seen in Figure 16 that during run E-6 the circulation remained stable for the better part of two hours as the helium bath was warmed from $1.60^{\circ}K$ to $1.76^{\circ}K$ then cooled to $1.45^{\circ}K$. Over this temperature range ρ_s/ρ_λ changes from 0.90 to 0.70. It is interesting to observe that during runs E-6 and E-7 stability at the level of two quantum units seems to have been favored at the higher temperatures, whereas stability at three quantum units predominated at $1.2^{\circ}K$.

During run E-1, at a time when the circulation was fairly stable at three quantum units, an attempt was made to measure the ellipticity of the normal modes of the wire. The assembly carrying the tube and wire was turned 45° from its usual position and photographs were taken of the decaying beat pattern. In such an orientation, where the axes of the normal modes lie at 90° and 180° to the direction of the magnetic field, the modulation of the beat pattern is a minimum. The envelope of the beat pattern, neglecting the transient response from the amplifier, has the form

$$(1 + R^4 + 2R^2 \cos[\Delta\omega(t-\Delta t)])^{\frac{1}{2}} e^{-\lambda t} \qquad (124)$$

where $R = \dfrac{\Delta\omega+\Delta\omega_o}{\Delta\omega_n}$ is the ratio of the major axis of each elliptical mode to its minor axis. Δt is the time delay of the amplifier. For run E-1, at a time when the circulation was

three quantum units at 1.2°K, R was equal to 1.83. The envelope function has been computed for these conditions, using values of $\Delta\omega_o$, Δt, and $1/\lambda$ taken from Table 1c, and is plotted against time in Figure 28. Amplitudes measured from a photograph of the beat pattern are also plotted on Figure 28, having been normalized to the scale of the calculated curve. The agreement is quite good. If no circulation had been present the curve would have followed the dashed line in Figure 28.

Finally, as additional evidence that the apparatus really measured quantized circulation in the fluid it should be pointed out that stable circulation was observed at the quantum levels using wires of different diameter and mass per unit length, and using different values of $\Delta\omega_o$ with the same wire. For examples of the latter point compare $\Delta\omega_o$ for runs D-1 and D-6, and E-1 and E-6.

A third significant result of this experiment is that the maximum value at which the apparent circulation around the wire is observed to remain stable depends markedly on the diameter of the wire. It is evident from a comparison of histograms for runs with different wires that as the diameter of the wire has been increased the maximum value of stable circulation observed has also increased. With wire C, of diameter 25 μ, stable circulations larger than one quantum unit were rarely observed. With wire D, of diameter 39 μ, stable circulations

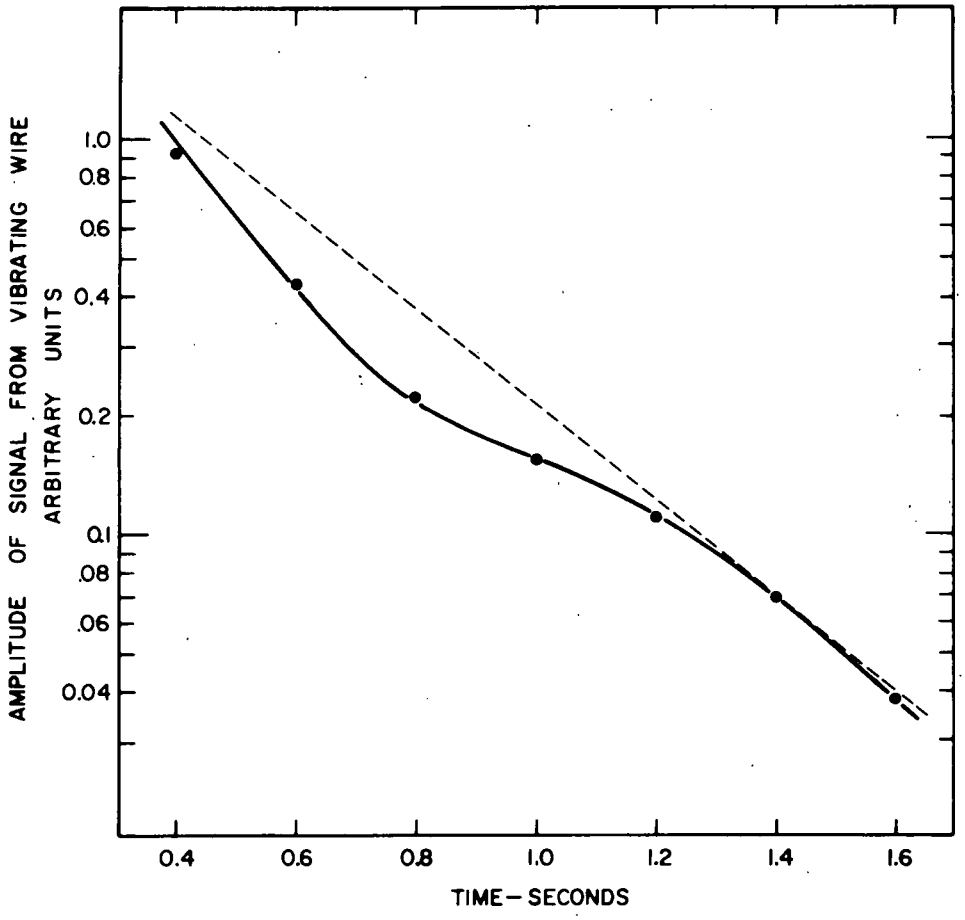

Figure 28. Signal Amplitude as a Function of Time with Normal Modes Excited Unequally. The solid curve was calculated assuming three quantum units of circulation. The dashed line was calculated assuming zero circulation.

larger than two units were rarely observed. With wire E, of diameter 75 μ, and wire H, of diameter 96 μ, stable circulations larger than about 3.2 units were rarely observed. Stable circulations at the level of four quantum units or more have not been observed at all. These results are consistent with the fact that Vinen, using a wire 25 μ in diameter, saw stable circulation only at the one-quantum level.[61]

The effect of steady rotation of the tube and wire on the apparent circulation is exemplified by run H-2, plotted in Figure 18. Previous to the beginning of this plot the apparatus was cooled through T_λ to 1.20°K with the assembly carrying the tube and wire stationary. At about the eighth hour the apparatus was warmed to a temperature above T_λ, where the wire and tube assembly was set into rotation counter-clockwise looking from above at 3.2 rad sec^{-1}. Then the apparatus was cooled back through T_λ to 1.20°K, where the rotation was brought to a stop. At about the tenth hour the apparatus was warmed to 4.2°K and more liquid helium was transferred into the dewar. Then the wire and tube assembly was set into rotation clockwise at 2.8 rad sec^{-1} and cooled through T_λ to 1.20°K, where again the rotation was brought to a stop. Four more times during the run the apparatus was warmed to a temperature above T_λ then cooled back to 1.20°K while rotating at about 3.2 rad sec^{-1}. Twice, during the time intervals marked C and E, the rotation was

clockwise. During the intervals marked F and G the rotation was counter-clockwise. One time, during the interval marked D, the apparatus was rotated counter-clockwise at 2.7 rad sec^{-1} while the temperature was held steady at 1.20°K.

Figure 18 shows that immediately after the rotation of the wire and tube assembly was brought to a stop the apparent circulation was found each time at an abnormally high value, up to 6.8 quantum units, and with the same sense as the rotation, clockwise or counter-clockwise around the wire. (Following rotation D measurements were delayed too long to see large circulation.) However, the circulation was not stable; in each case it decayed steadily to zero in about four minutes. Thereafter it either remained stable at zero or drifted to some other value in a direction seemingly unrelated to the direction in which the tube and wire had just been rotated.

If measurements could be made with the tube and wire rotating there are considerations which suggest how the circulation around the wire should depend on the rotation speed. Hydrodynamic arguments given by Griffiths[62] suggest that a higher rotation speed is necessary in order to establish a given circulation around the wire than would be expected on the basis of the thermodynamic arguments used by Vinen.[63] It was not clear whether either of these two approaches applied to this experiment, since measurements were not made until after the rotation

of the tube and wire had been stopped. Nevertheless, the rotation speeds used in this experiment were generally chosen to satisfy Griffiths' proposed criterion for the establishment of two quantum units of circulation around the wire, which is that $\Omega \geq \kappa/6\pi a^2$. Here Ω is the angular frequency of rotation of the vessel and a is the radius of the wire. In practice this criterion led to rotation speeds of the order of several radians per second, whereas Vinen used rotation speeds of the order of a few radians per minute.

It should also be pointed out that it is quite possible for circulation to exist around the wire even though no steady rotation of the apparatus has taken place. For example, Figure 18 shows that in run H-2 after the apparatus was cooled from 4.2° to 1.20° the first time, with the assembly carrying the tube and wire stationary, circulation as large as two quantum units was observed in both the clockwise and counter-clockwise directions. Moreover, stable circulations at the level of three quantum units were observed in runs with fiber E even when no steady rotation of the apparatus had taken place.

On some occasions, for example several times during run E-7, the wire was heated with a direct current in attempts to see whether or not heating would influence the circulation around the wire in some understandable way. It was found that currents dissipating 3 mW of power, if turned on for a minute or more,

did seem to affect the apparent circulation, but that the effect was not lasting. For example, during the time interval marked B in Figure 17 wire E was heated at the level of 3 mW, and when the direct current was turned off the circulation was found to have a value of four quantum units, the largest value observed during that run. However, the circulation quickly decayed back to the level of two quantum units, where it had been before the current was turned on. In general it was not possible to predict just what effect heating the wire would have on the circulation. However, it was sometimes a successful means of shifting the circulation to zero near the beginning of a run, so that a suitable intrinsic frequency splitting could be measured and established for the wire.

It was generally true of long runs, lasting about ten hours or more, that the apparent circulation drifted more rapidly near the beginning of the run than toward the end. Runs E-6 and E-7 are good examples of this effect. In each case the circulation tended to be more stable after the eighth or ninth hour of the run than it had been before. During much shorter runs this relative stability did not appear at all until the last hour of the run, when the anomalous kind of stability described earlier would set in.

B. Error

The error estimates to be assigned to the measured values of circulation recorded in Figures 16-26 in general represent limits of resolution for the instruments in the experiment. Random fluctuations in the data were too small to contribute significantly to the total error. For example, the smallest displacement of the first node of the beat pattern which was observable on the screen of the oscilloscope was 0.5 mm, whereas over a period of 100 sec or more during which the apparent circulation was stable the standard error in the measurements of the node position was almost always less than 0.5 mm. For another example the standard error in a set of readings for the mass of the wire was always less than the smallest estimated division on the scale of the microbalance, which was 1 μg.

There are three principal sources of instrumental error in this experiment: the measurement of the effective mass of the wire; the determination of the node position on the screen of the oscilloscope; and the determination of the shift in the node position introduced by the selective amplifier. Another important source of error is uncertainty in the assumed value of ρ_s, which is known only to within about 1% at 1.2°K.

The apparent circulation $\bar{\kappa}$ is equal to $\Delta\omega_\kappa \frac{\sqrt{\mu_x\mu_y}}{\rho_s}$. For a wire of circular cross-section $\sqrt{\mu_x\mu_y} = \mu$, where μ is the sum of the mass per unit length of the wire itself plus $\pi a^2(\rho_s+K\rho_n)$.

Here a is the radius of the wire and K is one of Stokes' functions plotted in Figure 2. For a wire of elliptical cross-section $\sqrt{\mu_x \mu_y}$ is equal to the sum of the mass per unit length of the wire itself plus $\pi ab(\rho_s + K\rho_n)$ where a and b are the semi-major and semi-minor axes of the ellipse. In practice the contribution of the fluid to $\sqrt{\mu_x \mu_y}$ was 3% to 6% of the total.

Measurements of the mass of the wire itself were considered accurate to 2 μg, which gives a fractional error of 1% for wire D down to 0.2% for wire H. Wire C must be excepted from this estimate because it was never weighed directly. Its mass density was taken to be the average of the mass densities of the two end pieces left over when it was cut from the middle of a longer fiber. The error in the mass of wire C was taken to be 4 μg, or 4%. The error in the length of each wire was 0.2%.

The contribution of the fluid to the effective mass of the wire was computed in practice as if the wires were circular, even though under a microscope the major and minor axes of a cross-section frequently differed from each other by as much as 10%. Percentage errors in $\bar{\kappa}$ due to this possible 10% asymmetry are tabulated for the various wires in Table 2. In addition the contribution of the fluid to the effective mass of the wire was computed in practice as if K were equal to 1, neglecting the normal fluid which is accelerated by the vibrating wire because of viscous drag. Percentage errors in $\bar{\kappa}$ from this source are also tabulated in Table 2.

Error in the measured beat period of the wire was thought to have just two important sources, which were error in the node position on the screen of the oscilloscope and error in the time delay of the amplifier. The error in the node position was in nearly every case just the limit of resolution of the graticule, $\pm$ 0.2 mm. The fractional error in the beat period with zero circulation due to error in the node position ranged generally from 0.2% to 0.5%. With non-zero circulation the fractional error was larger, and depended on the circulation.

The sweep speed of the oscilloscope could be accurately calibrated, and was very nearly linear in the region of the screen where measurements of the node position were commonly made. Error in timing the onset of the beat pattern was negligible. The time display of the oscilloscope was triggered by the same current pulse which excited the wire, and the onset of the display was adjusted to the zero position on the graticule with the sweep speed turned up to expand the time scale. Of course the sweep speed had to be reduced again in order to measure beat periods.

The approximate time delay of the amplifier was computed from measurements of the decay times of the wire and amplifier as discussed in chapter IV. These measurements were performed by determining the distance along the screen of the oscilloscope over which the amplitude of the decaying envelope from the wire or the ringing amplifier was judged to decrease by

one-half. The measurements were thought to be accurate to within about 1 mm, or 3%. In practice the delay time of the amplifier was nearly equal to its own time constant for decay; the wire had only a small effect. Consequently the error in the time constant of the wire had only a small effect on the error in the time delay.

The approximate time delay computed from these measurements was subject to a correction of about 10% ± 5% which is also discussed in chapter IV. The total probable error in the time delay was therefore about 6%. What is more pertinent is an estimate of the error in the beat period of the wire introduced by error in the time delay. Generally it was 0.2% or 0.3% of the beat period with zero circulation.

Of course the calculation for the approximate time delay is correct only when the amplifier is at resonance with the wire. The amplifier was tuned for resonance by ringing it and measuring its frequency with the electronic counter. The method was tested with the wire vibrating in vacuum. In repeated trials it was not difficult to reproduce the node position to an accuracy better than the resolution of the oscilloscope screen. Consequently this adjustment was not thought to be a significant source of error.

We consider now the extent to which error in the measured beat period of the wire produces error in $\Delta\omega_{\mu}$, the frequency

splitting due to circulation. Let τ be the measured time interval between the onset of the beat pattern and the appearance of the first node on the screen of the oscilloscope. Let τ_o be the maximum time interval, when the apparent circulation is zero, and let $\Delta\tau$ be the time delay of the amplifier. Then the beat period of the wire is $2(\tau - \Delta\tau) = 2\pi/\Delta\omega$, or with zero circulation, $2(\tau_o - \Delta\tau) = 2\pi/\Delta\omega_o$. The frequency splitting due to circulation is given by

$$(\Delta\omega_\kappa)^2 = (\Delta\omega)^2 - (\Delta\omega_o)^2$$

$$= [\pi/(\tau-\Delta\tau)]^2 - [\pi/(\tau_o-\Delta\tau)]^2. \quad (125)$$

Notice that two independent measurements of the time interval to the node, both τ and τ_o, enter into the calculation of $\Delta\omega_\kappa$. Each measurement contributes independently to the error in $\Delta\omega_\kappa$. The time delay $\Delta\tau$ also enters the calculation twice but introduces just a single error because it was measured only once. In fact the error it does introduce tends to cancel out of the calculation.

The extent to which error in each measurement contributes error to $\Delta\omega_\kappa$ is given by differentiation.

$$\frac{\delta(\Delta\omega_\kappa)}{\Delta\omega_\kappa} \text{ due to } \delta\tau = -\left(\frac{\Delta\omega}{\Delta\omega_\kappa}\right)^2 \frac{\delta\tau}{\tau-\Delta\tau} \quad (126)$$

$$\frac{\delta(\Delta\omega_\kappa)}{\Delta\omega_\kappa} \text{ due to } \delta\tau_o = \left(\frac{\Delta\omega_o}{\Delta\omega_\kappa}\right)^2 \frac{\delta\tau_o}{\tau_o-\Delta\tau} \quad (127)$$

$$\frac{\delta(\Delta\omega_\kappa)}{\Delta\omega_\kappa} \text{ due to } \delta(\Delta\tau) = \left(\frac{\Delta\omega_o}{\Delta\omega_\kappa}\right)^2 \left(\left|\frac{\Delta\omega}{\Delta\omega_o}\right|^3 - 1\right) \frac{\delta(\Delta\tau)}{\tau_o - \Delta\tau}. \quad (128)$$

Here $\delta\tau$, $\delta\tau_o$, and $\delta(\Delta\tau)$ are the errors in τ, τ_o, and $\Delta\tau$ respectively. The first of these terms, for example, is the fractional error in $\Delta\omega_\kappa$ which would be produced by a given error in τ if $\delta\tau_o$ and $\delta(\Delta\tau)$ were zero. Since the apparent circulation $\bar{\kappa}$ is just proportional to $\Delta\omega_\kappa$, it is also the fractional error in $\bar{\kappa}$ provided that all other errors are zero. These terms have been evaluated at various quantum levels of circulation for the runs represented by histograms in Figures 19-26, and are tabulated as percentage errors in Table 2. It is interesting to observe that as the circulation increases the terms which result from error in the node position get smaller, whereas the term which results from error in the time delay gets larger.

The error assigned to ρ_s was estimated by comparing the values computed by Reynolds et al, with other values obtained from data of Dash and Taylor.[64] Reynolds et al computed ρ_s using values of ρ_n obtained from measurements of the speed of second sound; whereas Dash and Taylor measured ρ_n by observing the period and damping of disks in torsional oscillation. The two sets of values for ρ_s differ by about 1% of ρ, the total fluid density, over the temperature range covered in this experiment. The error in ρ_s due to uncertainty in the temperature as measured in this experiment was at most 0.1%.

Wire	Run	$\bar{\kappa}$ (h/m)	Percentage error in $\bar{\kappa}$ due to error in:						
			μ			τ_o	τ	$\Delta\tau$	ρ_s
			A	B	C				
C	1	1.0	4	0.3	0.2	2	3	2	1.0
		2.0	4	0.3	0.2	1	2	6	1.0
	4	1.0	4	0.3	0.2	2	3	1	1.0
D	1	1.0	1	0.4	0.2	5	6	1	1.0
		2.0	1	0.4	0.2	1	3	1	1.0
	4(1.2°K)	1.0	1	0.4	0.2	4	4	1	1.0
		2.0	1	0.4	0.2	1	2	2	1.0
	6	1.0	1	0.4	0.2	0.5	1.0	0.8	1.0
		2.0	1	0.4	0.2	0.2	0.8	1.0	1.0
E	1	3.0	0.5	0.5	0.2	0.2	1.0	0.5	1.0
	3	2.0	0.5	0.5	0.2	0.4	0.7	0.4	1.0
		3.0	0.5	0.5	0.2	0.2	0.6	0.4	1.0
	5	3.0	0.5	0.5	0.2	0.3	0.7	0.5	1.0
	6(1.2°K)	1.0	0.5	0.5	0.2	2.6	3.2	0.4	1.0
		2.0	0.5	0.5	0.2	0.6	1.1	0.5	1.0
		3.0	0.5	0.5	0.2	0.2	0.9	0.7	1.0
	(1.6°K)	2.0	0.5	0.5	0.3	1.3	1.3	0.4	1.2
		3.0	0.5	0.5	0.3	0.6	0.8	0.5	1.2
	7(1.2°K)	3.0	0.5	0.5	0.2	0.3	1.0	0.7	1.0
	(1.6°K)	2.0	0.5	0.5	0.3	0.9	1.3	0.6	1.2
H	2	1.0	0.2	0.6	0.1	1.4	2.0	0.2	1.0
		3.0	0.2	0.6	0.1	0.3	0.8	0.2	1.0

Table 2. Errors for Runs Represented in Figures 19-26. The columns headed A, B, C contain percentage errors in $\bar{\kappa}$ due to (A) error in weighing the wire itself, (B) neglecting possible asymmetry of the wire, and (C) neglecting the added virtual mass of the wire due to viscous drag of the normal fluid.

VII. CONCLUSION

The results of this experiment show that it has been possible to repeat the Vinen experiment successfully and to extend it in three important ways. The first of these extensions was apparent improvement in the sensitivity of the electrical system which detects the vibrations of the wire. Because of this increased sensitivity it has been possible to make virtually continuous records of apparent circulation as a function of time for periods of several hours, and to make measurements over a temperature range from $1.2^{\circ}K$ to $1.9^{\circ}K$. The second important extension was to use wires of larger diameter in addition to a wire of diameter 25 μ, the size that Vinen used. By far the most convincing evidence for quantization of circulation was obtained with the larger wires. The third extension was measurement of the direction of the circulation around the wire as well as its magnitude.

There are two principal results of this experiment. The first is that motion of the superfluid can persist around the wire for long periods of time even though the assembly which carries the wire and surrounding tube is stationary. Moreover, this motion is in general not steady. Smooth changes in apparent circulation take place throughout a run, changes which can include reversals in sign. The second principal result is that

the apparent circulation tends to show markedly greater stability at the anticipated quantum levels than at other values. Long periods of stability have been observed at the level of zero, one, two, and three quantum units. These observations support the Onsager-Feynman hypothesis that circulation of superfluid helium is quantized in units of h/m. Another significant result of the experiment is that as the wire diameter has been increased, the maximum value of stable circulation observed has also increased.

However, the details of the fluid dynamics in this experiment remain far from clear. The observations of circulation values intermediate to the quantum levels and of spontaneous changes in circulation are not understood. Vinen proposed the explanation that a fraction of a quantum unit might be measured when one end of a free vortex line becomes attached to the wire at some point along its length. $\kappa(z)$ would change at such a point by an amount equal to the circulation of the free vortex. The apparent circulation around the wire would change smoothly as this point of attachment drifted along the wire. Stable values of circulation would be measured when no free vortex was attached to the wire, so that circulation was uniform along the wire. (We have seen that in this case the apparent circulation would equal the actual circulation of the superfluid.) However, the observation of transitions

between stable levels of +3 and -3 quantum units with no evidence for stability at intermediate levels would seem according to Vinen's model to require the existence of free vortex lines with circulation as large as six quantum units. It is very difficult to imagine that such vortices do in fact exist, because of the large energy they would have. The vortex rings observed by Rayfield and Reif and others had one unit of circulation.

It would be interesting to measure circulation around the wire with the assembly carrying the wire and surrounding tube still rotating, when the liquid might be in equilibrium in a rotating state. It was evident during this experiment from observations of the apparent circulation made immediately following rotation, that if the fluid is in equilibrium during rotation the equilibrium is destroyed when rotation is stopped. It may be that equilibrium in rotation is difficult to achieve. (In fact no reliable way was found in this experiment of cooling the liquid in equilibrium even without rotation.) Vinen was able to make measurements in rotation but saw no evidence of stable circulation. Measurements were not attempted during rotation in this experiment because of the noise level.

If they should be possible such measurements would be interesting because it is possible to calculate the equilibrium value of circulation around the wire, assuming quantized

circulation and the existence of quantized free vortex lines in the superfluid.[65] Proposals have also been made concerning the influence of normal fluid on free vortex lines during rotation, and of consequent effects on the circulation around the wire.[66] In addition, judging from Figure 18, it should be possible to observe stable circulation at higher quantum levels with the apparatus rotating than has been observed in the present experiment.

REFERENCES

References 1-5 are recommended as general sources.

1. F. London, Superfluids, Vol. II (Wiley, New York, 1954, reprinted by Dover, New York, 1964).

2. K. R. Atkins, Liquid Helium (Cambridge University Press, 1959).

3. I. M. Khalatnikov, An Introduction to the Theory of Superfluidity, translated by P. C. Hohenberg (Benjamin, New York, 1965).

4. G. Careri, Director, Proceedings of the International School of Physics "Enrico Fermi", Course XXI, Liquid Helium (Academic Press, New York, 1963).

5. C. T. Lane, Superfluid Physics (McGraw-Hill, New York, 1962).

6. E. L. Andronikashvili, J. Phys. (U.S.S.R.) 10, 201 (1946); Zh. Eksperim. i Teor. Fiz. 16, 780 (1946); Zh. Eksperim, i Teor. Fiz. 18, 424 (1948).

7. L. D. Landau, Phys. Rev. 60, 357 (1941); J. Phys. (U.S.S.R.) 5, 71 (1941); J. Phys. (U.S.S.R.) 8, 1 (1944); J. Phys. (U.S.S.R.) 11, 91 (1947); Phys. Rev. 75, 884 (1949).

8. L. D. Landau and I. M. Khalatnikov, Zh. Eksperim. i Teor. Fiz. 19 637, 709 (1949).

9. L. D. Landau, J. Phys. (U.S.S.R.) 5, 71 (1941).

10. F. London, Nature 141, 643 (1938); Phys. Rev. 54, 1947 (1938).

11. J. Bardeen, in Proceedings of the IXth International Conference on Low Temperature Physics, Columbus, Ohio, August 31-September 4, 1964, edited by J. G. Daunt et al (Plenum Press, New York, 1965) p. 3.

12. W. L. McMillan, Phys. Rev. 138, A442 (1965).

13. L. Onsager, Nuovo Cimento 6, Suppl. 2, 249 (1949).

14. R. P. Feynman, in Progress in Low Temperature Physics, edited by C. J. Gorter, (North-Holland, Amsterdam, 1955) Vol. I, Chap. II.

15. G. W. Rayfield and F. Reif, Phys. Rev. 136, A1194 (1964).

16. G. Gamota and T. M. Sanders, Phys. Rev. Letters 15, 949 (1965).

17. P. L. Richards and P. W. Anderson, Phys. Rev. Letters 14, 540 (1965).

18. H. E. Hall and W. F. Vinen, Proc. Roy. Soc. (London) A238, 204 (1956).

19. H. E. Hall, Proc. Roy. Soc. (London) A245, 546 (1958).

20. R. L. Douglass, Phys. Rev. 141, 192 (1966).

21. W. F. Vinen, Proc. Roy. Soc. (London) A260, 218 (1961).

22. D. J. Griffiths, Proc. Roy. Soc. (London) A277, 214 (1964).

23. L. A. Segel, Quart. Appl. Math. 18, 335 (1961).

24. G. G. Stokes, Mathematical and Physical Papers (Cambridge, 1901) Vol. 3, p. 38.

25. J. T. Stuart, in Laminar Boundary Layers, edited by L. Rosenhead (Clarendon Press, Oxford, 1963) p. 390.

26. M. Abramowitz and I. Stegun, Handbook of Mathematical Functions (N. B. S. Appl. Math. Series 55, Washington, D. C., 1964) p. 358.

27. E. Jahnke and F. Emde, Tables of Functions (Dover, New York, 1945) 4th ed., p. 252.

28. Reference 23.

29. R. P. Kanwal, Z. angew. Math. Mech. 35, 17 (1955).

30. H. Lamb, Hydrodynamics (Cambridge University Press, 1932, reprinted by Dover, New York, 1945) 6th ed., p. 83.

31. Reference 30, p. 78.

32. Reference 30, p. 681.

33. P. M. Morse, Vibration and Sound (McGraw-Hill, New York, 1948) 2d ed., p. 166.

34. Reference 33.

35. R. Courant and D. Hilbert, Methods of Mathematical Physics (Interscience, New York, 1953) Vol. 1, p. 363.

36. H. V. Neher, in Procedures in Experimental Physics, edited by J. Strong (Prentice-Hall, Englewood Cliffs, New Jersey, 1938) p. 188.

37. E-Solder 3021, Epoxy Products, Inc., Irvington, N.J.

38. 40 parts Maraglas Type A, The Marblette Corp., Long Island City, N.Y.; 10 parts Cardolite, Minnesota Mining & Mfg. Co., St. Paul, Minn.; 1 part benzyldimethylamine.

39. Oil seal #34013, National Motor Bearing Co.

40. Cenco Hyvac, Central Scientific Co., Chicago, Ill.

41. Bodine Electric Co., Chicago, Illinois.

42. Reference 41.

43. Model SH-14, Minarik Electric Co., 228 E. Third St., Los Angeles, Calif.

44. Supercon, Division of National Research Corp., Natick, Mass.

45. H. S. Martin & Sons, Evanston, Ill.

46. Microvac #212-H-10, F. J. Stokes Co., Division of Pennsalt Chemicals Corp., Philadelphia, Pa.

47. Allen-Bradley Co., 136 West Greenfield Ave., Milwaukee, Wisc.

48. Type 162 Waveform Generator, Tektronix, Inc., Beaverton, Ore.

49. Type 161 Pulse Generator, Tektronix, Inc.

50. Type 163 Pulse Generator, Tektronix, Inc.

51. Type 1232-A Tuned Amplifier and Null Detector, General Radio Co., West Concord, Mass.

52. Type 561 Oscilloscope, Tektronix, Inc.

53. Type 63 Differential Amplifier, Tektronix, Inc.

54. Type 67 Time Base, Tektronix, Inc.

55. Type 5343L Electronic Counter, Hewlett-Packard Co., Palo Alto, California.

56. Type 1233A Power Amplifier, General Radio Co.

57. Type 161 Pulse Generator, Tektronix, Inc.

58. TG-1 GeoTran, Norris-Thermador Corp., 5217 S. Boyle Ave., Los Angeles, Calif.

59. Reference 21.

60. J. M. Reynolds, R. G. Hussey, D. P. Thibodeux, B. E. Tucker, and R. F. Folse, The Oscillation of Cylinders and Spheres in Liquid Helium II, Tech. Doc. Report ML TDR 64-314 (Louisiana State University, 1964).

61. Reference 21.

62. Reference 22.

63. Reference 21.

64. J. G. Dash and R. D. Taylor, Phys. Rev. 105, 7 (1957).

65. Reference 21.

66. Reference 22.

ACKNOWLEDGMENTS

The author wishes to express his grateful appreciation to his adviser, Professor William Zimmermann, Jr., for his guidance and support during all of this work.

He also gratefully acknowledges the support given this work by the U. S. Air Force Office of Scientific Research and more recently the U. S. Atomic Energy Commission. He is also grateful for the tenure of a National Science Foundation Cooperative Graduate Fellowship during part of this work.